

# Transmark

AERODYNAMIC TESTS IN THE  
SIMPLON TUNNEL (pp)  
(TRANSMARK (RESEARCH) PART)

AERODYNAMIC TESTS IN THE  
SIMPLON TUNNEL (pp)  
(TRANSMARK (RESEARCH) PART)

by  
TRANSMARK  
(Transportation Systems and Market Research Ltd.)  
for  
Euro-Tunnel

Date: 5/1/89  
Report Ref: 613-8E  
File No.: -

Enterprise House  
169 Westbourne Terrace  
London W2 6J

Tel. No. 01-723 3411  
Tlx. No. 8953218 BRITMK G  
Fax. No. 01-258 1938

# TRANSMARK (RESEARCH)

AERODYNAMIC TESTS IN THE  
SIMPLON TUNNEL (pp)  
(TRANSMARK (RESEARCH) PART)

by

TRANSMARK  
(Transportation Systems & Market Research Ltd)

for

Euro-Tunnel

Date : 5/1/89

Report Ref : 613-8E

File No : -

**Key Words :**  
TUNNEL AERODYNAMICS  
FRICTION FACTORS  
PRESSURE LOSS  
COEFFICIENTS  
LEAKAGE BETWEEN  
TUNNELS  
FLOW VELOCITY PROFILES

This report was prepared for Transmark under the terms of a contract agreement. The contents are confidential and will not be divulged to a third party without the prior permission of Transmark.

## CONTENTS

*(of SNCF and TRANSMARK (Research) parts of reports)*  
*(Page numbers refer to Transmark (Research) contribution only)*

	Page
* 1. SUMMARY	
+ 2. OBJECTIVES	
* 3. GEOMETRICAL CHARACTERISTICS	
* 3.1 Tunnel	
* 3.2 Train	
* 4. EQUIPMENT AND TEST PROGRAMME	
5. EXPERIMENTAL TECHNIQUES AND EQUIPMENT	1
5.1 Tunnel	1
5.1.1 Location of measuring points	1
5.1.2 Transmark (Research) measuring equipment	
* 5.1.3 SNCF measuring equipment	
* 5.1.4 Sundry equipment	
5.2 On the Train	
* 5.2.1 Measuring equipment on the locomotives	
* 5.2.2 Pressure measuring equipment on the test trains	
6. RESULTS	4
6.1 Coefficient of Friction of Tunnel	
* 6.1.1 Steady analysis	
* 6.1.1.1 Principle of analysis	
* 6.1.1.2 Basic results	
* 6.1.1.3 Interpretation of results	
* 6.1.1.4 Conclusions	
6.1.2 Unsteady analysis	4
6.1.2.1 Principle of analysis	4
6.1.2.2 Results	7
6.1.2.3 Comments	8

CONTENTS (*Cont'd*)

	Page
6.1.3 Conclusion	8
6.2 Coefficient of Friction of the Train	10
* 6.2.1 Determination from the train	
* 6.2.1.1 Method adopted	
* 6.2.1.2 Maximum pressure loss along the train at 160 km/h	
* 6.2.1.3 Calculation of $C_{f_{TR}}$	
* 6.2.1.4 Analysis of the results	
6.2.2 Determination from the tunnel	10
6.2.2.1 Principle of analysis	10
6.2.2.2 Results	13
6.2.2.3 Comments	13
6.2.3 Conclusion	
6.3 Cross-Passage Pressure Loss Coefficients	15
6.3.1 Principle of analysis	15
6.3.2 Results	19
6.3.3 Comments	21
6.4 Loss Coefficients for Train Ends	25
6.4.1 Principle of analysis	25
6.4.2 Results	29
6.4.3 Comments	30
6.5 Leakage between Tunnels with Doors Closed	31
6.5.1 Flow measurements	31
6.5.2 Comments	33
* 6.6 Aerodynamic Coefficient of Train	
* 6.6.1 Measurement of the resistance to forward movement - General	
* 6.6.2 Primary components of the resistance to forward movement	
* 6.6.3 Secondary components of the resistance to forward movement	
* 6.6.3.1 Influence of profile	
* 6.6.3.2 Effect of curves	

CONTENTS (*Cont'd*)

## Page

* 6.6.3.3	Influence of wind	
* 6.6.4	Measuring method used	
* 6.6.4.1	Principle of the method	
* 6.6.4.2	Execution of measurements	
* 6.6.5	Results	
* 6.6.6	Analysis of results	
* 6.6.7	Comparison with the results of the May 87 series of tests	
* 6.6.8	Conclusions	
* 6.7	Pressure Variations on the Sides of the Vehicle	
* 6.7.1	Steady effects	
* 6.7.2	Unsteady effects	
6.8	Piston Duct Lateral Effects	34
6.8.1	Relationship between train position and air velocity	34
* 6.8.2	Pressure variations on the opposite sides of the vehicles	
* 6.8.3	Variations according to height	
* 6.8.4	Variations according to distance along the train	
* 6.9	Air Velocity in the Space between Train and Tunnel	
* 6.9.1	Mesuring principle	
* 6.9.2	Analysis of phenomena	
* 6.9.3	Ground/mobile comparison	
* 6.9.4	Comparative results	
* 6.9.5	Conclusion	
6.10	Velocity Profiles in the Cross-Passages and in the Tunnel	36
* 6.11	Misceilaneous measurements	
* 6.11.1	Pressure variations in the vestibules	
* 6.11.2	Air velocity in the train	
6.12	Selection of runs for simulation	

CONTENTS (*Cont'd*)

	Page
x 7. CONCLUSION	40

\* Provided by SNCF.

+ Provided by Euro Tunnel.

x Provided jointly by SNCF and Transmark (Research).

**LIST OF TABLES**  
*(Transmark (Research) Part)*

TABLE NO	TITLE
5.1.1.1	Instruments used for trackside measurements.
5.1.1.2	Role of instruments at measurement stations.
6.1.2.1	Calculated tunnel friction factors.
6.2.2.1	Tabulation of train friction factors.
6.3.1	Overall cross passage pressure loss coefficients (conditions "a" and "b").
6.3.2	Overall cross passage pressure loss coefficients (conditions "c" and "d").
6.3.3	Component pressure loss coefficients (Test Train in Tunnel 1).
6.3.4	Component pressure loss coefficients (Test Train in Tunnel 2).
6.4.1	Tabulation of train nose pressure loss coefficients.
6.4.2	Tabulation of train tail pressure loss coefficients.
6.8.1	Largest instantaneous flow velocities in cross passage as test train passes (9.12.87).
6.8.1.2	Largest instantaneous flow velocities in cross passage as test train passes (10.12.87).



**LIST OF TABLES**  
*(Transmark (Research) Part)*

FIG NO	TITLE
5.1.1.1	Layout of instrumentation in tunnel.
5.1.1.2a	Disposition of instruments at measurement stations A-H (looking towards Brig).
5.1.1.2b	Disposition of instruments at measurement stations I-O (K-O viewed looking towards Brig).
5.3	Recording station - Niche 6, Tunnel 2.
5.4	Static pressure sensing plate for tunnel wall.
5.5	ERA Gust Anemometer.
6.1.2.1	Flow velocity measurements at stations A and H. Train in Tunnel 1. (Run 34011, 3.12.87).
6.1.2.2	Characteristic Grid.
6.1.2.3	Characteristic at left hand end of duct.
6.1.2.4	Characteristic at right hand end of duct.
6.1.2.5	Run 801 input pressure histories at stations A and G - accelerating flow.
6.1.2.6	Run 801 flow velocity simulations using various friction factors - accelerating flow (Station A).
6.1.2.7	Run 801 input pressure histories at stations A and G - retarding flow.
6.1.2.8	Run 801 flow velocity simulations using various friction factors - retarding flow (Station A).
6.2.2.1	Pressure excursion produced by the passage of the test train past a stationary point in the tunnel.
6.2.2.2	Control volume for annulus.
6.2.2.3	Distribution of train friction factor measurements.

(Cont'd)

FIG NO	TITLE
6.3.1	Stations for evaluating cross passage pressure loss coefficients.
6.3.2	Cross passage flow conditions.
6.3.3	Behaviour of Channels 13, 14 and 15.
6.3.4	Behaviour of Channels 7, 8 and 9.
6.3.5	Differences between pressure channels.
6.3.6	Dynamic head of flow in cross passage.
6.3.7	Evaluation of total pressure loss coefficients.
6.3.8	Total pressure loss coefficients extracted from Ref 1.
6.3.9	Comparisons with extrapolated pressure loss coefficients deduced from Ref 1.
6.4.1	Pressure changes generated by the nose and tail.
6.4.2	Flow over nose (relative to train).
6.4.3	Flow over tail (relative to train).
6.4.4	Distribution of train nose pressure loss coefficient measurements.
6.4.5	Distribution of train tail pressure loss coefficient.
6.5.1	Train in Tunnel 1 Run 34011 3.12.87 flow velocities and pressures in and adjacent to cross passage 30.
6.5.2	Train in Tunnel 2 Run 34028 8.12.87 flow velocities and pressures in and adjacent to cross passage 30.
6.8.1.1	Flow behaviour in cross passage 30 Run 34065 9.12. 87 - Test Train in Tunnel 1 (Direction Brig - Iselle).
6.8.1.2	Run 34065 9.12.87 - Velocity excursions in cross passage shown on expanded time scale with nose and tail passing events.

*(Cont'd)*

FIG NO	TITLE
6.8.1.3	Run 34065, 9.12.87 - Train passing events obtained from infra red sensors.
6.8.1.4	Flow behaviour in Cross Passage 30 Run 34028 9.12.87. Test Train in Tunnel 2 (Direction Iselle - Brig).
6.8.1.5	Flow behaviour in Cross Passage 30 Run 34012 9.12.87 Test Train in Tunnel 1 (Direction Brig - Iselle).
6.10.1	Traversing anemometer.
6.10.2	Horizontal and vertical traverse points showing measured values of $U_T/U_{Ref}$ .
6.10.3	Distribution of points for determining mean flow velocity (Based on recommendation given in BS 848).
6.10.4	Representation of horizontal and vertical velocity distributions using 1/7th power law profiles.

## 5. EXPERIMENTAL TECHNIQUES AND EQUIPMENT

### 5.1 Tunnel

#### 5.1.1 Location of measurement points

Measurements at fixed locations in the tunnel were carried out by teams from SNCF and Transmark (Research). The measurements were performed at fourteen stations designated A to O. These were located between 4.7 km and 5.9 km from the Brig portal and are shown in Fig 5.1.1.1. Fig 5.1.1.1 also shows the instruments deployed at each station. A formal list of the instruments used at each station is presented in Table 5.1.1.1. Figs 5.1.1.2a and 5.1.1.2b illustrate the disposition of the instruments at the stations. The function of the instruments at each station is outlined in Table 5.1.1.2.

All the measurements were recorded in Niche 6, Tunnel 2, Fig 5.1.1.3.

#### 5.1.2 Transmark (Research) measurement equipment

The Transmark (Research) team was responsible for performing the measurements at stations A, O, G, H, J, N and O. The signals were recorded on UV paper and on a 42 channel tape recorder. The same tape recorder was also used for recording the signals from SNCF's equipment.

The static pressures at stations A, G, J and N were measured using Shaevitz absolute pressure transducers. A Druck absolute pressure transducer was used for the purpose of measuring the static pressure at station D. At each location the pressures were sensed through static pressure measuring plates mounted on the walls. A diagram showing the design of the plate is given in Fig 5.1.2.1.

The direction of flow at station A was determined using a wind vane mounted on a rotary potentiometer.

Flow velocities in the range 0-15 m/s were determined at stations A, H, J and O using eight bladed Abbirko vane anemometers. When the doors in cross passage 30 were opened, however, the vane anemometer at J was replaced with a four bladed device to enable it to measure flow velocities in the range 0-30 m/s.

ERA gust anemometers were deployed at H, J and O for the purpose of measuring sudden changes in flow velocity and flow velocities beyond the range of the vane anemometers. At stations H and J gust anemometers were mounted on both sides

of the tunnel. In cross passage 30 two gust anemometers were deployed to measure the flow velocity behaviour at the half height and three quarter height levels, Fig 5.1.1.2b.

Fig 5.1.2.2 shows a gust anemometer. The instrument has a response of 10 Hz and in its standard form is fitted with a perforated "table tennis" ball 38 mm in diameter. The perforated ball is mounted on a tube which deflects when the ball is exposed to a flow. The tube is attached to a strain gauged beam and the strain gauges give a signal which is proportional to the dynamic head of the stream. The ball is perforated to minimise its sensitivity to Reynolds number effects. The instrument is calibrated in a wind tunnel and flow velocity is ascertained by taking the square root of the product of the calibration constant and the signal from the strain gauges.

With the 38 mm diameter balls, the gust anemometer are limited to measuring a maximum velocity of 30 m/s. Since flow velocities in excess of this were expected in the running tunnels and cross passages, smaller diameter perforated balls were made available. These were 22 mm in diameter and extended the operating limit of the anemometers to 60 m/s.

Radar guns were positioned in Tunnels 1 and 2 for determining service train speed profiles. The guns were located at 6 km from the Brig end of the tunnel. In Tunnel 1, the gun was orientated towards the Brig portal and in Tunnel 2 towards Iselle. In Tunnel 1 the gun gave speed profiles for the section between the Brig portal and the 6 km position. In Tunnel 2 speed profiles were obtained from approximately the tunnel mid point to the niche at 6 km.

A "mobile" or transportable vane anemometer was provided for measuring velocity profiles in Tunnel 2. This exercise will be dealt with more fully in Section 6.10.

TABLE 5.1.1.1

## INSTRUMENTS USED FOR TRACKSIDE MEASUREMENTS

LOCATION	MEASURED QUANTITY	INSTRUMENT	MAKER/TYPE	CHANNEL NO	HEIGHT ABOVE RAIL LEVEL H, mm
A	Static Pressure	Absolute pressure transducer	Shaevitz P792-0103	17	1500
A	Flow Velocity	Vane anemometer	Abbirko	10	1150
A	Flow Direction	Direction vane mounted on potentiometer		11	1500
B	Static Pressure (Until 1/12)	Differential pressure transducer	Validyne DP7	25	3500
C	Static Pressure (From 2/12)	Differential pressure transducer	Validyne DP7	25	3500
C	Flow Velocity	Gust anemometer	ERA	35	~1000
D	Static Pressure	Absolute pressure transducer	Druck PD CR 101A	16	1500
E	Static Pressure (Until 2/12)	Differential pressure transducer	Validyne DP7	33	3500
E	Static Pressure (Until 2/12)	Differential pressure transducer	Validyne DP7	34	3500
F	Static Pressure	Differential pressure transducer	Validyne DP7	30	3500
G	Static Pressure	Absolute pressure transducer	Shaevitz P 792-0103	15	1500
H	Flow Velocity	Gust anemometer	ERA	5	1880
H	Flow Velocity	Gust anemometer	ERA	6	1880
H	Flow Velocity	Vane anemometer	Abbirko	9	1230
I	Flow Velocity	Gust anemometer	ERA	36	Rail Level
J	Flow Velocity	Gust anemometer	ERA	3	1200
J	Flow Velocity	Gust anemometer	ERA	4	1630
J	Flow Velocity	Vane anemometer	Abbirko	8	450, 1000*
J	Flow Velocity (pm 9/12 & 10/12 only)	Vane anemometer	Abbirko	12	Mobile
J	Static Pressure	Absolute pressure transducer	Shaevitz P 792-0103	14	1000
K	Static Pressure	Differential pressure transducer	Validyne DP7	26	3500
K	Static Pressure	Differential pressure transducer	Validyne DP7	27	500
K	Static Pressure	Differential pressure transducer	Validyne DP7	28	3500
K	Static Pressure	Differential pressure transducer	Validyne DP7	29	500
L	Flow Velocity	Gust anemometer	ERA	37	~1000
M	Static Pressure	Differential pressure transducer	Validyne DP7	31	3500
M	Static Pressure	Differential pressure transducer	Validyne DP7	32	3500
M	Static Pressure (Until 1/12)	Differential pressure transducer	Validyne DP7	33	500
M	Static Pressure (Until 1/12)	Differential pressure transducer	Validyne DP7	34	500
N	Static Pressure	Absolute pressure transducer	Shaevitz P 792-0103	13	1500
O	Flow Velocity	Gust anemometer	ERA	1	1150
O	Flow Velocity	Gust anemometer	ERA	2	1150
O	Flow Velocity	Gust anemometer	Abbirko	7	1100

\*From 10.12.87

TABLE 5.1.1.2

## ROLE OF INSTRUMENTS AT MEASUREMENT STATIONS

MEASUREMENT PLANE	LOCATION OF MEASUREMENT PLANE	BASIC FUNCTIONS AND APPLICATIONS OF INSTRUMENTS AT MEASUREMENT PLANE
A	Tunnel 1 4528 m from Brig Portal	Measurement of pressure and flow velocity evaluation of tunnel friction factor, train friction factor, train nose pressure loss coefficient, train tail pressure loss coefficient.
B	Tunnel 1 4702 m from Brig Portal	Measurement of static pressure in tunnel leg of cross passage junction.
C	Tunnel 1 5322 m from Brig Portal	Measurement of static pressure and flow velocity in tunnel leg of cross passage junction
D	Tunnel 1 5539 m from Brig Portal	Measurement of static pressure evaluation of train friction factor, train nose pressure loss coefficient, train tail pressure loss coefficient.
E	Tunnel 1 5704 m from Brig Portal	Measurement of static pressure in tunnel leg of cross passage junction.
F	Tunnel 1 5724 m from Brig Portal	Measurement of static pressure in tunnel leg of cross passage junction.
G	Tunnel 1 5739 m from Brig Portal	Measurement of static pressure evaluation of tunnel friction factor, train friction factor, train nose pressure loss coefficient, train tail pressure loss coefficient, cross passage pressure loss coefficients.
H	Tunnel 1 5874 m from Brig Portal	Measurement of flow velocity evaluation of tunnel friction factor, train friction factor, train nose pressure loss coefficient, train tail pressure loss coefficient, cross passage pressure loss coefficient.
I	Cross passage 29	Measurement of flow velocity.
J	Cross passage 30	Measurement of static pressure and flow velocity, leakage flows with doors closed evaluation of static and stagnation pressure loss coefficients for cross passage.
K	Tunnel 2 4747 m from Brig Portal	Measurement of static pressure in tunnel leg of cross passage junction.
L	Tunnel 2 5347 m from Brig Portal	Measurement of flow velocity in tunnel leg of cross passage junction.
M	Tunnel 2 5747 m from Brig Portal	Measurement of static pressure in tunnel leg of cross passage junction.
N	Tunnel 2 5762 m from Brig Portal	Measurement of static pressure evaluation of train friction factor, train nose pressure loss coefficient, train tail pressure loss coefficient, cross passage pressure loss coefficient.
O	Tunnel 2 5897 m from Brig Portal	Measurement of flow velocity evaluation of train friction factor, train nose pressure loss coefficient, train tail pressure loss coefficient, cross passage loss coefficient.

SIMPLON TUNNEL DEC. 1987

## TRANSDUCERS/CAPTEURS

- GUST ANEMOMETER
- VANE ANEMOMETER
- STATIC PRESSURE
- x DIRECTION VANE

## CHANNELS/VOIES (TRANSMARK (RESEARCH) Nos.)

1-17 - TRANSMARK (RESEARCH)

25-37 - SNCF

## NOTE

25(1) - UNTIL 1/12

25(2) - FROM 2/12

33(1) - UNTIL 2/12

34

32(2) - FROM 3/12

34

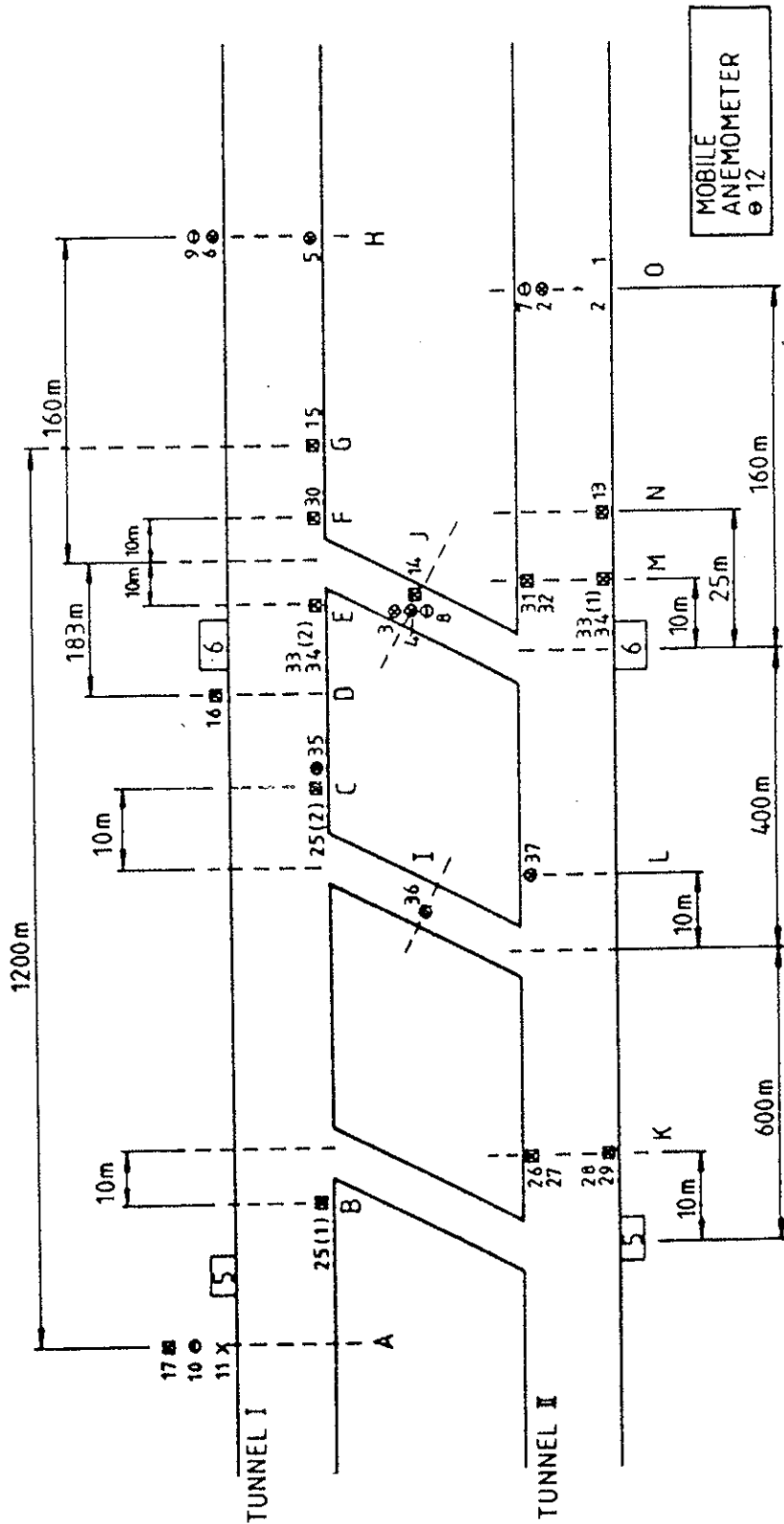


FIG. 5.1.1.1. LAYOUT OF INSTRUMENTATION IN TUNNEL I



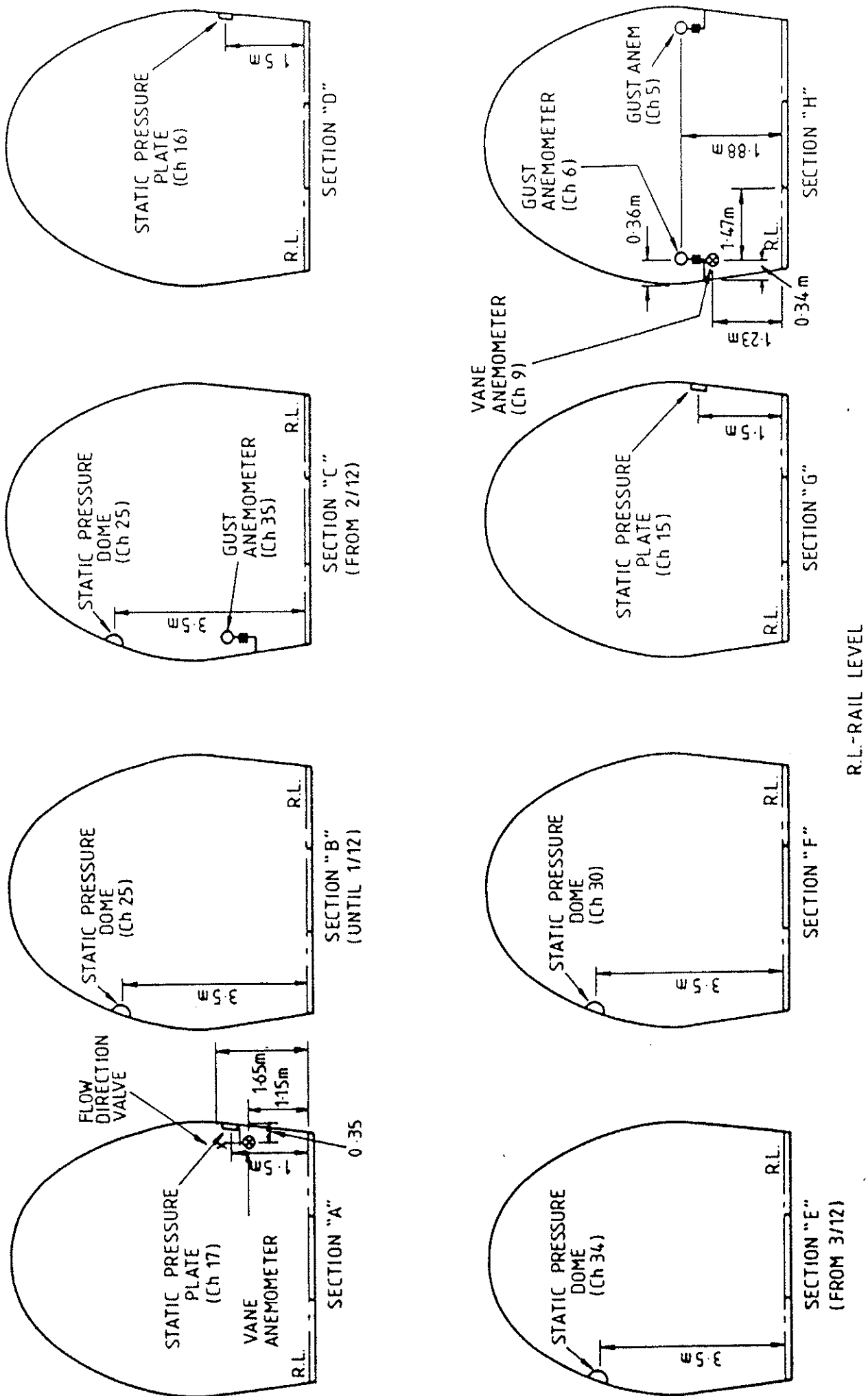


FIG. 5.1.1.2a. DISPOSITION OF INSTRUMENTS AT MEASUREMENT STATIONS A-H

FIG. 5.1.1.2b.

TRANSMARK

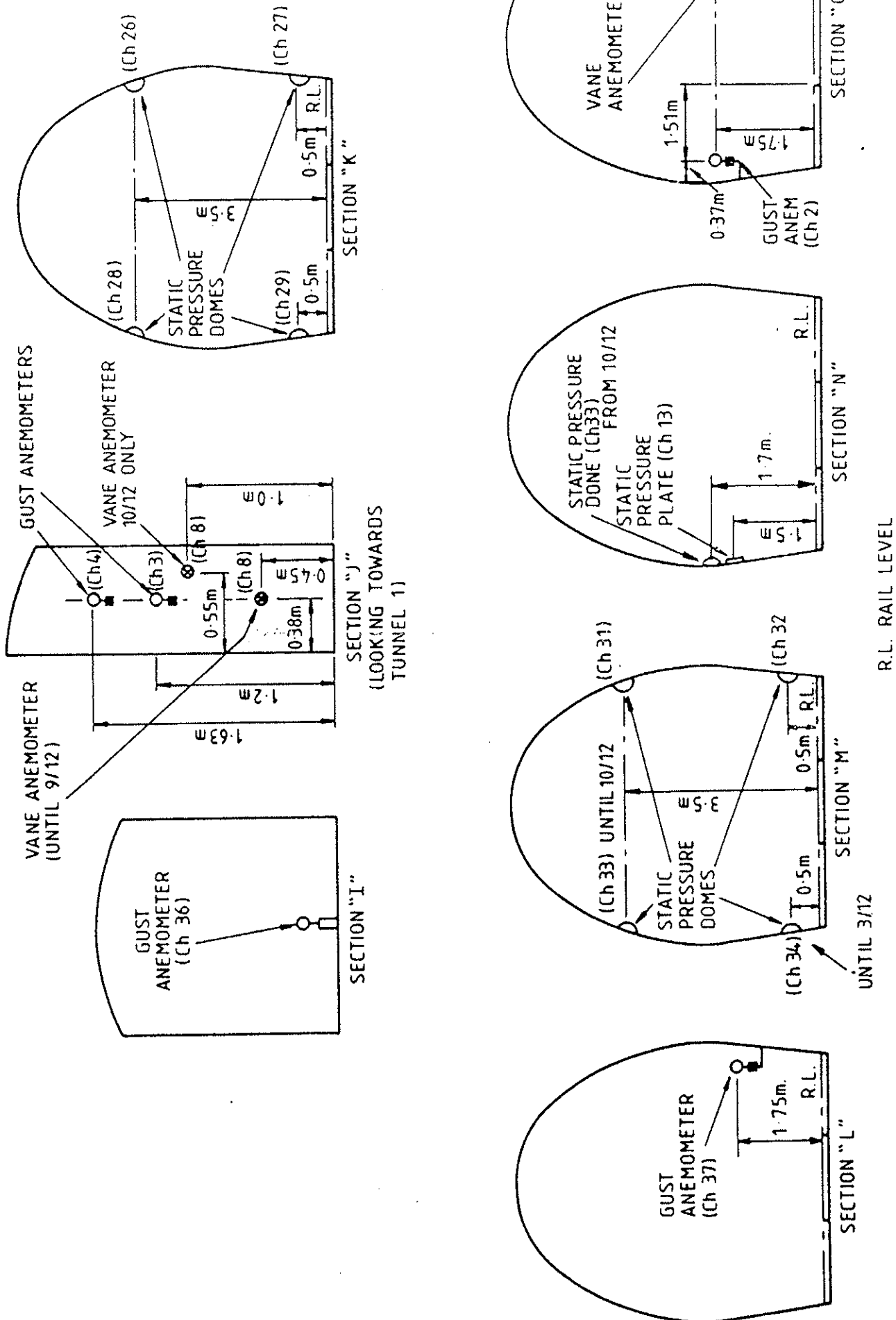


FIG. 5.1.1.2b. DISPOSITION OF INSTRUMENTS AT MEASUREMENT STATIONS I-O

FIG. 5.3.

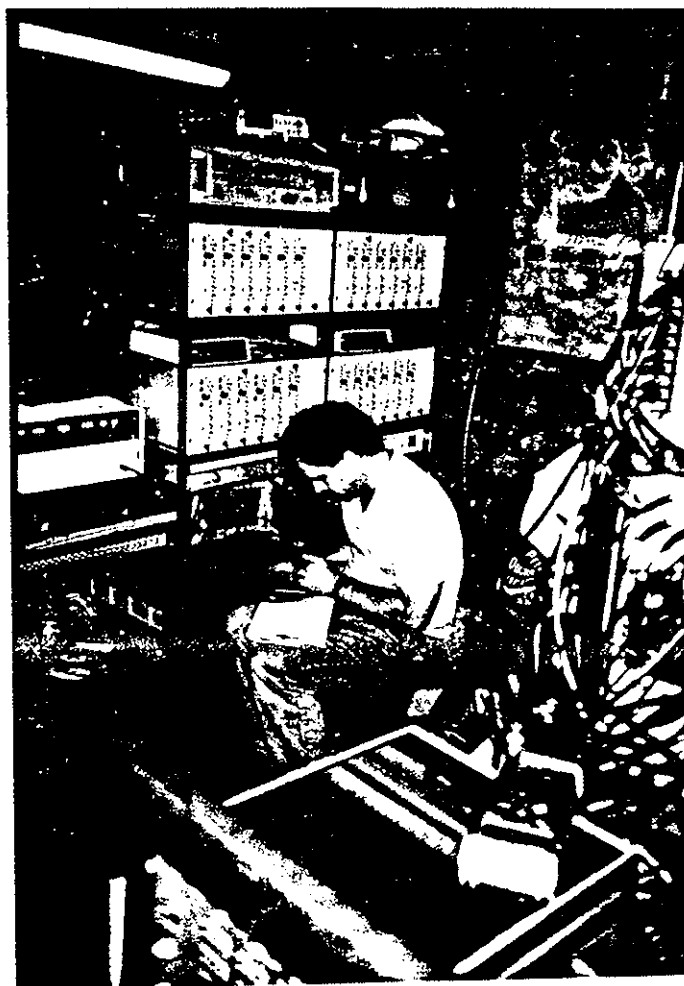


FIG. 5.3. RECORDING STATION - NICHE 6  
TUNNEL 2

FIG. 5.4.

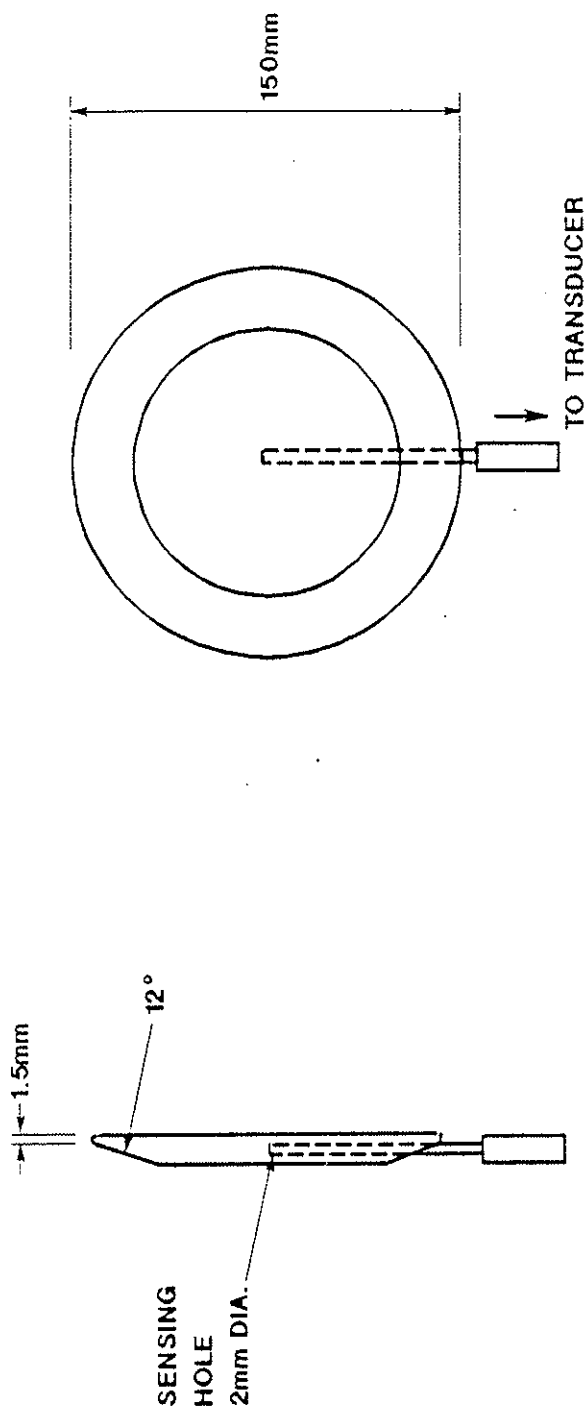


FIG. 5.4. STATIC PRESSURE SENSING PLATE  
FOR TUNNEL WALL

FIG. 5.5.

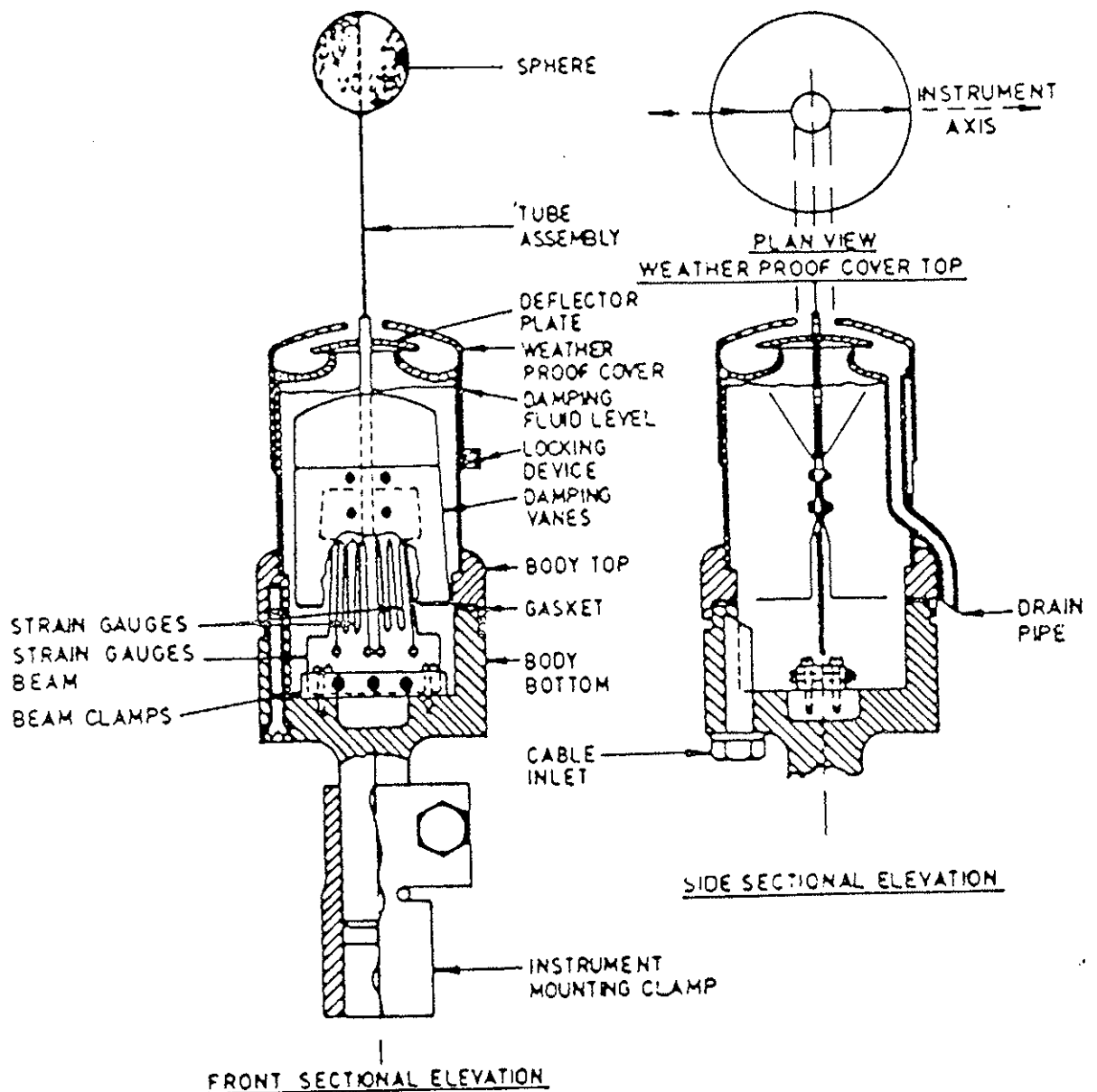


FIG. 5.5. ERA GUST ANEMOMETER

## NOTATION FOR SECTION 6.1.2

### *Roman Letters*

a	speed of sound in air
D	hydraulic diameter
f	friction factor for tunnel
p	static pressure
V	flow velocity
T	time
x	distance co-ordinate

### *Greek Letters*

$\rho$	air density
--------	-------------

### *Sufficies*

A	point A
B	point B
P	point P

## 6. TUNNEL FRICTION FACTOR

### 6.1.2 Unsteady analysis

#### 6.1.2.1 Principle of analysis

An alternative method for determining the tunnel friction factor is to consider the flow in the tunnel as unsteady. The method involves treating the 1211 m long section between stations A and G, Fig 5.1 as a plain duct. The method is only applicable to measurements obtained with the cross passage doors closed.

The leakage between the tunnels as a whole is significant with the doors closed. Over the relatively short section A to G, however, the leakage is small and is therefore, ignored in the analysis. This is justified on the grounds that the flow velocities as measured by the vane anemometers at A and H (135 m downstream of G) are very similar, implying that there is little loss of flow. Fig 6.1.2.1 compares the flow velocities at both stations for a draught generated by a train movement in Tunnel 1.

When a train enters Tunnel 1, the flow in section A-G will accelerate by wave action. Then, after the train passes through the section, the flow will progressively decay. An important factor in promoting the reduction of the flow velocity is the effect of leakage between the running tunnels as a whole.

Now the pressure histories at A and G are known from measurement. As a result they can be used as static pressure boundary conditions for the ends of the duct A-G. The flow between the boundaries can be modelled as an unsteady flow using the method of characteristics. The flow behaviour will depend on the magnitude of the tunnel wall friction factor. Thus by carrying out calculations for a range of friction factors one can assess which value of friction factor results in the most satisfactory calculation of the flow velocity behaviour at station A. The resulting friction factor represents the friction factor of the tunnel.

Calculations can be performed for an accelerating airflow generated by the entry of a train into the tunnel and for the retardation of the flow following transit of trains through the section A-G. The calculation is not designed to handle the movement of trains through A-G. It is only intended to model the acceleration of the airflow prior to arrival of the train at the section or the retardation of the flow after the train has left.

### Theoretical details

In analysing the unsteady flow, density changes are ignored since these are small. A finite speed of sound is, however, employed to model the effect of wave action. The governing equations are, therefore, identical to those used in solving unsteady flow problems in the field of hydraulics.

Equations of motion.

Continuity

$$\frac{1}{\rho} \frac{\partial P}{\partial t} + \frac{1}{\rho} \frac{\partial P}{\partial x} \cdot V + a^2 \frac{\partial V}{\partial x} = 0 \quad (1)$$

Momentum

$$\frac{1}{\rho} \frac{\partial P}{\partial x} + \frac{v \partial v}{\partial x} + \frac{\partial v}{\partial t} + \frac{fv^2}{2D} = 0 \quad (2)$$

Equations 1 and 2 may be recast into the following equations for the rightward (C<sup>+</sup>) and leftward (C<sup>-</sup>) propagating characteristics.

$$\begin{aligned} \frac{1}{\rho} \frac{dP}{dt} + a \frac{dV}{dt} + \frac{afV^2}{2D} &= 0 & C^+ \text{ characteristics} \\ \frac{dx}{dt} &= V + a \end{aligned}$$

$$\begin{aligned} \frac{1}{\rho} \frac{dP}{dt} - a \frac{dV}{dt} - \frac{afV^2}{2D} &= 0 & C^- \text{ characteristics} \\ \frac{dx}{dt} &= V - a \end{aligned}$$

assuming that  $v$  is small compared with  $a$

$$\frac{dx}{dt} = a \text{ for } C^+ \text{ characteristic}$$

$$\frac{dx}{dt} = -a \text{ for } C^- \text{ characteristic}$$



The characteristics equations can be re-cast into a finite difference form and solved with respect to a grid in  $x - t$  space, Fig 6.1.2.2. A marching procedure is employed whereby the calculation is advanced in time by small successive time steps  $\Delta T$ . To ensure that the calculation remains within the zone of dependence and stable, the magnitude of  $\Delta T$  must be such that:

$$\Delta T \leq \frac{\Delta X}{a}$$

where  $\Delta X$  is the mesh length.

The  $C^+$  and  $C^-$  characteristics re-cast infinite difference form are as follows:

$$C^+ \quad \frac{1}{\rho} (P_P - P_A) + a (V_P - V_A) + \frac{afV_A^2 \Delta T}{2D} = 0 \quad 3$$

$$C^- \quad \frac{1}{\rho} (P_P - P_B) - a (V_P - V_B) - \frac{afV_B^2 \Delta T}{2D} = 0 \quad 4$$

In the above equations the suffices A and B refer to known conditions at the foot of the characteristics, see Fig 6.1.2.2.

Equations 3 and 4 can be combined to give the static pressure and flow velocity at the point P (Fig 6.1.2.2).

$$P_P = \frac{1}{2} \left[ (P_A - P_B) + a\rho (V_A - V_B) - \frac{af\Delta T}{2D} (V_A^2 - V_B^2) \right] \quad 5$$

$$V_P = \frac{1}{2} \left[ (V_A - V_B) + \frac{1}{\rho a} (P_A - P_B) - \frac{f\Delta T}{2D} (V_A^2 + V_B^2) \right] \quad 6$$

Equations 5 and 6 can be applied to give the pressure and velocity at all mesh points at the end of the time step,  $\Delta T$ , except those at the boundaries.

At the boundaries the pressure is known.

For the left hand end, Fig 6.1.2.3, the flow velocity follows from

$$V_p = \frac{1}{\rho a} (P_p - P_B) + V_B - \frac{fV_B^2 \Delta T}{2D} \quad 7$$

For the right hand end, Fig 6.1.2.4, the flow velocity follows from

$$V_p = -\frac{1}{\rho a} (P_p - P_A) + V_A - \frac{fV_A^2 \Delta T}{2D} \quad 8$$

Having established the flow velocities and pressures at the end of the time step, the calculation can be repeated for successive time increments.

### 6.1.2.2 Results

Using the above calculation method friction factors are deduced using a process which involves replicating the measurement of the mean flow velocity at Station A. The calibration exercise for obtaining the mean flow velocity carried out in Tunnel 2, see Section 6.10, suggests that the vane anemometers as positioned in the running tunnels measure a velocity which is very close to the mean velocity. Nevertheless, in addition, calculations have been performed for relationships between the mean and measured velocity as follows :

$$U_{MEAN} = 1.1 U_{MEASURED}$$

$$U_{MEAN} = 1.2 U_{MEASURED}$$

This allows the sensitivity of the calculation of the friction factor to the measurement of the mean velocity to be assessed.

The input pressures for one run Run 801, will now be considered in some detail. Two cases were examined; accelerating flow and retarding flow.

Fig 6.1.2.5 shows the input pressure histories at sections A and G for the accelerating flow case. The resulting simulation of the measured velocity at Section A (taking  $U_{MEAN} = U_{MEASURED}$ ) is shown in Fig 6.1.2.6. Fig 6.1.2.6 indicates that the best fit between the measured and simulated flow velocities was obtained for a friction factor of 0.007.

The input pressure histories at A and G for the retarding flow case are shown in Fig 6.1.2.7 and the resulting modelling of the measured velocity at A given in Fig 6.1.2.8. Here the best fit was obtained for a friction factor of 0.006.

A remarkable feature of the simulations is the closeness with which they model the unsteady flow behaviour.

Nine other runs were examined in detail and the friction factors deduced from all the simulations of the flow velocity behaviour are presented in Table 6.1.2.1. Table 6.1.2.1 includes the results of simulations for  $U_{MEAN} = U_{MEASURED}$  and  $U_{MEAN} = 1.2 U_{MEASURED}$  as well as  $U_{MEAN} = U_{MEASURED}$ . For  $U_{MEAN} = U_{MEASURED}$ , the average friction factor is 0.0069. For a 10% increase in the ratio  $U_{MEAN}/U_{MEASURED}$  there is a 20% decrease in the friction factor. This is to be expected since the instantaneous pressure difference is proportional to the dynamic head. The strong dependence of the friction factor on the velocity ratio underlines the importance of determining the mean velocity accurately.

#### 6.1.2.3 Comments

An unsteady flow analyses has yielded an average friction factor for the tunnel of 0.0069. Results from the analyses of individual runs show a high degree of consistency with one another.

#### 6.1.3 Conclusion

The steady state analysis has yielded a friction factor of 0.0072 and the unsteady flow analysis a value of 0.0069. Taking the average of the two figures suggests a friction factor for the tunnel of 0.0071.

TABLE 6.1.2.1

## CALCULATED TUNNEL FRICTION FACTORS - UNSTEADY METHOD

			$U_{\text{MEAN}} = U_{\text{MEASURED}}$ FRICTION FACTOR		$U_{\text{MEAN}} = 1.1 U_{\text{MEASURED}}$ FRICTION FACTOR		$U_{\text{MEAN}} = 1.2 U_{\text{MEASURED}}$ FRICTION FACTOR	
DATE	SBB RUN NO	BR RUN NO	BEFORE TRAIN	AFTER TRAIN	BEFORE TRAIN	AFTER TRAIN	BEFORE TRAIN	AFTER TRAIN
4/11	34015	402	0.008	0.007	0.006	0.006	0.005	0.005
4/11	34019	404	0.007	0.007	0.006	0.006	0.005	0.005
7/11	34057	701	0.007	0.007	0.0055	0.0055	0.0045	0.005
7/11	34065	705	0.006	0.006	0.005	0.005	0.004	0.0045
8/11	34011	801	0.007	0.006	0.0055	0.0055	0.0045	0.0045
8/11	34015	802	0.006	0.007	0.005	0.006	0.004	0.005
8/11	34019	803	0.0065	0.006	0.005	0.005	0.004	0.004
3/11	34015	303	NA	0.0075	NA	0.006	NA	0.005
3/11	Not a test train 128 km/h	305	0.008	0.0075	0.007	0.006	0.0055	0.0055
3/11	34019	306	0.0075	0.008	0.006	0.0065	0.005	0.0055

$$f_{AV} = 0.0069$$

$$f_{AV} = 0.0057$$

$$f_{AV} = 0.0048$$

NA - Not Available

FIG. 6.1.2.1.

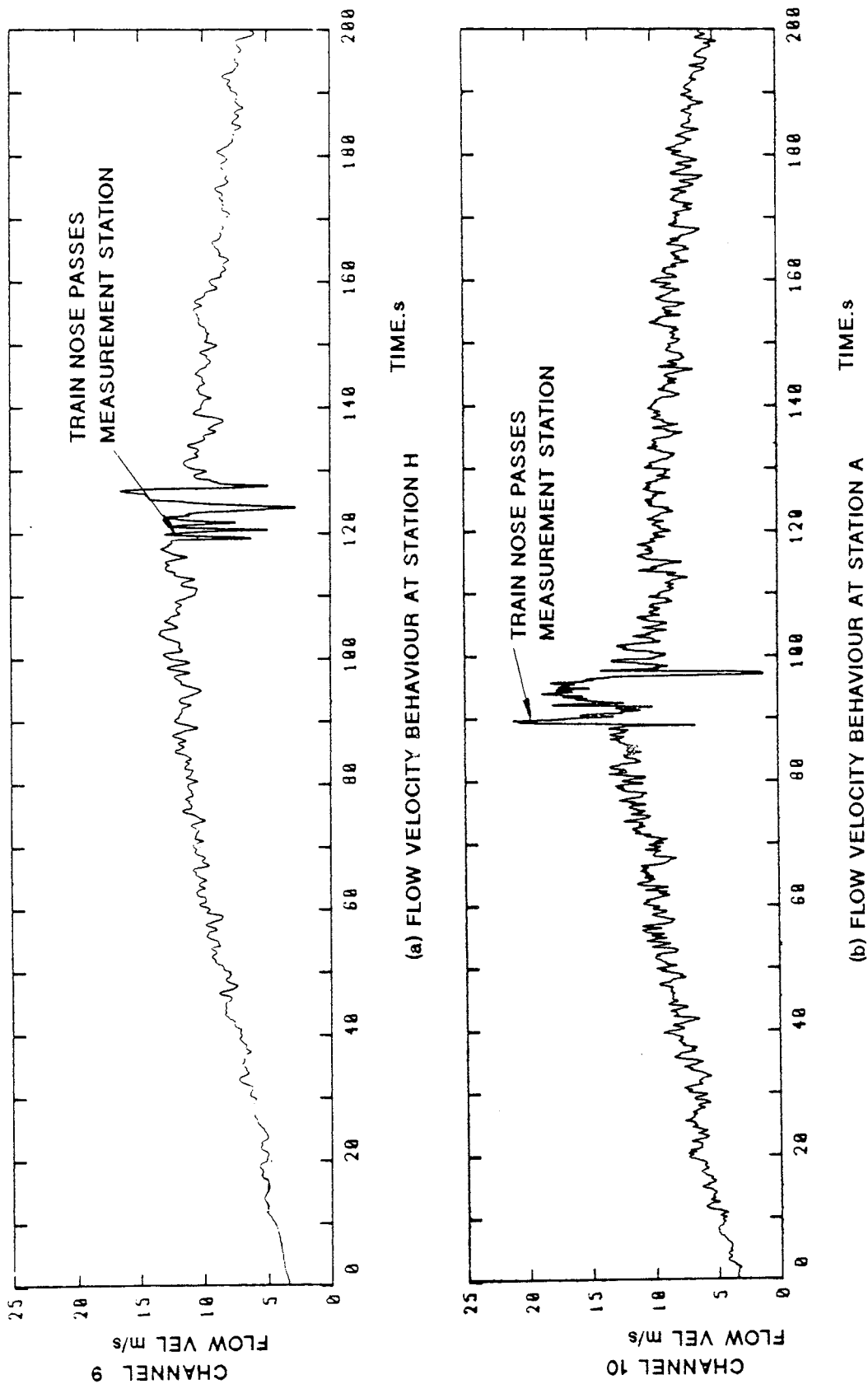


FIG. 6.1.2.1. FLOW VELOCITY MEASUREMENTS AT STATIONS A AND H  
TRAIN IN TUNNEL 1

FIG. 6.1.2.2, 6.1.2.3, 6.1.2.4.

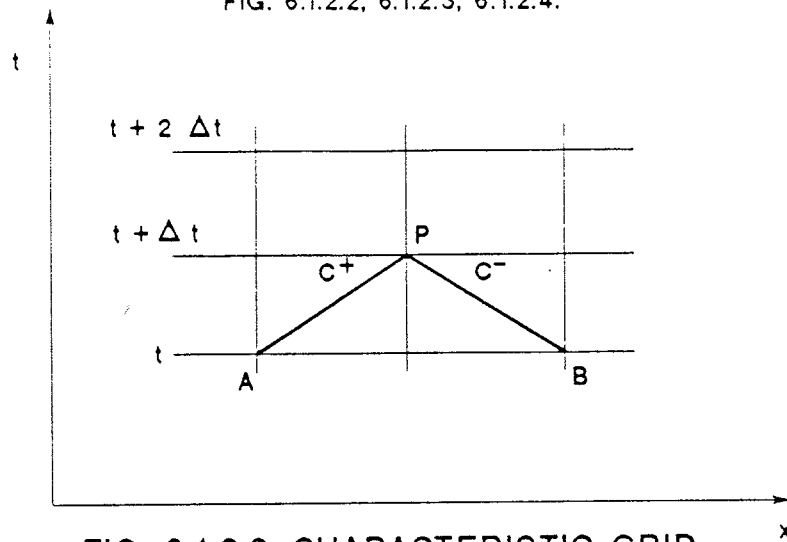


FIG. 6.1.2.2. CHARACTERISTIC GRID

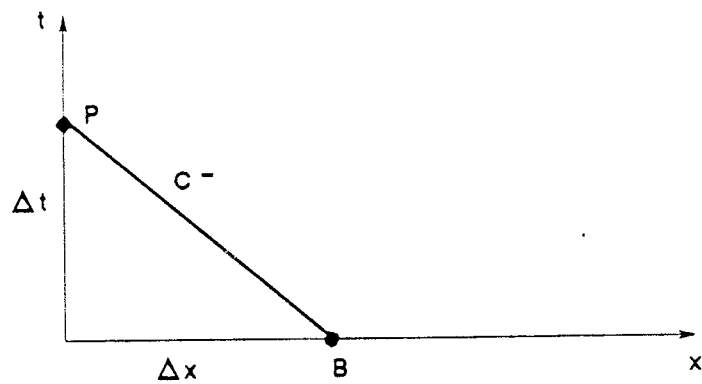


FIG. 6.1.2.3. CHARACTERISTIC AT LEFT HAND END OF DUCT

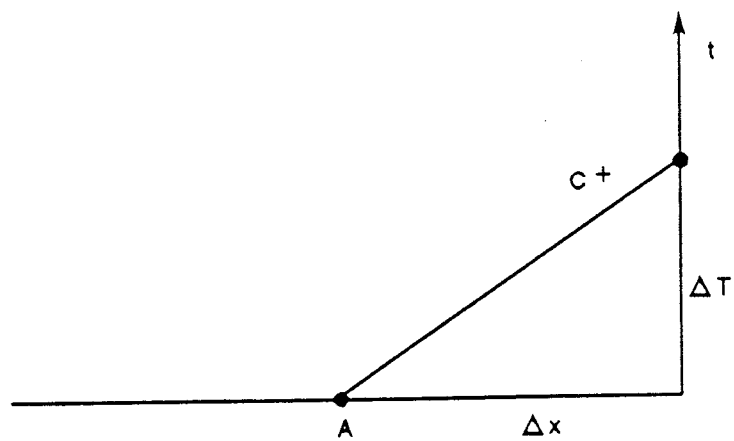


FIG. 6.1.2.4. CHARACTERISTIC AT RIGHT HAND END OF DUCT

FIG. 6.1.2.5.

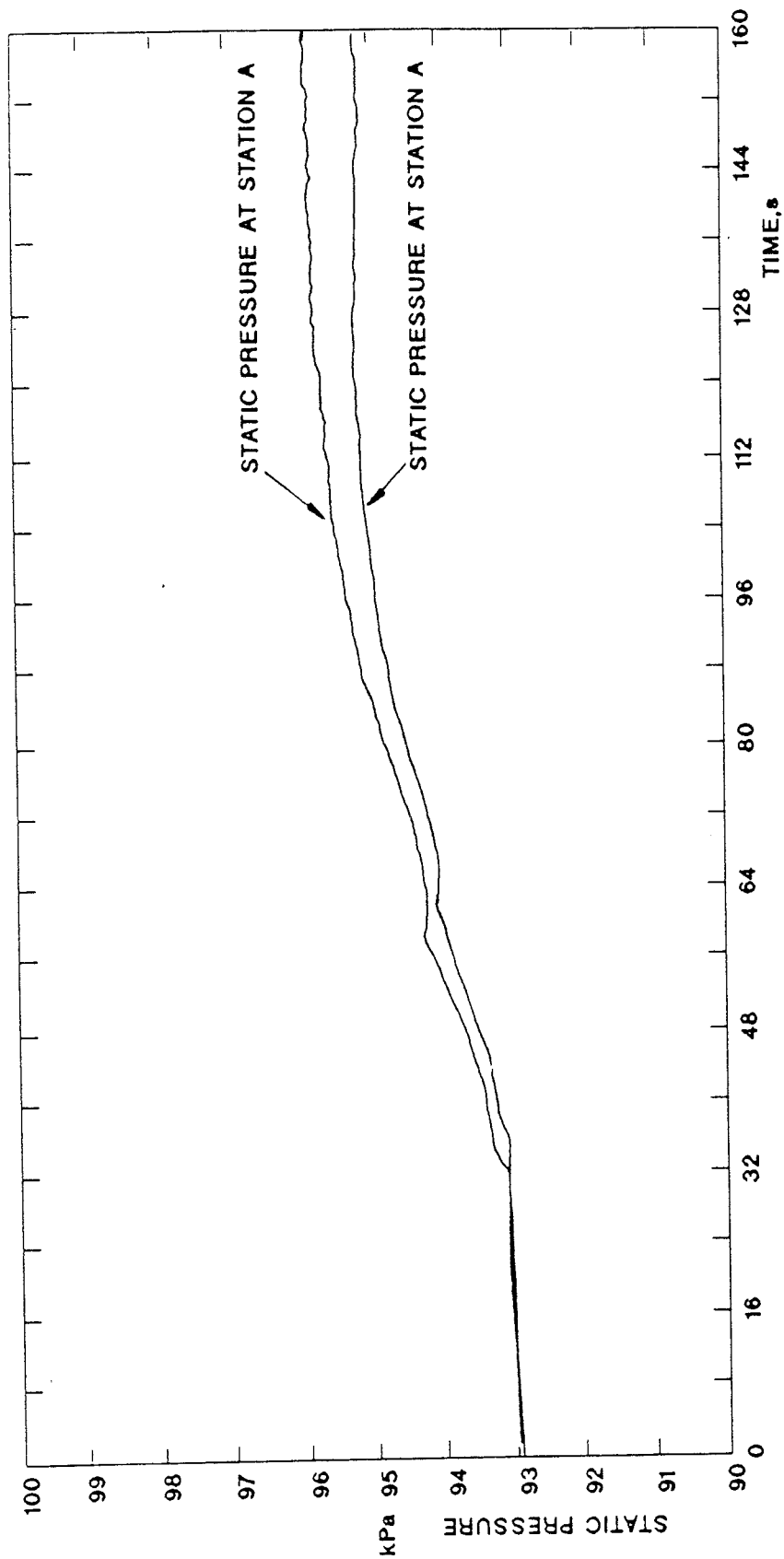


FIG. 6.1.2.5. RUN 801 INPUT PRESSURE HISTORIES AT STATIONS  
A AND B - ACCELERATING FLOW

FIG. 6.1.2.6.

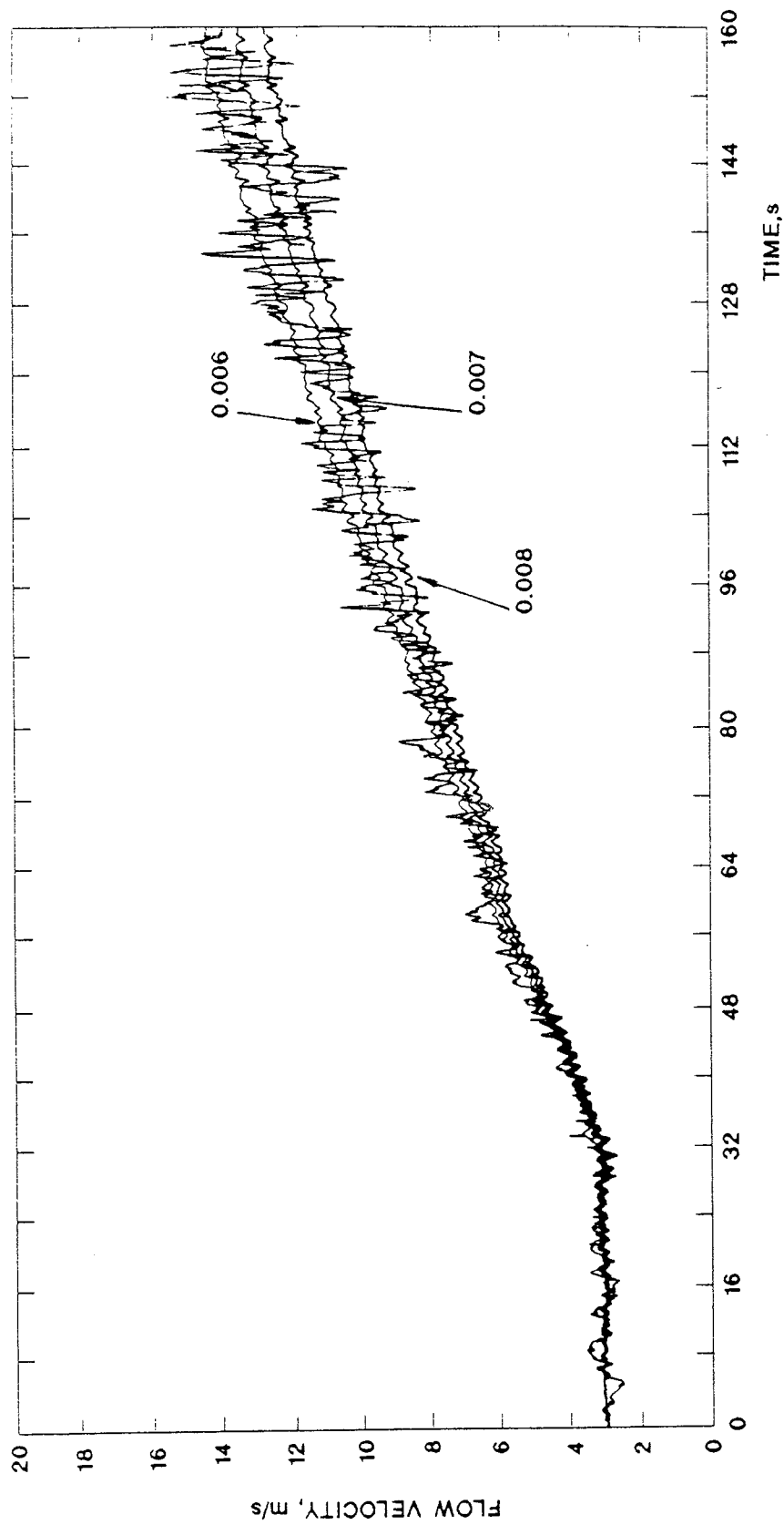


FIG. 6.1.2.6. RUN 801 FLOW VELOCITY SIMULATIONS USING VARIOUS  
FRICTION FACTORS - ACCELERATING FLOW (STATION A)



FIG. 6.1.2.7.

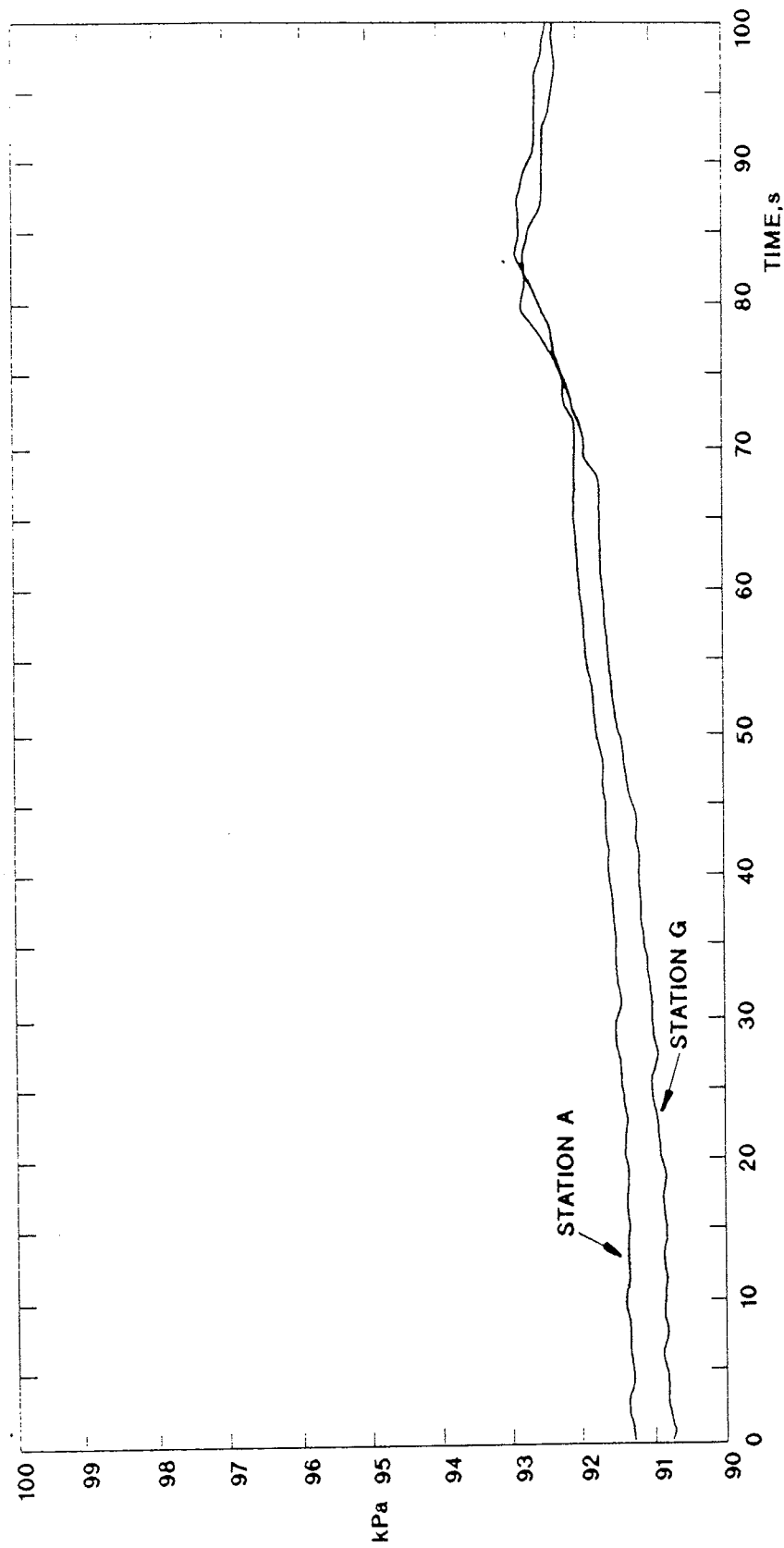


FIG. 6.1.2.7. RUN 801 INPUT PRESSURE HISTORIES AT STATIONS  
A AND G - RETARDING FLOW

FIG. 6.1.2.8.

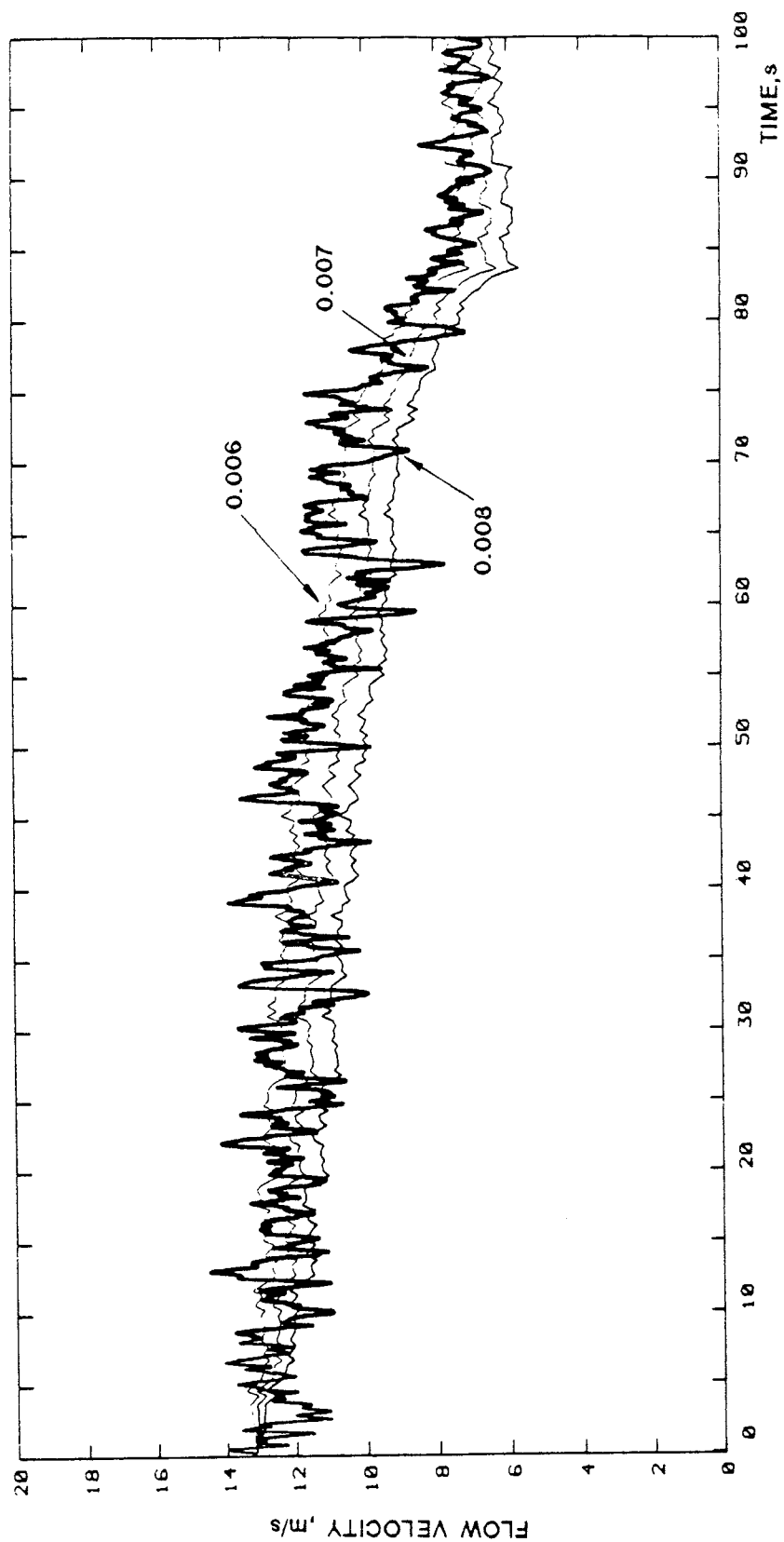


FIG. 6.1.2.8. RUN 801 FLOW VELOCITY SIMULATIONS USING VARIOUS FRICTION FACTORS  
RETARDING FLOW (STATION A)

## NOTATION FOR SECTION 6.2.2

### *Roman Letters*

$A_{an}$	cross sectional area of annulus between train and tunnel
$f_{tr}$	train friction factor
$f_{tu}$	tunnel friction factor
$l$	train length
$\Delta p_f$	pressure difference between the front and rear of the train
$S_{tr}$	train perimeter
$S_{tu}$	tunnel perimeter
$U$	flow velocity in annulus relative to tunnel
$U_1$	flow velocity in annulus relative to train
$U_T$	flow velocity in open tunnel relative to tunnel
$V$	train velocity

### *Greek Letters*

$$\phi \quad \text{area ratio} \quad \left\{ 1 - \frac{\text{train c/s area}}{\text{tunnel c/s area}} \right\}$$

$\rho$  air density

$X_{f_{tr}}$  tolerance on train friction factor

$X_{\Delta p_f}$  tolerance on pressure drop between front and rear of annulus

$X_U$  tolerance on flow velocity in annulus relative to tunnel

$X_{U_1}$  tolerance on flow velocity in annulus relative

## 6.2 Friction Factor for Train

### 6.2.2 Determination from tunnel

#### 6.2.2.1 Principle of analysis

The train friction factor may be determined from the excursion in pressure which is generated when a train passes a stationary point in a tunnel. Fig 6.2.2.1 shows an example of such an excursion. This depicts the passage of the test train past the pressure transducer at Station E in Tunnel 1. The nose produces a sudden fall in pressure. This is followed by a more gradual fall in pressure as the sides of the train draw past and then an increase in pressure as the tail sweeps by the transducer. The pressure excursion is largely a function of the reduction in flow area caused by the passage of the train but is also influenced by local viscous flow effects. The gradual fall in pressure AB is dependent on friction in the annular gap between the train and the tunnel and may be applied to determine the train friction factor. In order, however, to deduce the train friction factor from AB, it is also necessary to determine the flow velocity in the annulus.

This may be obtained from one of the flow metering points in the tunnel, eg Channel 9 in Tunnel 1 or Channel 7 in Tunnel 2. The flow velocity in the train/tunnel annulus may be found using the continuity equation from the flow velocity in the open tunnel just before the nose of the train passes.

In order to deduce an expression for the train friction factor let us now apply the momentum equation to the flow in the annulus. Referring to Fig 6.2.2.2, we have :-

$$\Delta p_f A_{an} = \frac{1}{2} \rho U_1^2 S_{tr} l f_{tr} + \frac{1}{2} \rho U |U| S_{tu} l f_{tu} \quad \text{eq.1}$$

In the above  $\Delta p_f$  is the difference in pressure between the front and rear of the annulus. It is equivalent to the fall in pressure AB which is generated as the sides of a train pass a stationary point in a tunnel.  $U$  and  $U_1$  are the flow velocities in the annulus relative to the tunnel and train respectively. They may be obtained from the flow velocity ahead of the train by continuity

$$\text{ie } U = \frac{V - U_T}{\phi} \quad \text{eq.2}$$

$$\text{and } U_1 = \frac{V - U_T}{\phi} \quad \text{eq.3}$$

Rearranging eq. 1 gives an expression for  $f_{tr}$  :

$$f_{tr} = \frac{\phi^2}{(V - U_T)^2 S_{tr}} \left\{ \frac{\Delta \rho_f A_{an}}{\frac{1}{2} \rho l} - \frac{V - U_T}{\phi} - V \left( \frac{V - U_T}{\phi} - V \right) S_{tu} f_{tu} \right\} \quad \text{eq.4}$$

$f_{tu}$  is the friction factor for the tunnel which has been derived in Section 6.1.

Uncertainties in the determination of the pressure and the flow velocity in the annulus have an important influence on the accuracy of  $f_{tr}$ .

If we have a quantity  $y$  which is a function of independent variables  $a, b, c$  etc then the tolerance  $X_y$  on  $y$  is related to the tolerances  $X_a, X_b, X_c$  etc on the quantities  $a, b$  and  $c$  by the equation

$$X_y^2 = \left( \frac{a}{y} \frac{\partial y}{\partial a} \right)^2 X_a^2 + \left( \frac{b}{y} \frac{\partial y}{\partial b} \right)^2 X_b^2 + \left( \frac{c}{y} \frac{\partial y}{\partial c} \right)^2 X_c^2 + \quad \text{eq. 5}$$

From eq. 5, writing  $f_{tr}$  in terms of the velocities  $U$  and  $U_1$ , gives the following expression for the tolerance on  $f_{tr}$ .

$$X_{f_{tr}} = \sqrt{\left[ 4 X_{U_1}^2 + \left( \frac{2 A_{an} \Delta p_f}{\rho U_1^2 S_{tr} l f_{tr}} \right)^2 X_{\Delta p_f}^2 + \left( \frac{2 U^2 S_{tu} f_{tu}}{U_1^2 S_{tr} f_{tr}} \right) X_U^2 \right]} \quad \text{eq.6}$$

Let us now consider a specimen error estimation involving Run 34057 of 8 December 1987 using the pressure channel, Ch 17 and the flow velocity channel, Ch 9. During this run the train speed was 42.9 m/s and the length 452.7 m. The pressure drop along the annulus and the flow velocity ahead of the train deduced from Ch 17 and Ch 9 were 5050 N/m<sup>2</sup> and 13.2 m/s respectively.

Now from equation 4,

$$f_{tr} = \frac{(0.569)^2}{(42.9 - 13.2)^2 \cdot 11} \left\{ \frac{5050 \cdot (23.2 - 10)}{\frac{1}{2} \cdot 1.15 \cdot 452.7} \left| \frac{42.9 - 13.2}{0.569} - 42.9 \right| \right. \\ \left. \left[ \left( \frac{42.9 - 13.2}{0.569} \right) - 42.9 \right] \times 18.9 \times 0.0069 \right\} = 0.00817$$

From equation 6,

$$\frac{2 A_{an} \Delta p_f}{\rho U_1^2 S_{tr} f_{tr}} = \frac{2 \cdot 13.2 \cdot 5050}{1.15 \cdot (52.2)^2 \cdot 11 \cdot 452.7 \cdot 0.00817} = 1.0458$$

$$\frac{2 U^2 S_{tu} f_{tu}}{U_1^2 S_{tr} f_{tr}} = \frac{2 \cdot (9.3)^2 \cdot 18.9 \cdot 0.0069}{(52.2)^2 \cdot 11 \cdot 0.00817} = 0.0921$$

Hence,

$$X_{f_{tr}} = \left\{ 4 X_{U_1}^2 + 1.0937 X_{\Delta p_f}^2 + 0.0085 X_U^2 \right\}^{\frac{1}{2}} \quad \text{eq.7}$$

Realistic tolerances are

$$X_{U_1} = \pm 5\%, X_U = \pm 5\% \text{ and } X_{\Delta p_f} = \pm 5\%$$

Thus,

$$X_{f_{tr}} = \pm 11.3\%$$

The above result indicates that the errors in pressure and velocity measurement combine to give quite large uncertainties in the result for the friction factor. These may be minimised by analysing a large number of test results. In this exercise a total of 78 results have been analysed. In Tunnel 1 pressure excursions have been taken from Channels 15, 16 and 17 with the flow velocity deduced from Channel 9. In Tunnel 2

the pressure excursions for analysis have been obtained from Channel 13 and the flow velocities extracted from Channel 7.

#### 6.2.2.2 Results

The results of the analysis are presented in Table 6.2.2.1. They are plotted on a histogram in Fig 6.2.2.3 and are not too far divorced from a normal distribution. The average value is 0.00819 and the mean standard deviation is 0.000841 or 10.3% of the average value. The 95% confidence interval of the average value is  $\pm 2.3\%$ .

#### 6.2.2.3 Comments

The friction factor of 0.00819 is fairly typical of a modern train and compares well with a figure of 0.0081 deduced for a HST travelling in a single track tunnel.

TABLE 6.2.2.1

## TABULATION OF TRAIN FRICTION FACTORS

DATE	RUN NO	TUNNEL	TRAIN LENGTH m	TRAIN VELOCITY m/s	TRAIN FRICTION FACTOR				CONDITIONS OF TRAIN MOVEMENT
					Ch 13 Station N Tunnel 2	Ch 15 Station G Tunnel 1	Ch 16 Station O Tunnel 1	Ch 17 Station A Tunnel 1	
3.12.87	34011	1	347.1	45.1		0.00863	0.00841	0.00800	Test train only.
3.12.87	34015	1	347.1	45.0		0.00906	0.00880	0.00802	
3.12.87	34016	2	↑ 347.1	44.8	0.00781				
3.12.87	34019	1	347.1	45.2		0.00898	0.00860	0.00771	
3.12.87	34020	2	347.1	44.9	0.00790				
			Coaches						Ferry train between PK 6 and Central Station.
3.12.87	34023	1	347.1	45.0		0.00913	0.00954	0.00827	Crossing with another train at Central Station.
3.12.87	34024	2	347.1	44.6	0.00707				
3.12.87	34027	1	↑ 347.1	44.4		0.00911	0.00985	0.00836	
3.12.87	34028	2	347.1	44.4	0.00818				
			12 Veh						
3.12.87	34057	1	241.5	45.6		0.00913	0.00907	0.00786	Crossing with other train on Swiss side.
3.12.87	34058	2	↑ 241.5	44.4	0.00771				
3.12.87	34062	2	241.5	45.4	0.00767				
3.12.87	34065	1	241.5	44.7		0.00899	0.00903	0.00854	
3.12.87	34066	2	241.5	44.5	0.00785				
3.12.87	34069	1	241.5	44.7		0.00811	0.00835	0.01069	Ferry train at PK 6 130s before test train.
			8 Veh Coaches						
7.12.87	34057	1	452.7	43.6		0.00899	0.00864	0.00740	Passing with other train on Italian side.
7.12.87	34058	2	↑ 452.7	44.7	0.00794				
7.12.87	34061	1	452.7	42.9		0.00975	0.00919	0.00806	
7.12.87	34062	2	452.7	44.7	0.00785				
7.12.87	34065	1	452.7	44.0		0.00897	0.00897	0.00667	
7.12.87	34066	2	452.7	44.7	0.00756				Test train only.
7.12.87	34069	1	↑ 452.7	44.7		0.00760	0.00735	0.00656	
7.12.87	34070	2	452.7	44.7	0.00755				
			16 Veh Coaches						
									Crossing at Central Station test train only.
8.12.87	34011	1	452.7	43.3		0.00894	0.00872	0.00761	Crossing at PK 6 with Freight Train.
8.12.87	34016	1	452.7	44.7		0.00793	0.00775	0.00674	
8.12.87	34019	1	452.7	44.0		0.00877	0.00863	0.00727	
8.12.87	34020	2	452.7	41.5	0.00690				
8.12.87	34023	1	↑ 452.7	41.0		0.00831	0.00875	0.00806	
8.12.87	34024	2	452.7	43.3	0.00780				Ferry train between PK 6 and Central Station. Ferry train stops at PK 6 100s after test train.
8.12.87	34027	1	452.7	41.1		0.00757	0.00763	0.00689	
8.12.87	34028	2	452.7	44.7	0.00843				
8.12.87	34057	1	452.7	42.9		0.00966	0.00929	0.00817	
8.12.87	34058	2	452.7	44.7	0.00667				
8.12.87	34061	1	↑ 452.7	44.7		0.00702	0.00729	0.00637	Crossing with Ferry train at PK 6.
8.12.87	34062	2	452.7	44.7	0.00838				
8.12.87	34066	2	452.7	43.8	0.00845				
8.12.87	34069	1	452.7	42.0		0.00829	0.00798	0.00755	
8.12.87	34070	2	452.7	44.7	0.00765				
									Ferry train in Tunnel 45s before test train.



FIG. 6.2.2.1.

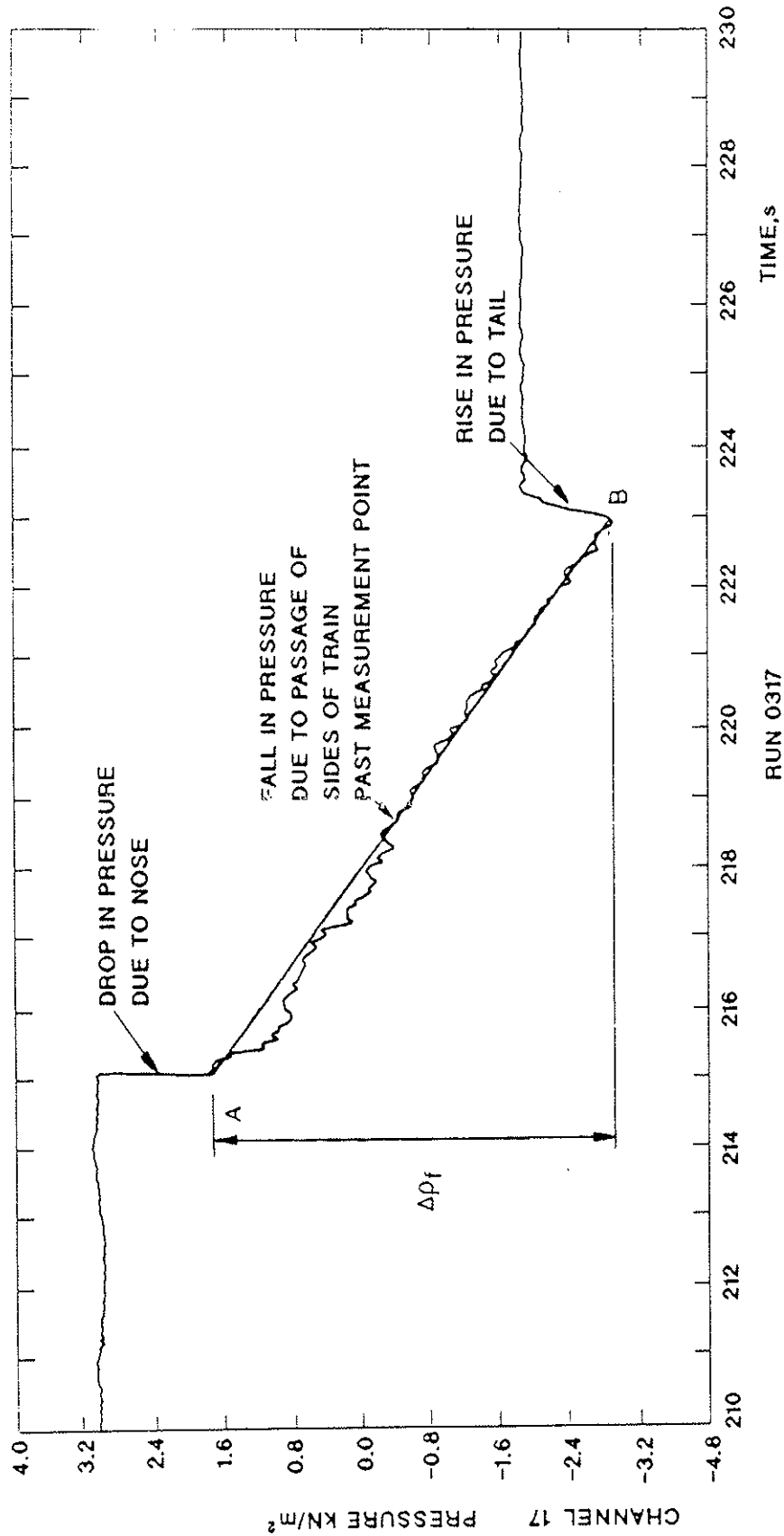


FIG. 6.2.2.1. PRESSURE EXCURSION PRODUCED BY THE PASSAGE OF THE TEST TRAIN PAST A STATIONARY POINT IN THE TUNNEL

FIG. 6.2.2.2.

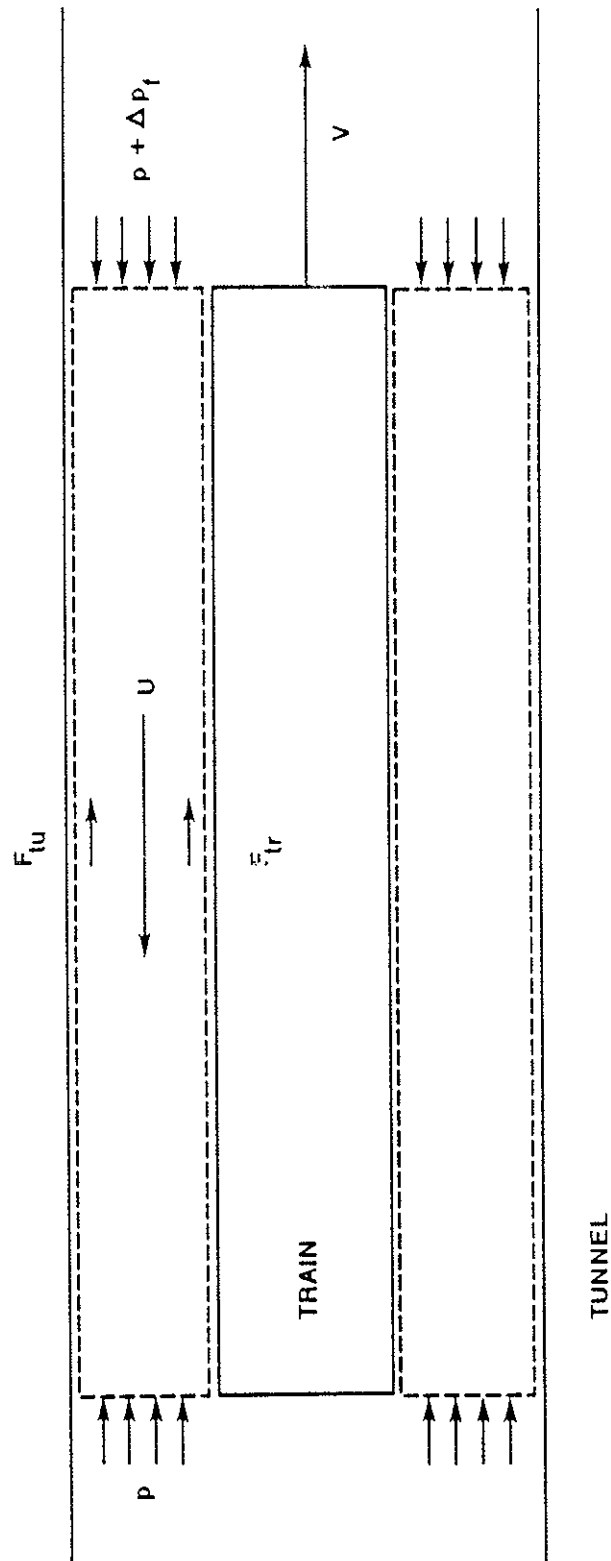


FIG. 6.2.2.2. CONTROL VOLUME FOR ANNULUS

FIG. 6.2.2.3.

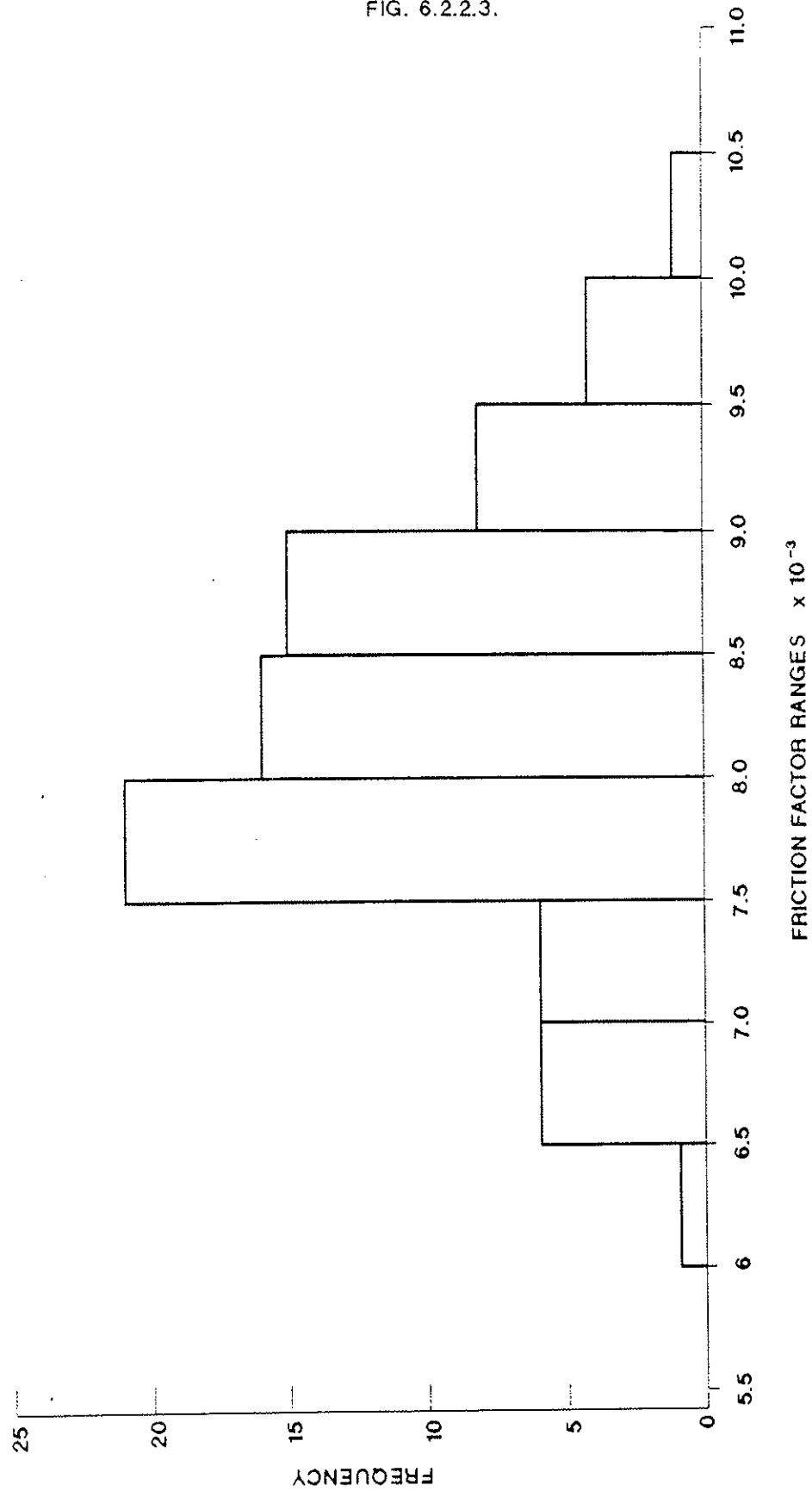


FIG. 6.2.2.3.DISTRIBUTION OF TRAIN FRICTION FACTOR MEASUREMENTS

## NOTATION FOR SECTION 6.3

### *Roman Letters*

K	total pressure loss coefficient
k	static pressure loss coefficient
p	static pressure
V	flow velocity
Q	volume flow

### *Greek Letters*

$\rho$	air density
--------	-------------

### *Sufficies*

1, 2, 3	stations 1, 2 and 3
12	denotes loss from 1 to 2
21	denotes loss from 2 to 1
23	denotes loss from 2 to 3
32	denotes loss from 3 to 2
13	denotes loss from 1 to 3
31	denotes loss from 3 to 1
T	denotes total volume flow

## 6.3 Cross Passage Loss Coefficients

### 6.3.1 Principle of analysis

Pressure loss coefficients for the lined cross passage, cross Passage 30, have been evaluated using pressure data from Channels 13, 14 and 15 and velocity data from Channels 7, 8 and 9. The evaluations were carried out using data obtained on 9 December 1987 and 10 December 1987 when tests were conducted with the cross passage doors open. The location of the channels is given on Fig 5.1.1.1. The flow velocity recordings in the running tunnel, Ch 7 and Ch 9, were carried out about 150 m away from the cross passage to ensure that the measurements were made in a region of attached flow.

For the purpose of evaluating the coefficients, the channels are grouped as follows, see also Fig 6.3.1.

Station 1	Ch 9, Ch 15
Station 2	Ch 8, Ch 14
Station 3	Ch 7, Ch 13

Coefficients have been evaluated for four basic flow conditions, Fig 6.3.2.

These are :

- (a) train in Tunnel 1 approaching cross passage (dividing flow)
- (b) train in Tunnel 1 moving away from cross passage (joining flow)
- (c) train in Tunnel 2 approaching cross passage (dividing flow)
- (d) train in Tunnel 2 moving away from cross passage (joining flow).

For each condition total and static pressure loss coefficients have been determined for the following :

- (i) the flow through the complete cross passage
- (ii) the "inlet" flow from the tunnel to the throat of the cross passage
- (iii) the "outlet" flow from the throat of the cross passage to the tunnel.

The coefficients are defined with respect to the stations shown on Fig 6.3.1 as follows :

1. Flow from Tunnel 1 to Tunnel 2 (ie conditions (a) and (d)).

(i) Flow through the complete cross passage,

total pressure loss :

$$K_{13} = \frac{p_1 - p_3 + \frac{1}{2} \rho V_1^2 - \frac{1}{2} \rho V_3^2}{\frac{1}{2} \rho V_2^2}$$

static pressure loss :

$$k_{13} = \frac{p_1 - p_3}{\frac{1}{2} \rho V_2^2}$$

(ii) "inlet" flow from Tunnel 1 to cross passage throat,

total pressure loss :

$$K_{12} = \frac{p_1 - p_2 + \frac{1}{2} \rho V_1^2 - \frac{1}{2} \rho V_2^2}{\frac{1}{2} \rho V_2^2}$$

static pressure loss :

$$k_{12} = \frac{p_1 - p_2}{\frac{1}{2} \rho V_2^2}$$

- (iii) "outlet" flow from cross passage throat to Tunnel 2,

total pressure loss :

$$K_{23} = \frac{p_2 - p_3 + \frac{1}{2} \rho V_2^2 - \frac{1}{2} \rho V_3^2}{\frac{1}{2} \rho V_2^2}$$

static pressure loss :

$$k_{23} = \frac{p_2 - p_3}{\frac{1}{2} \rho V_2^2}$$

2. Flow from Tunnel 2 to Tunnel 1 (ie conditions (b) and (c)).

- (i) Flow through the complete cross passage,

total pressure loss :

$$K_{31} = \frac{p_3 - p_1 + \frac{1}{2} \rho V_3^2 - \frac{1}{2} \rho V_1^2}{\frac{1}{2} \rho V_2^2}$$

static pressure loss :

$$k_{31} = \frac{p_3 - p_1}{\frac{1}{2} \rho V_2^2}$$

- (ii) "inlet" flow from Tunnel 2 to cross passage throat,

total pressure loss :

$$K_{32} = \frac{p_3 - p_2 + \frac{1}{2} \rho V_3^2 - \frac{1}{2} \rho V_2^2}{\frac{1}{2} \rho V_2^2}$$

static pressure loss :

$$k_{32} = \frac{p_3 - p_2}{\frac{1}{2} \rho V_2^2}$$

(iii) "outlet" flow from cross passage throat to Tunnel 1,

total pressure loss :

$$K_{21} = \frac{p_2 - p_1 + \frac{1}{2} \rho V_2^2 - \frac{1}{2} \rho V_1^2}{\frac{1}{2} \rho V_2^2}$$

static pressure loss :

$$k_{21} = \frac{p_2 - p_1}{\frac{1}{2} \rho V_2^2}$$

We will now present an example to illustrate the results of individual steps in the calculations. The example uses data from Run 34011 of 10 December. This features the test train running in Tunnel 1. Data was gathered for the train approaching and moving away from the cross passage enabling loss coefficients to be established for conditions (a) and (b). The example also serves to show how well behaved the results are.

Fig 6.3.3 shows the behaviour of the pressure Channels 13, 14 and 15. As the train approaches the cross passage an increase in pressure is registered by Channel 15. This is followed by a sudden fall in pressure as the train passes the pressure measurement point and then a progressive rise in pressure as the train moves away. This behaviour is also exhibited to some extent by Channel 14 which records the variation of static pressure in the cross passage. A much less pronounced variation in pressure is registered by Channel 13 in Tunnel 2 due to the losses in the cross passage.

Fig 6.3.4 illustrates the behaviour of the flow velocity Channels 7, 8 and 9. Channel 9 gives the variation of flow velocity in Tunnel 1. This is characterised by an increase in the flow velocity as the train approaches the anemometer and then a sudden fall as the nose passes. As the tail passes a rise in velocity is experienced. This is then



followed by a progressive fall in velocity as the train moves away. In the cross passage (Channel 8), the flow velocity variation is much more pronounced. As the train approaches the cross passage, the flow velocity rises to around 30 m/s. It then falls and reverses as the train goes past. A deceleration of the flow subsequently takes place as the train moves away from the cross passage. In Tunnel 2 (Channel 7) an acceleration of the flow occurs as the train approaches the cross passage followed by a deceleration as the train moves away. The disturbance, however, is much less marked than those in Tunnel 1 and the cross passage.

Fig 6.3.5 shows the variation with time of the following differences in static pressure :

Ch 15 - Ch 13 ie  $p_1 - p_3$

Ch 15 - Ch 14 ie  $p_1 - p_2$

Ch 14 - Ch 13 ie  $p_2 - p_3$

Prior to and following the train passing the cross passage, the pressure differences vary approximately linearly with time.

The variation of the flow dynamic head in the cross passage ( $1/2 \rho V^2$ ) is shown in Fig 6.3.6 and behaves approximately linearly as the train approaches and moves away from the cross passage. There is, however, some deviation from linear behaviour as the flow retards following 120 s.

Fig 6.3.7 shows the evaluation of the total pressure loss coefficients for condition (a) (ie  $K_{13}$ ,  $K_{12}$  and  $K_{23}$ ) and condition (b) (ie  $K_{31}$ ,  $K_{32}$  and  $K_{21}$ ). The constancy of the coefficients is quite remarkable.  $K_{31}$ ,  $K_{32}$  and  $K_{21}$ , however, deviate from constant values after 160 s. At this stage, the dynamic head in the cross passage and the static pressure differences are small. As a result the evaluation of the loss coefficients will be susceptible to error.

The general behaviour of the static pressure loss coefficients is similar to the total pressure loss coefficients.

### 6.3.2 Results

The principal objective is to determine the overall pressure loss coefficients for the cross passage for all four flow conditions. The loss coefficients have been evaluated for test train runs on 9 and 10 December and are shown in Tables 6.3.1 and 6.3.2. Table 6.3.1 gives the total and static pressure loss coefficients for the test train in Tunnel 1 (conditions a and b). Table 6.3.2 presents the loss coefficients for test train

movements in Tunnel 2. Average coefficients with their standard deviations (sd) and 95% confidence intervals are as follows :

Condition (a)

$$\begin{array}{lll} K_{13} = 4.19 & sd = 0.76 & 95\% \text{ int } \pm 42\% \\ k_{13} = 4.03 & sd = 0.69 & 95\% \text{ int } \pm 40\% \end{array}$$

Condition (b)

$$\begin{array}{lll} K_{31} = 2.06 & sd = 0.49 & 95\% \text{ int } \pm 55\% \\ k_{31} = 2.29 & sd = 0.51 & 95\% \text{ int } \pm 52\% \end{array}$$

Condition (c)

$$\begin{array}{lll} K_{31} = 2.61 & sd = 0.41 & 95\% \text{ int } \pm 36\% \\ k_{31} = 2.62 & sd = 0.46 & 95\% \text{ int } \pm 41\% \end{array}$$

Condition (d)

$$\begin{array}{lll} K_{13} = 2.83 & sd = 0.41 & 95\% \text{ int } \pm 33\% \\ k_{13} = 3.06 & sd = 0.47 & 95\% \text{ int } \pm 35\% \end{array}$$

The magnitudes of the "component" pressure loss coefficients  $K_{12}$ ,  $K_{23}$ ,  $K_{32}$  and  $K_{21}$  etc have been determined from runs conducted on the afternoon of 9 December. The values for conditions (a) and (b) are shown in Table 6.3.3 and values for (c) and (d) are presented in Table 6.3.4.

The loss coefficients for a branch are dependent on the ratios of

- (i) cross sectional area of the branch to the main duct
- (ii) the flow in the branch to the total flow.

Published loss coefficients for branches are often presented as functions of area and flow ratios. To assist in the process of comparing the loss coefficients with other data, average flow ratios have been established for conditions (a) - (d) and are given below :

(a)	(b)	(c)	(d)
$\frac{Q_2}{Q_T} = 0.15$	$\frac{Q_2}{Q_T} = 0.14$	$\frac{Q_2}{Q_T} = 0.14$	$\frac{Q_2}{Q_T} = 0.11$

Static pressure measuring channels were provided by SNCF in Tunnels 1 and 2 close to the cross passage. The locations of these are shown in Fig 5.1.1.1. Two channels, Ch 31 in Tunnel 1 and Ch 33 in Tunnel 2 have been used to provide comparative total pressure loss coefficients. These have been determined for Run 34015 of 9 December and are appropriate to conditions (a) and (b). The coefficients obtained are given below with the equivalent values obtained from Channels 15 and 13.

Condition (a)

$$K_{13} \text{ (Ch 31/33)} = 3.0$$

$$K_{13} \text{ (Ch 15/13)} = 3.4$$

Condition (b)

$$K_{31} \text{ (Ch 31/33)} = 2.0$$

$$K_{31} \text{ (Ch 15/13)} = 1.9$$

The degree of correspondence is good.

### 6.3.3 Comments

Conditions (a) and (c) are equivalent to each other as are (b) and (d). There are, however, quite substantial differences in the loss coefficients for each of the equivalent conditions. These are probably due to geometric asymmetry in the cross passage. The differences in the total pressure loss coefficients are summarised below :

Conditions (a) and (c)

	(a)	(c)	$\left( (K_{13(a)} - K_{31(c)}) / K_{13(a)} \right) \%$
$K_{13}$	4.19	2.61	38%

Conditions (b) and (d)

	(b)	(d)	$\left( (K_{31(b)} - K_{13(d)}) / K_{31(b)} \right) \%$
$K_{31}$	2.06	2.83	-38%

The average losses are smaller for flow from Tunnel 2 to Tunnel 1 than for flow from Tunnel 1 to Tunnel 2.

Broadly speaking the total pressure loss coefficients for the full cross passage are of a very similar magnitude to the equivalent static pressure loss coefficients.

Good correspondence exists between loss coefficients deduced from pressure channels provided by Transmark (Research) and SNCF.

The cross passage geometry is quite unusual. As a result there is very little published information available with which to compare the measured coefficients. Miller gives total pressure loss coefficients for a 60° angle branch presented as functions of area and flow ratio, Fig 6.3.8. The area ratio of the cross passage to the running tunnel is 0.065 and the flow ratios lie between 0.11 and 0.15. This means the configuration lies outside the data presented on the curves and comparisons have to be effected using extrapolated information.

Comparisons with coefficients extrapolated from Miller's data are made for the "component" pressure loss coefficients established from the results of the afternoon of 9 December. The comparisons are presented in Fig 6.3.9. To be compatible with Miller's definition of total pressure loss coefficient, the measured total pressure loss coefficients have been recast using the total flow dynamic head as the non-dimensionalising factor. The levels of agreement are quite good for cases (ii), (iii) and (iv). There is, however, a large discrepancy between the extrapolated loss coefficient and the measured value for case (i). No published data has been found for dividing flow conditions A and B involving inclined branches.

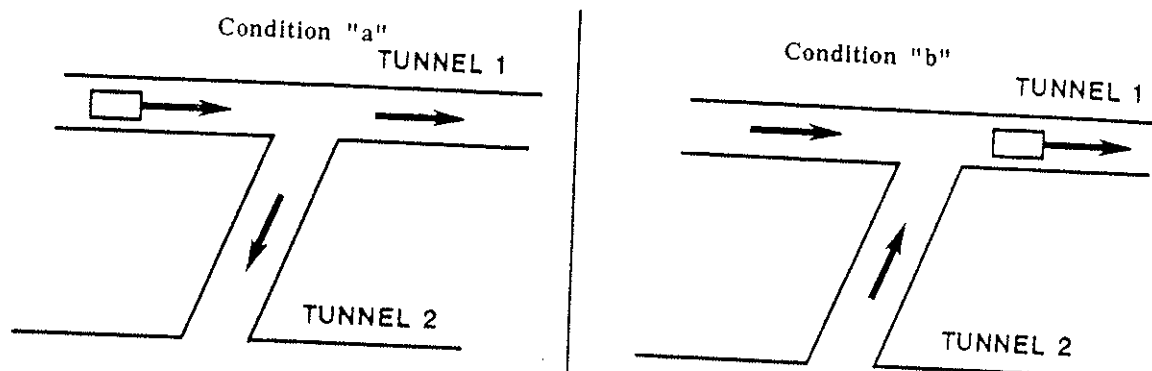
For cases (i) and (iv), Fig 6.3.9, the measured loss coefficient for the branch is based on the static pressure at stations 1 and 3 respectively. To be fully compatible with Miller's definition, the respective loss coefficient should be based on the pressures at X and Y (Fig 6.3.9). Miller's data shows, however, that the pressure difference across the mouth of the branch is small. Hence direct comparison between Miller's coefficients and the measured values for cases (i) and (iv) is justified.

The comparisons are somewhat tenuous in that quite radical extrapolations have had to be made in order to use Miller's data. In broad terms, however, the extrapolations suggest that the coefficients are realistic.

#### 6.3.4 Reference

1. Miller D S, "Internal Flow Systems" BHRA Fluid Engineering, Cranfield, 1978.

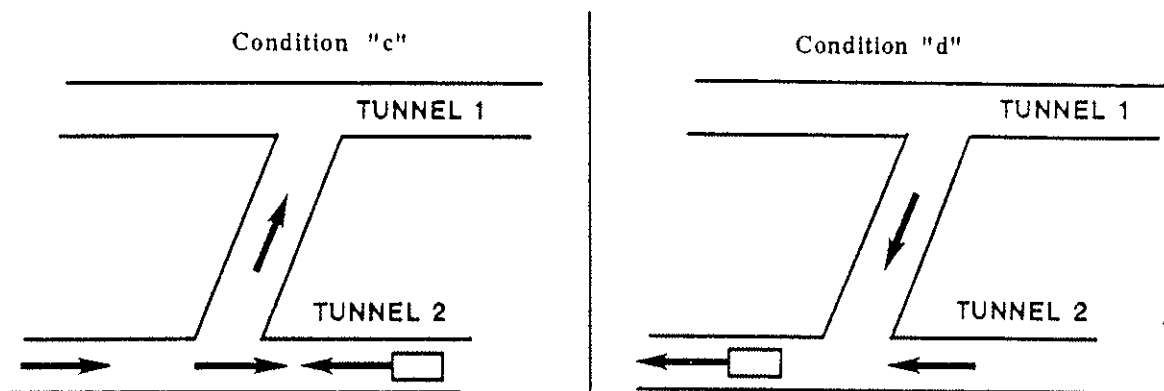
TABLE 6.3.1

OVERALL CROSS PASSAGE PRESSURE LOSS COEFFICIENTS  
(CONDITIONS "a" AND "b")

RUN NO	DATE	TOTAL PRESSURE LOSS COEFFICIENT	STATIC PRESSURE LOSS COEFFICIENT	TOTAL PRESSURE LOSS COEFFICIENT	STATIC PRESSURE LOSS COEFFICIENT	CONDITIONS OF TRAIN MOVEMENT
34011	9/12	3.6	3.5	2.1	2.1	Test train only. Express V = 140 km/h in Tunnel 2 90s after test train.
34015	9/12	3.4	3.4	1.9	2.0	
34019	9/12	3.5	3.3	1.7	2.0	
34057	9/12	4.2	4.1	2.2	2.3	Ferry train V = 90 km/h in Tunnel 2 90s before test train.
34061	9/12	5.1	4.9	-	-	Test train only.
34065	9/12	5.3	4.9	2.6	2.7	Test train only.
34069	9/12	4.7	4.4	2.6	2.9	Ferry train V = 90 km/h in Tunnel 2 25s after test train.
34011	10/12	4.3	4.1	1.6	1.9	Express V = 140 km/h in Tunnel 2 200s before test train.
34028	10/12	2.7	2.6	1.0	1.2	Test train only.
34061	10/12	4.3	4.2	2.2	2.5	-
34065	10/12	4.6	4.4	2.6	2.9	-
34069	10/12	4.6	4.5	2.2	2.7	Ferry train V = 90 km/h in Tunnel 2 just before test train.
Average Value		4.2	4.0	2.1	2.3	Express V = 140 km/h in Tunnel 2 180s before test train.

TABLE 6.3.2

OVERALL CROSS PASSAGE PRESSURE LOSS COEFFICIENTS  
(CONDITIONS "c" AND "d")

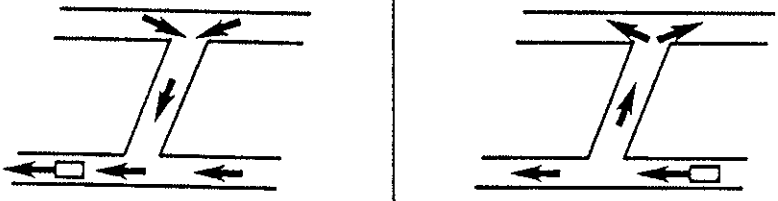


RUN NO	DATE	TOTAL PRESSURE LOSS COEFFICIENT	STATIC PRESSURE LOSS COEFFICIENT	TOTAL PRESSURE LOSS COEFFICIENT	STATIC PRESSURE LOSS COEFFICIENT	CONDITIONS OF TRAIN MOVEMENT
34016	9/12	2.1	2.0	3.0	3.2	Express V = 140 km/h 20s after test train.
34020	9/12	2.3	2.2	3.1	3.4	Train in Tunnel 1 180s before test train.
34062	9/12	-	-	2.5	2.6	Test train only.
34066	9/12	2.6	3.0	2.9	2.8	Test train only.
34070	9/12	3.5	3.5	2.6	2.6	Test train only.
34028	10/12	2.7	2.7	3.8	4.1	Express V = 180 km/h in Tunnel 1 120s after test train.
34058	10/12	2.2	2.2	2.6	2.8	Ferry train V = 90 km/h in Tunnel 1 240s before test train.
34062	10/12	2.6	2.5	2.4	2.7	Test train only.
34066	10/12	2.8	2.8	2.6	3.3	Simultaneous crossing with other train.
34070	10/12	2.7	2.7	2.8	3.1	Test train only.
Average Value		2.6	2.6	2.8	3.1	

TABLE 6.3.3

COMPONENT PRESSURE LOSS COEFFICIENTS  
(TEST TRAIN IN TUNNEL 1)

TEST DATA 9/12 (pm)

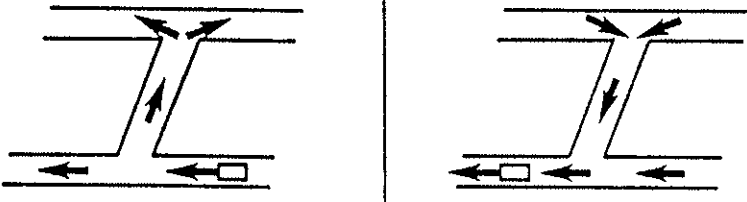
RUN NO	$K_{12}$	$K_{23}$	$K_{32}$	$K_{21}$
34069	2.3 (1.6)	2.0 (3.0)	1.3 (2.0)	1.7 (0.6)
34061	3.1 (2.2)	1.9 (2.8)	-	-
34065	2.9 (2.0)	2.3 (3.0)	1.3 (2.1)	1.4 (0.6)
34057	2.1 (1.2)	1.9 (3.0)	1.0 (1.9)	1.5 (0.3)
Average Value	2.6 (1.8)	2.0 (3.0)	1.2 (2.0)	1.5 (0.5)
				

( ) Total pressure loss coefficient.

TABLE 6.3.4

COMPONENT PRESSURE LOSS COEFFICIENTS  
(TEST TRAIN IN TUNNEL 2)

TEST DATA 9/12 (pm)

RUN NO	$K_{32}$	$K_{21}$	$K_{12}$	$K_{23}$
34066	1.4 (0.6)	1.8 (2.3)	1.1 (2.0)	1.7 (0.9)
34062	-	-	0.9 (1.9)	1.5 (0.6)
34070	1.3 (1.1)	2.1 (3.0)	1.0 (2.0)	1.5 (0.6)
Average Value	1.4 (0.9)	2.0 (2.7)	1.0 (2.0)	1.6 (0.7)
				

( ) Total pressure loss coefficient.



FIG. 6.3.1.

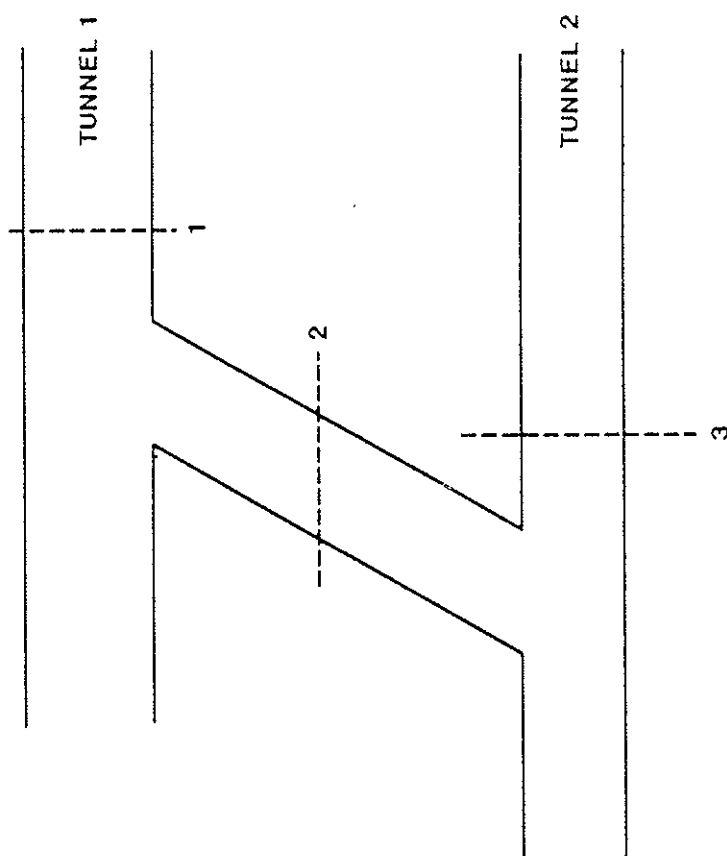


FIG. 6.3.1. STATIONS FOR EVALUATING CROSS PASSAGE PRESSURE LOSS COEFFICIENTS

FIG. 6.3.2.

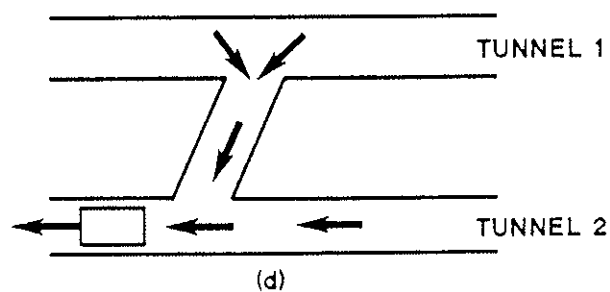
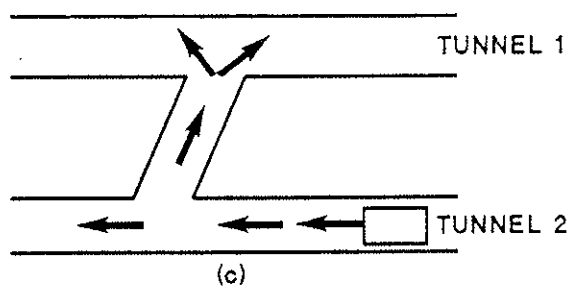
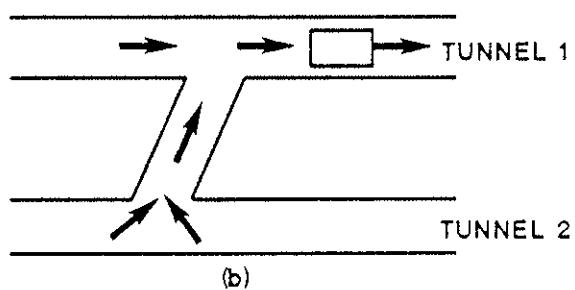
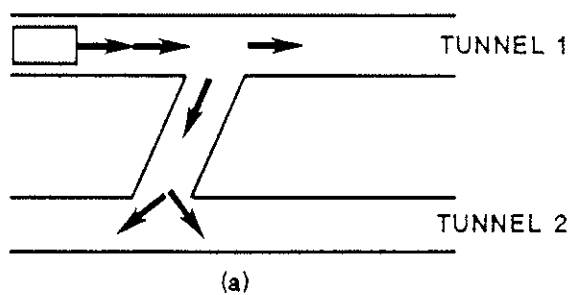


FIG. 6.3.3.

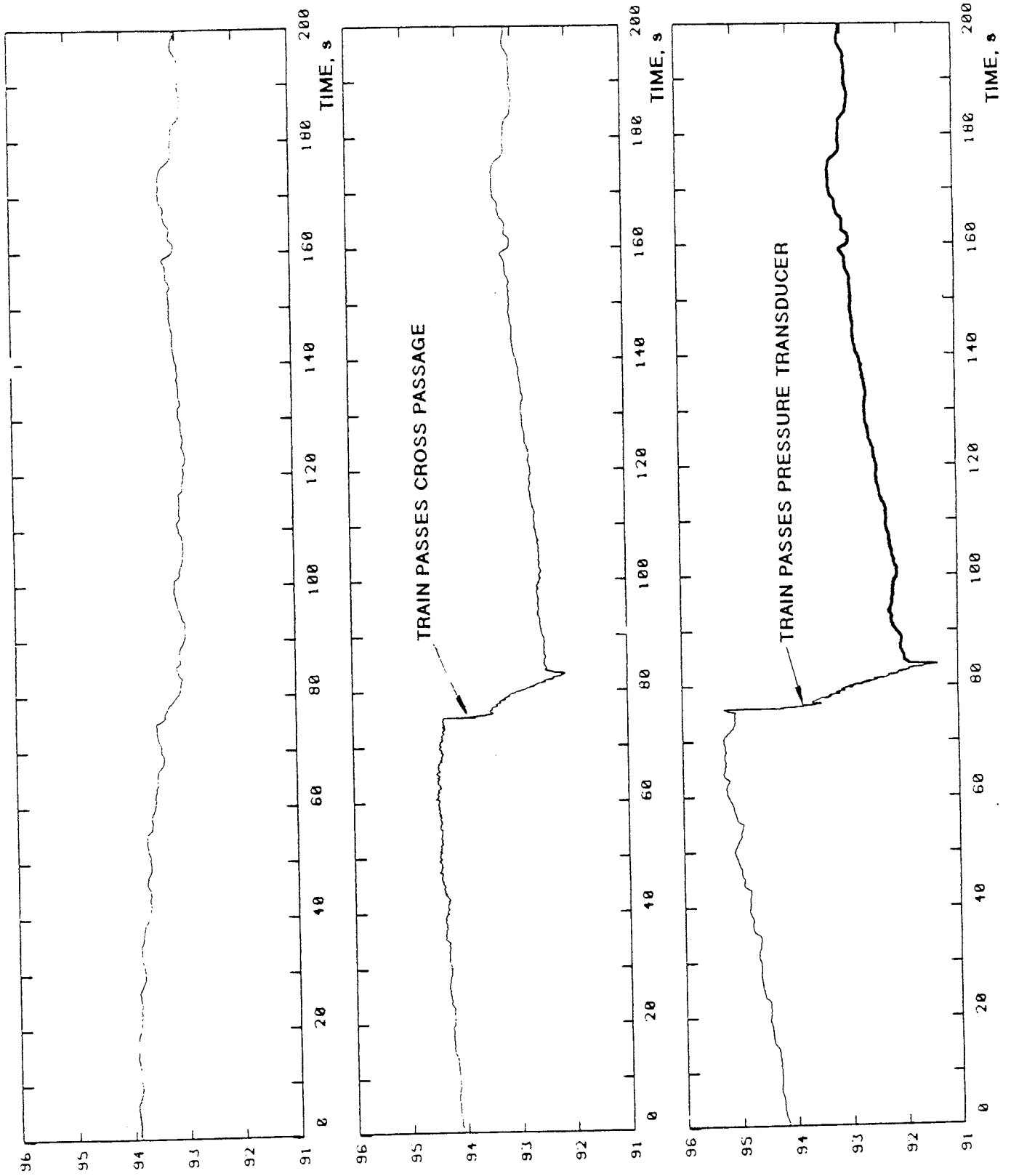


FIG. 6.3.3. BEHAVIOUR OF CHANNELS 13, 14 AND 15

FIG. 6.3.4

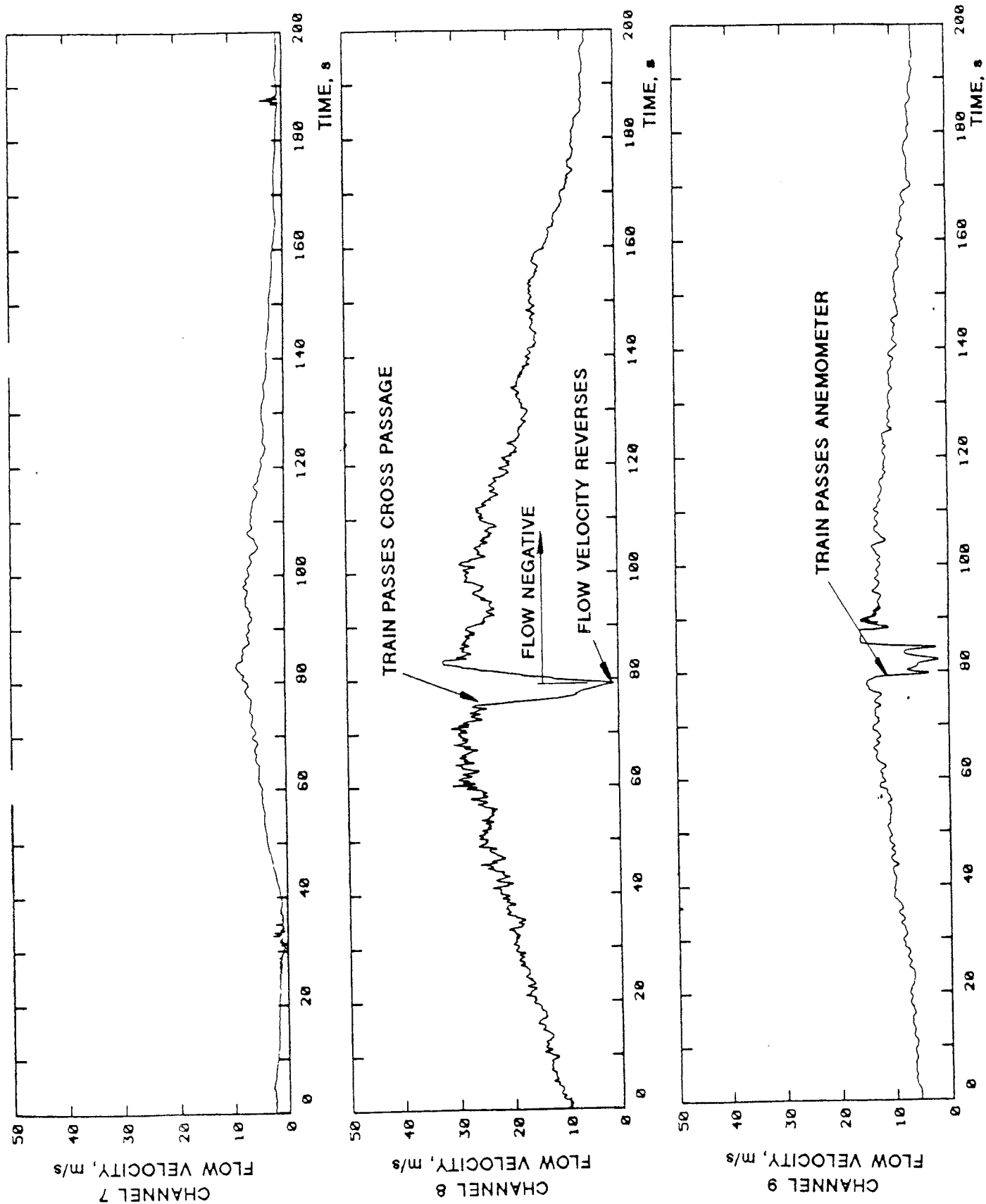


FIG. 6.3.4. BEHAVIOUR OF CHANNELS 7, 8 AND 9

FIG. 6.3.5.

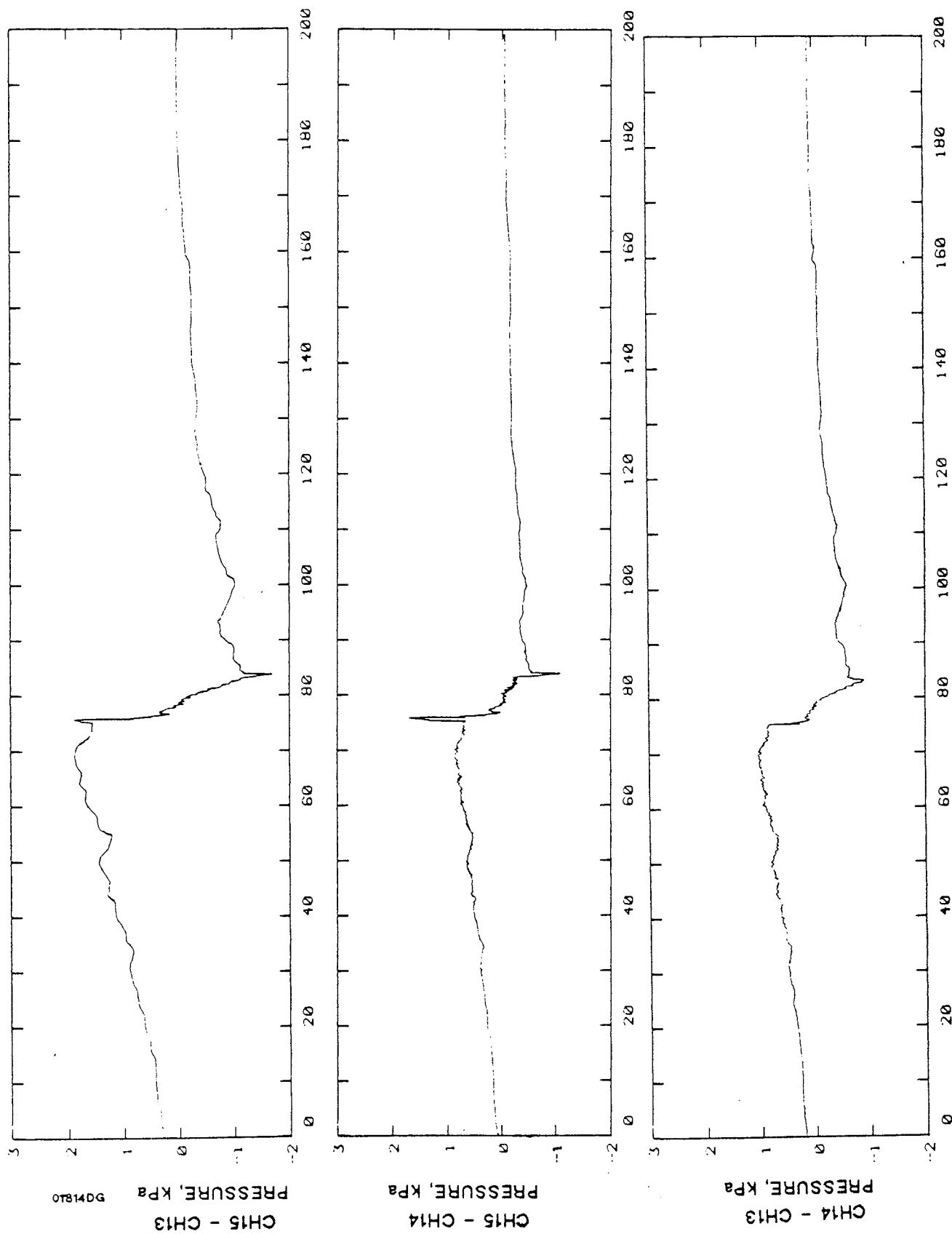


FIG. 6.3.5. DIFFERENCES BETWEEN PRESSURE CHANNELS

FIG. 6.3.6.

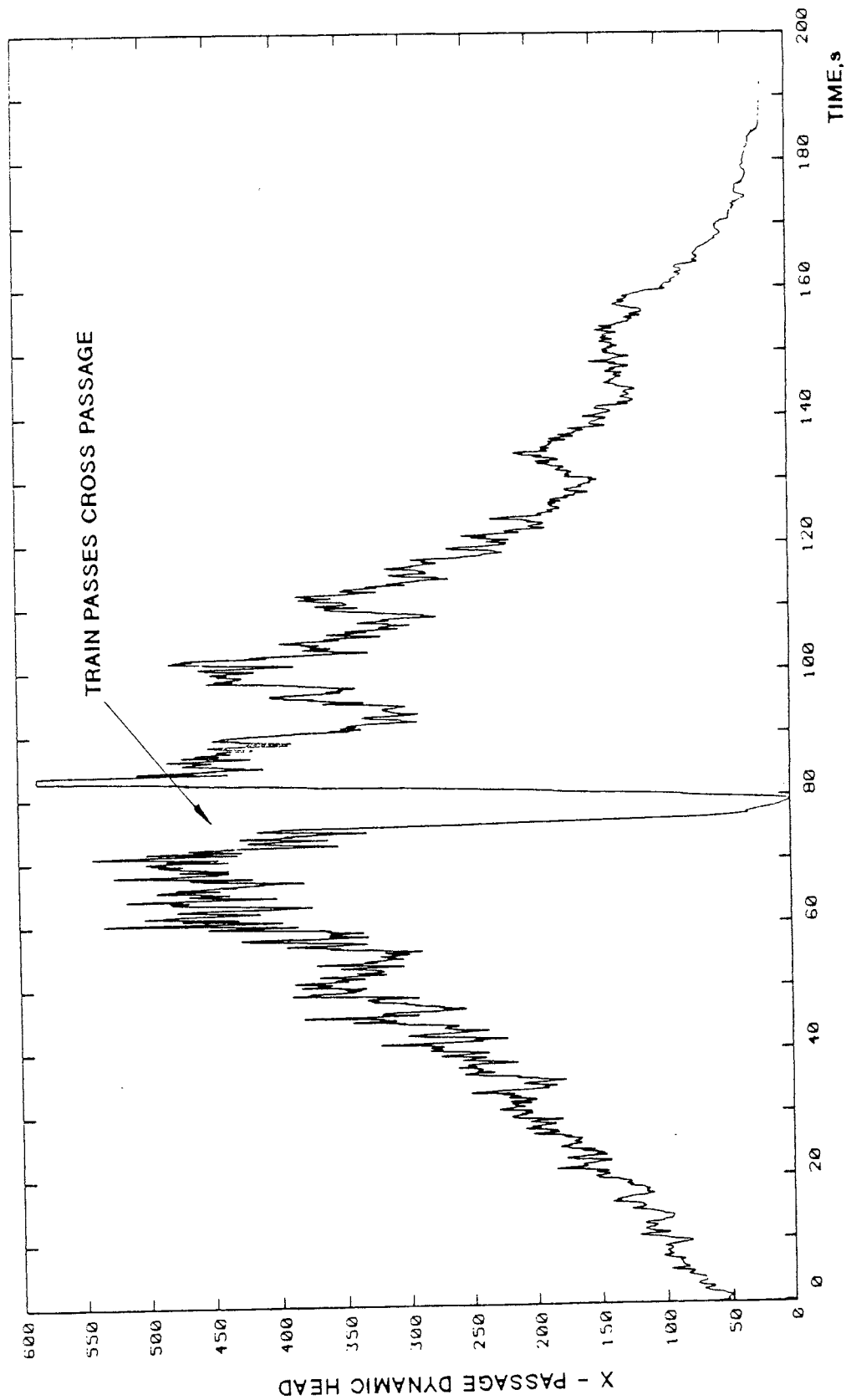


FIG. 6.3.6. DYNAMIC HEAD OF FLOW IN CROSS PASSAGE

FIG. 6.3.7.

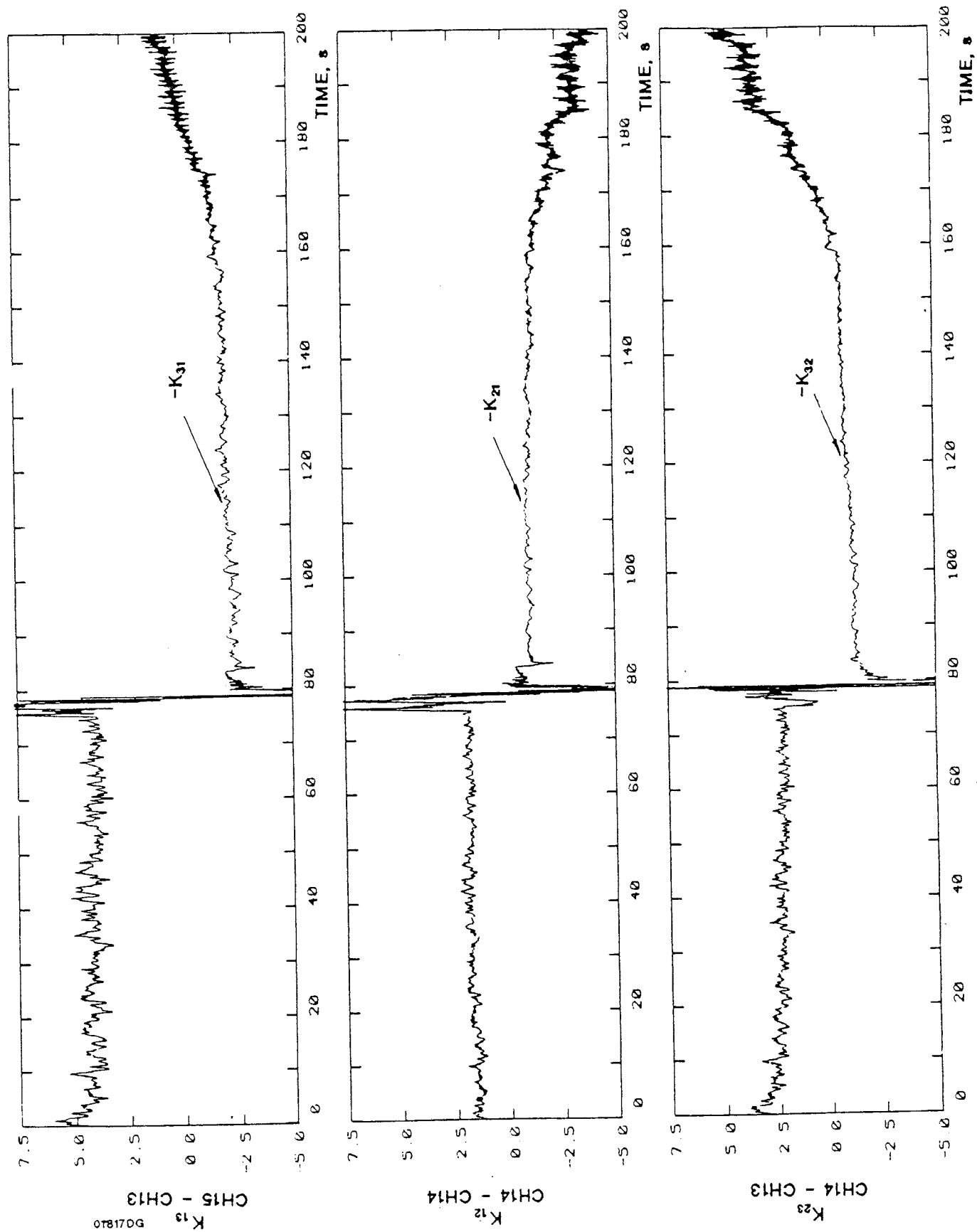
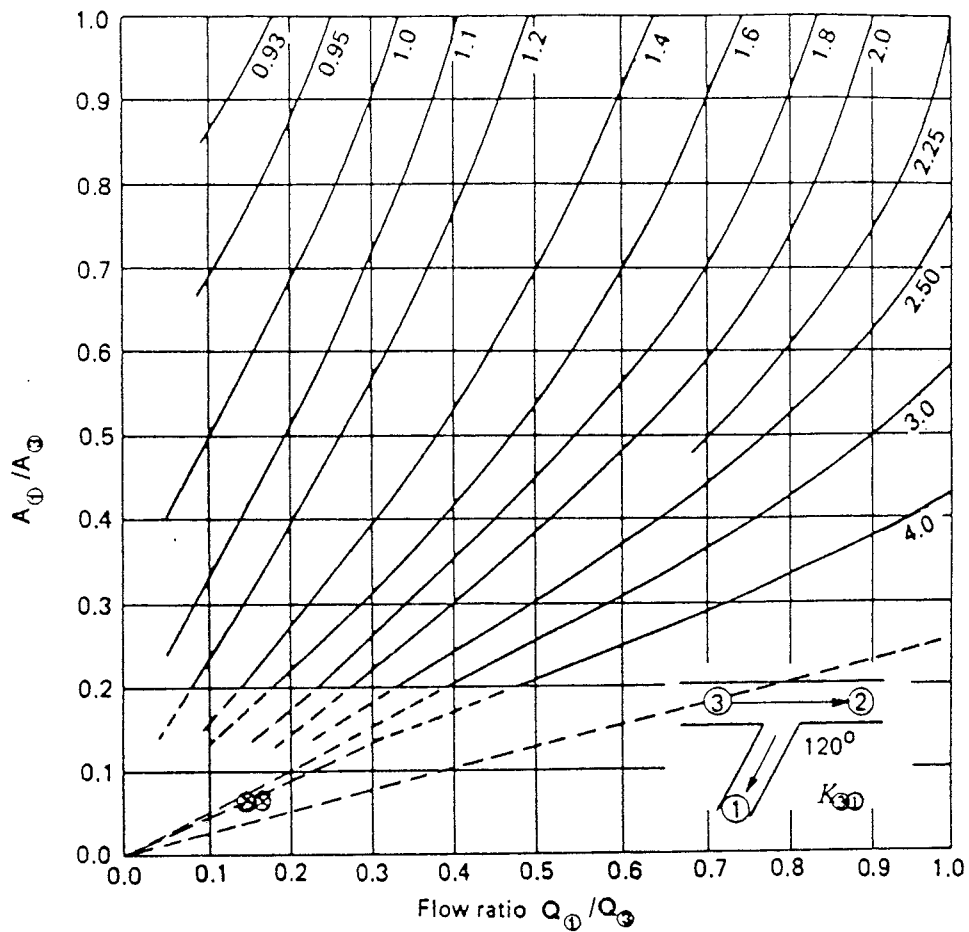


FIG. 6.3.7. EVALUATION OF TOTAL PRESSURE LOSS COEFFICIENTS

FIG. 6.3.8.

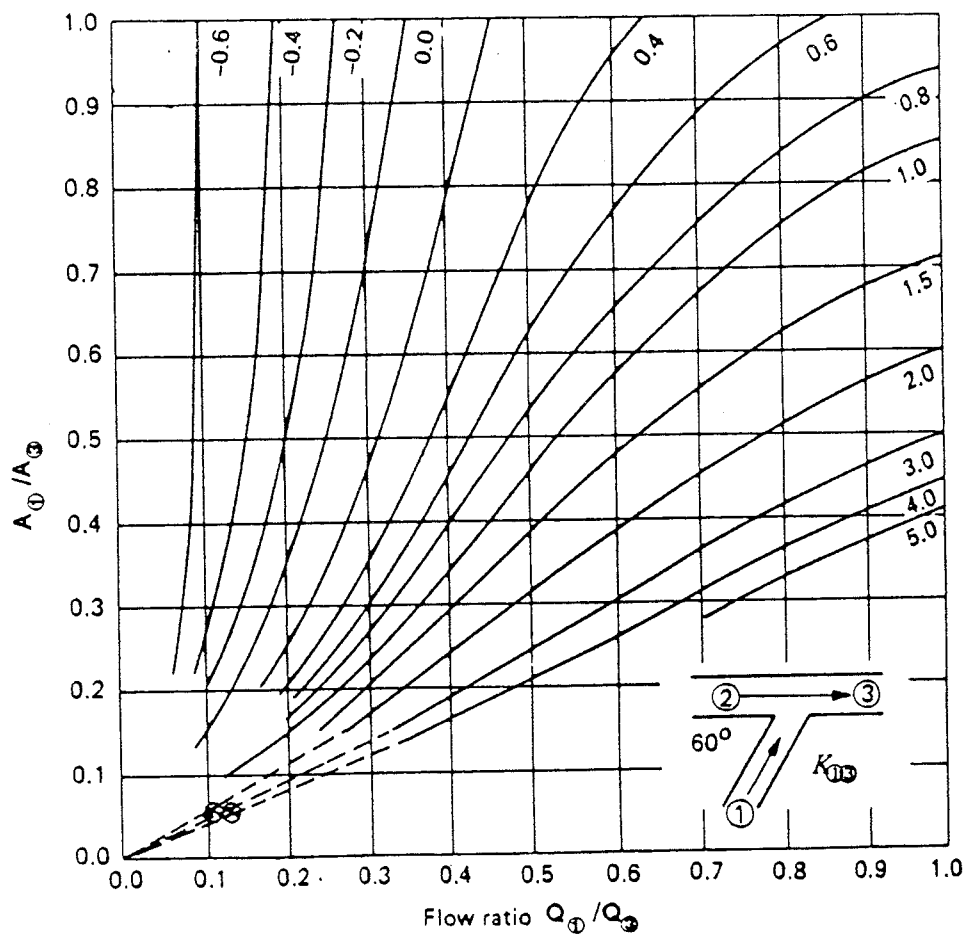


BY  
EXTRAPOLATION:

$$K'_{12} \approx 4.5$$

$$K'_{32} \approx 4.0$$

DIVIDING FLOW - BRANCH ANGLE  $120^\circ$  - LOSS COEFFICIENT  $K_{30}$



BY  
EXTRAPOLATION:

$$K'_{21} = 3.0$$

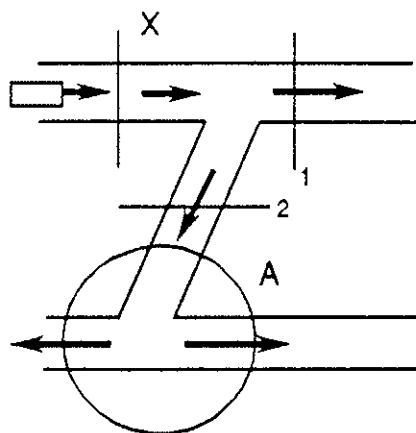
$$K'_{23} = 2.0$$

COMBINING FLOW - BRANCH ANGLE  $60^\circ$  - LOSS COEFFICIENT  $K_{10}$

FIG. 6.3.8. TOTAL PRESSURE LOSS COEFFICIENTS



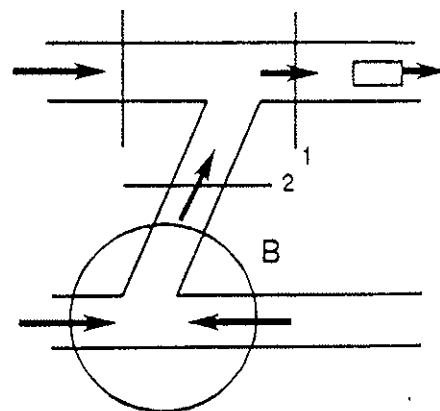
FIG. 6.3.9.



REF. 1  $K'_{12} \cong 4.5$

TEST  $K'_{12} \cong 9.6$

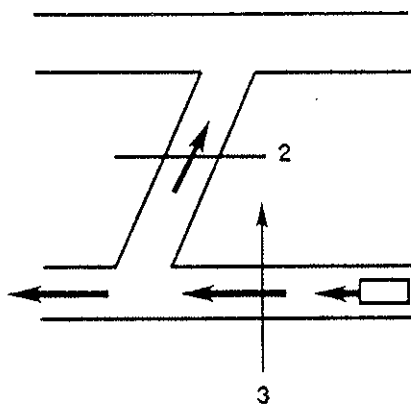
CASE (i)



REF. 1  $K'_{21} \cong 3.0$

TEST  $K'_{21} \cong 2.3$

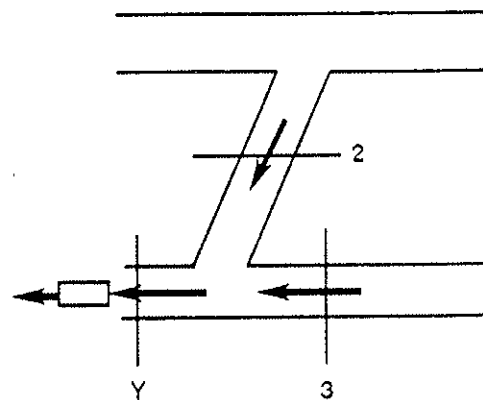
CASE (ii)



REF. 1  $K'_{32} \cong 4.0$

TEST  $K'_{32} \cong 4.2$

CASE (iii)



REF. 1  $K'_{23} \cong 2.0$

TEST  $K'_{23} \cong 2.0$

CASE (iv)

FIG. 6.3.9. COMPARISONS WITH EXTRA POLATED LOSS COEFFICIENTS DEDUCED FROM REF.1.

## NOTATION FOR SECTION 6.4

### *Roman Letters*

$H_0$	total pressure ahead of train nose
$H_1$	total pressure at leading end of annulus
$H_2$	total pressure at trailing end of annulus
$H_3$	total pressure behind train tail
$L_N$	pressure loss coefficient for nose
$L_T$	pressure loss coefficient for tail
$p_0$	static pressure ahead of train nose
$p_1$	static pressure at leading end of annulus
$p_2$	static pressure at trailing end of annulus
$p_3$	static pressure behind tail
$\Delta p_N$	$p_0 - p_1$
$\Delta p_T$	$p_3 - p_2$
$U_T$	flow velocity in open tunnel relative to tunnel
$U_0$	flow velocity in open tunnel relative to train
$U_1$	flow velocity in annulus relative to train
$V$	train velocity
$X_{L_N}$	tolerance on nose pressure loss coefficient
$X_{L_T}$	tolerance on tail pressure loss coefficient
$X_{\Delta p_N}$	tolerance on $\Delta p_N$
$X_{\Delta p_T}$	tolerance on $\Delta p_T$
$X_{U_1}$	tolerance on $U_1$

*Greek Letters*

$\rho$  air density

$\phi$  area ratio  $\left( 1 - \frac{\text{train c/s area}}{\text{tunnel c/s area}} \right)$

## 6.4 Loss Coefficients for Train Ends

### 6.4.1 Principle of analysis

The loss coefficients for the train ends comprise the nose pressure loss coefficient and the tail pressure loss coefficient. They may be determined from the pressure excursions generated by the passage of the train past a stationary point in the tunnel using a similar method to that for obtaining the train friction factor. A typical excursion is shown in Fig 6.4.1. The nose pressure loss coefficient may be derived from the fall in static pressure due to the nose  $\Delta p_N$  and the tail pressure loss coefficient may be established from the rise in pressure due to the tail  $\Delta p_T$ . The loss coefficients are based on the dynamic head of the flow in the annulus relative to the train so a knowledge of the flow velocity along the tunnel is required. This may be obtained from one of the flow metering points in the tunnel, typically Channel 9 in Tunnel 1 and Channel 7 in Tunnel 2.

Referring to Fig 6.4.2, the nose pressure loss coefficient is defined as

$$L_N = \frac{H_0 - H_1}{\frac{1}{2} \rho U_1^2} \quad \text{eq.1}$$

$$\text{Now } H_0 = p_0 + \frac{1}{2} \rho U_0^2$$

$$\text{and } H_1 = p_1 + \frac{1}{2} \rho U_1^2$$

$$\text{Thus } L_N = \frac{p_0 - p_1}{\frac{1}{2} \rho U_1^2} + \left( \frac{U_0}{U_1} \right)^2 - 1$$

But from continuity  $U_0 = U_1 \phi$ , hence

$$L_N = \frac{p_0 - p_1}{\frac{1}{2} \rho U_1^2} + (\phi^2 - 1)$$

Now  $\Delta p_N = p_0 - p_1$ , thus

$$L_N = \frac{\Delta p_N}{\frac{1}{2} \rho U_1^2} + (\phi^2 - 1) \quad \text{eq.2}$$

$U_1$  is the flow velocity in the annulus relative to the train. In terms of the velocity in the open tunnel  $U_1$  is given by

$$U_1 = \frac{V - U_T}{\phi} \quad \text{eq.3}$$

Referring to Fig 6.4.3, the tail pressure loss coefficient is defined as

$$L_T = \frac{H_2 - H_3}{\frac{1}{2} \rho U_1^2} \quad \text{eq.4}$$

$$\text{Now } H_2 = p_2 + \frac{1}{2} \rho U_1^2$$

$$\text{and } H_3 = p_3 + \frac{1}{2} \rho U_0^2$$

$$\text{Thus } L_T = \frac{p_2 - p_3}{\frac{1}{2} \rho U_1^2} + 1 - \left( \frac{U_0}{U_1} \right)^2$$

From continuity  $U_0 = U_1 \phi$  thus

$$L_T = \frac{-\Delta p_T}{\frac{1}{2} \rho U_1^2} + (1 - \phi^2) \quad \text{eq.5}$$

$U_1$  is obtainable from equation 3.

Equations 2 and 5 are the working relationships for determining  $L_N$  and  $L_T$  respectively. Like the train friction factor, the accuracy of  $L_N$  and  $L_T$  is heavily

dependent on the precision of the flow velocity and pressure measurements. This will now be illustrated using the error analysis employed in Section 6.2.2.1.

(a) Reliability of  $L_N$

From equation 5 Section 6.2.2.1, it can be shown that the tolerance on  $L_N$  is given by :

$$X_{L_N} = \pm \left\{ \frac{2 \Delta p_N}{\rho U_1^2} \frac{L_N}{L_N} \right\} \left( 4 X_{U_1}^2 + X_{\Delta p_N}^2 \right)^{\frac{1}{2}} \quad \text{eq.6}$$

Consider now a demonstration error estimation involving Run 34057 of 8 December using the pressure channel, Ch 17 and the flow velocity channel, Ch 9. For this run :

$$V = 42.9 \text{ m/s}$$

$$U_T = 13.2 \text{ m/s (from Ch 9)}$$

$$\Delta p_N = 1180 \text{ N/m}^2 \text{ (from Ch 17)}$$

Now  $\phi = 0.569$ , hence

$$U_1 = \frac{42.9 - 13.2}{0.569} = 52.2 \text{ m/s}$$

From equation 2,

$$L_N = \frac{2 \times 1180}{1.15 \times (52.2)^2} + (0.569)^2 - 1 = 0.0768$$

From equation 6,

$$\begin{aligned} X_{L_N} &= \pm \frac{0.753}{0.0768} \left( 4 X_{U_1}^2 + X_{\Delta p_N}^2 \right)^{\frac{1}{2}} \\ &= \pm 9.81 \left( 4 X_{U_1}^2 + X_{\Delta p_N}^2 \right)^{\frac{1}{2}} \end{aligned}$$

Realistic tolerances are

$$X_{U_1} = \pm 5\%, \Delta p_N = \pm 5\%$$

Thus

$$X_{L_N} = \pm 110\%$$

(b) *Reliability of  $L_T$*

From equation 5, Section 6.2.2.1 it can be shown that the tolerance on  $L_T$  is

$$X_{L_T} = \pm \left\{ \frac{\frac{2 \Delta p_T}{\rho U_1^2}}{\frac{L_T}{L_T}} \right\} \left( 4 X_{U_1}^2 + X_{\Delta p_N}^2 \right)^{\frac{1}{2}} \quad \text{eq.7}$$

As before, consider now an error estimation involving Run 34057 of 8 December using Ch 17 and Ch 9. For this run :

$U_1 = 52.2$  m/s (obtained from Ch 9 using continuity)

$\Delta p_T = -800$  N/m<sup>2</sup> (from Ch 17)

From equation 5,

$$L_T = - \frac{2 \times 800}{1.15 \times (52.2)^2} + 1 - (0.569)^2 = 0.165$$

From equation 7,

$$\begin{aligned} X_{L_T} &= \pm \frac{0.511}{0.165} \left( 4 X_{U_1}^2 + X_{\Delta p_T}^2 \right)^{\frac{1}{2}} \\ &= \pm 3.10 \left( 4 X_{U_1}^2 + X_{\Delta p_T}^2 \right)^{\frac{1}{2}} \end{aligned}$$

Realistic tolerances are

$$X_{U_1} = \pm 5\%, X_{\Delta p_T} = \pm 5\%$$

$$\text{Thus } X_{L_T} = \pm 34.7\%$$

It follows, therefore, that  $L_N$  and  $L_T$  are extremely sensitive to small errors in the determination of  $U_1$  and the pressure difference upon which the coefficient is based. The sensitivity of  $L_N$  to errors in  $U_1$  and  $\Delta p_N$  is particularly marked.

In view of this, it is important that average values of  $L_N$  and  $L_T$  are determined from a large number of samples. Average values of  $L_N$  and  $L_T$  have been obtained from the pressure excursions used for the train friction factor analysis described in Section 6.2.2. Each coefficient has been formed from the average of 78 results. In Tunnel 1 derivations have been obtained from Channels 15, 16 and 17 with Channel 9 supplying the flow velocity. In Tunnel 2 the derivations have been carried out using pressure data from Channel 13 and flow velocity data from Channel 7.

#### 6.4.2 Results

The results of the pressure loss coefficient analysis are shown in Tables 6.4.1 and 6.4.2. Table 6.4.1 shows the nose pressure loss coefficients and Table 6.4.2 the tail pressure loss coefficient. Histograms showing the distributions of the values of  $L_N$  and  $L_T$  are given in Figs 6.4.4 and 6.4.5 respectively.

The statistics are as follows :

- (a) Nose pressure loss coefficient,  $L_N$

average value = 0.10

mean standard deviation = 0.0604  
(60.5% of mean)

95% confidence interval of the average value =  $\pm 13.6\%$

- (b) Tail pressure loss coefficient,  $L_T$

average value = 0.203

mean standard deviation = 0.0659  
(32.5% of mean)

95% confidence interval of the average value =  $\pm 7.3\%$



### 6.4.3 Comments

The nose pressure loss coefficient for a HST in a tunnel of similar blockage ratio has been found to be 0.185<sup>1</sup>. This is somewhat larger than the value deduced for the nose of the test train. The smaller value for the test train is a little surprising since the nose is much more angular. The test train locomotives however, possess snow ploughs just beneath their buffer beams. It is possible that these could result in an overall improvement in the flow over the locomotive.

One would expect the tail pressure loss coefficient to be close to the Borda Carnot loss for an abrupt enlargement in a pipe. This is equal to the blockage ratio squared and for the test train running in the Simplon Tunnel would assume a value of around 0.17. The value obtained from the tests is slightly larger but of the expected order of magnitude.

### 6.4.4 Reference

1. Pope C W, Gawthorpe R G, and Richards S P, "An Experimental Investigation into the Effect of Train Shape on the Unsteady Flows Generated in Tunnels." 4th ISAVVT, Paper C2, University of York, BHRA Fluid Engineering, Cranfield, March 88.

TABLE 6.4.1

## TABULATION OF TRAIN NOSE PRESSURE LOSS COEFFICIENTS

DATE	RUN NO	TUNNEL	TRAIN LENGTH m	TRAIN VELOCITY m/s	NOSE PRESSURE LOSS COEFFICIENTS			
					Ch 13	Ch 15	Ch 16	Ch 17
3.12.87	34011	1	347.1	45.1		0.141	0.096	0.043
3.12.87	34015	1	347.1	45.0		0.134	0.134	0.103
3.12.87	34016	2	347.1	44.8	0.070			
3.12.87	34019	1	347.1	45.2		0.163	0.163	0.041
3.12.87	34020	2	347.1	44.9	0.080			
3.12.87	34023	1	347.1	45.0		0.124	0.172	0.093
3.12.87	34024	2	347.1	44.6	0.063			
3.12.87	34027	1	347.1	44.4		0.144	0.246	0.139
3.12.87	34028	2	347.1	44.4	0.128			
3.12.87	34057	1	241.5	45.6		0.152	0.152	0.095
3.12.87	34058	2	241.5	44.4	0.089			
3.12.87	34062	2	241.5	45.4	0.098			
3.12.87	34065	1	241.5	44.7		0.179	0.197	0.094
3.12.87	34066	2	241.5	44.5	0.089			
3.12.87	34069	1	241.5	44.7		0.105	0.105	0.196
7.12.87	34057	1	452.7	43.6		0.124	0.124	0.027
7.12.87	34058	2	452.7	44.7	0.071			
7.12.87	34061	1	452.7	42.9		0.151	0.125	0.081
7.12.87	34062	2	452.7	44.7	0.065			
7.12.87	34065	1	452.7	44.0		0.151	0.119	0.067
7.12.87	34066	2	452.7	44.7	0.084			
7.12.87	34069	1	452.7	44.7		0.130	-0.016	-0.085
7.12.87	34070	2	452.7	44.7	0.070			
8.12.87	34011	1	452.7	43.3		0.143	0.156	0.045
8.12.87	34015	1	452.7	44.7		0.102	0.120	0.024
8.12.87	34019	1	452.7	44.0		0.154	0.147	0.068
8.12.87	34020	2	452.7	41.5	0.016			
8.12.87	34023	1	452.7	41.0		0.136	0.152	0.143
8.12.87	34024	2	452.7	43.3	0.106			
8.12.87	34027	1	452.7	41.1		0.092	0.085	0.031
8.12.87	34028	2	452.7	44.7	0.116			
8.12.87	34057	1	452.7	42.9		0.192	0.192	0.077
8.12.87	34058	2	452.7	44.7	-0.060			
8.12.87	34061	1	452.7	44.7		0.010	-0.022	-0.049
8.12.87	34062	2	452.7	44.7	0.081			
8.12.87	34066	2	452.7	43.8	0.106			
8.12.87	34069	1	452.7	42.0		0.112	0.090	0.035
8.12.87	34070	2	452.7	44.7	0.081			

For conditions of train movement see Table 6.2.2.1.

TABLE 6.4.2

## TABULATION OF TRAIN TAIL PRESSURE LOSS COEFFICIENTS

DATE	RUN NO	TUNNEL	TRAIN LENGTH m	TRAIN VELOCITY m/s	TAIL PRESSURE LOSS COEFFICIENT			
					Ch 13	Ch 15	Ch 16	Ch 17
3.12.87	34011	1	347.1	45.1		0.196	0.309	0.179
3.12.87	34015	1	347.1	45.0		0.110	0.110	0.275
3.12.87	34016	2	347.1	44.8	0.195			
3.12.87	34019	1	347.1	45.2		0.170	0.229	0.251
3.12.87	34020	2	347.1	44.9	0.299			
3.12.87	34023	1	347.1	45.0		0.179	0.165	0.184
3.12.87	34024	2	347.1	44.6	0.258			
3.12.87	34027	1	347.1	44.4		0.187	0.126	0.271
3.12.87	34028	2	347.1	44.4	0.263			
3.12.87	34057	1	241.5	45.6		0.157	0.183	0.207
3.12.87	34058	2	241.5	44.4	0.150			
3.12.87	34062	2	241.5	45.4	0.144			
3.12.87	34065	1	241.5	44.7		0.230	0.179	0.208
3.12.87	34066	2	241.5	44.5	0.176			
3.12.87	34069	1	241.5	44.7		0.308	0.281	0.083
7.12.87	34057	1	452.7	43.6		0.172	0.202	0.298
7.12.87	34058	2	452.7	44.7	0.240			
7.12.87	34061	1	452.7	42.9		0.092	0.098	0.211
7.12.87	34062	2	452.7	44.7	0.165			
7.12.87	34065	1	452.7	44.0		0.168	0.200	0.339
7.12.87	34066	2	452.7	44.7	0.228			
7.12.87	34069	1	452.7	44.7		0.234	0.269	0.354
7.12.87	34070	2	452.7	44.7	0.225			
8.12.87	34011	1	452.7	43.3		0.108	0.086	0.217
8.12.87	34015	1	452.7	44.7		0.155	0.211	0.312
8.12.87	34019	1	452.7	44.0		0.200	0.186	0.256
8.12.87	34020	2	452.7	41.5	0.239			
8.12.87	34023	1	452.7	41.0		0.141	0.076	0.304
8.12.87	34024	2	452.7	43.3	0.179			
8.12.87	34027	1	452.7	41.1		0.189	0.210	0.291
8.12.87	34028	2	452.7	44.7	0.149			
8.12.87	34057	1	452.7	42.9		0.073	0.157	0.166
8.12.87	34058	2	452.7	44.7	0.259			
8.12.87	34061	1	452.7	44.7		0.278	0.229	0.284
8.12.87	34062	2	452.7	44.7	0.130			
8.12.87	34066	2	452.7	43.8	0.145			
8.12.87	34069	1	452.7	42.0		0.150	0.186	0.191
8.12.87	34070	2	452.7	44.7	0.290			

For conditions of train movement see Table 6.2.2.1.

FIG. 6.4.1.

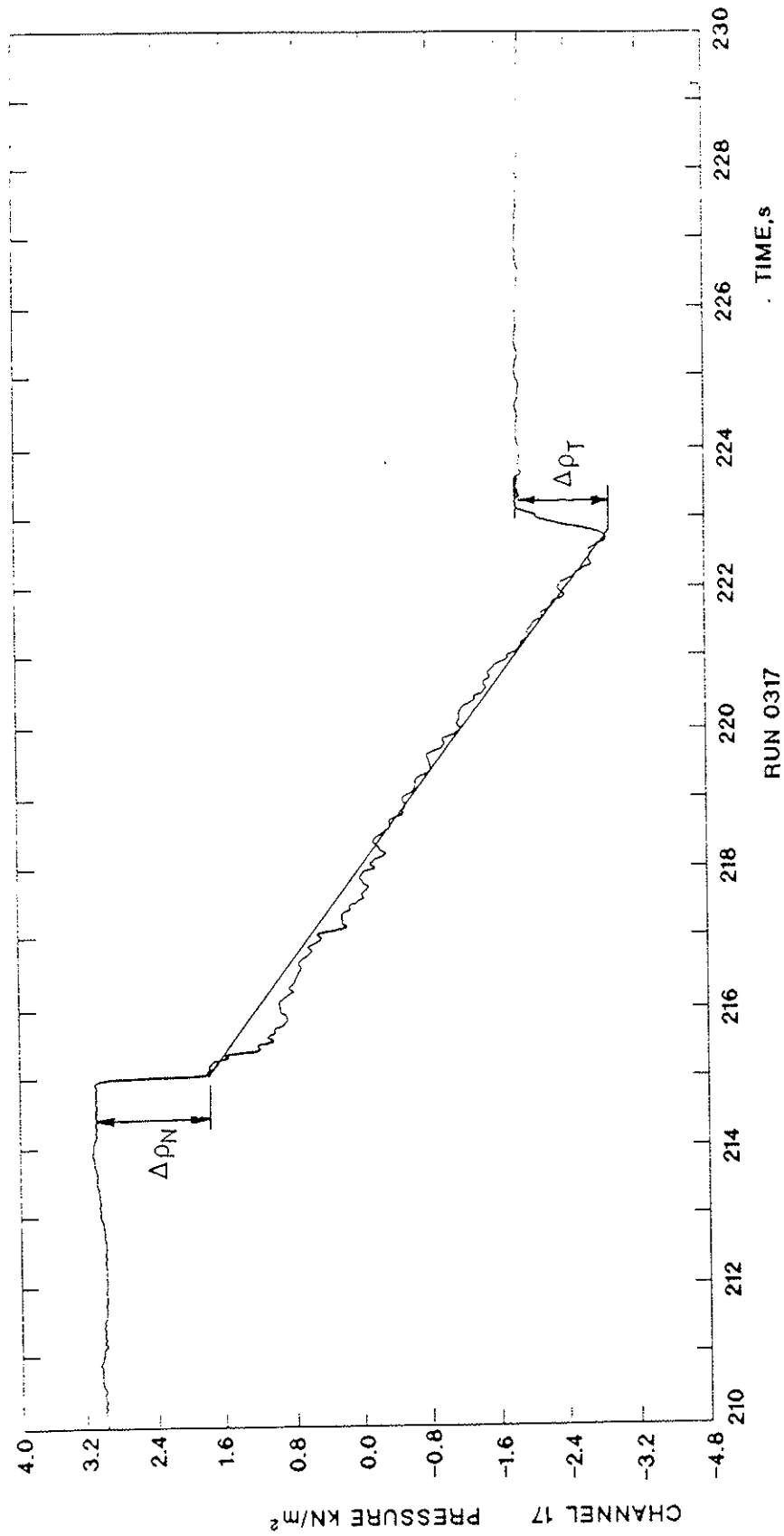


FIG. 6.4.1. PRESSURE CHANGES GENERATED BY THE NOSE AND TAIL

FIG. 6.4.2, &amp; 6.4.3.

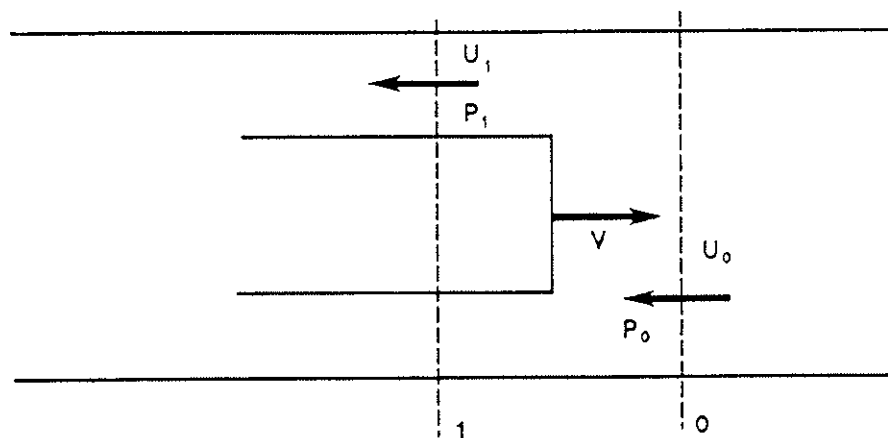
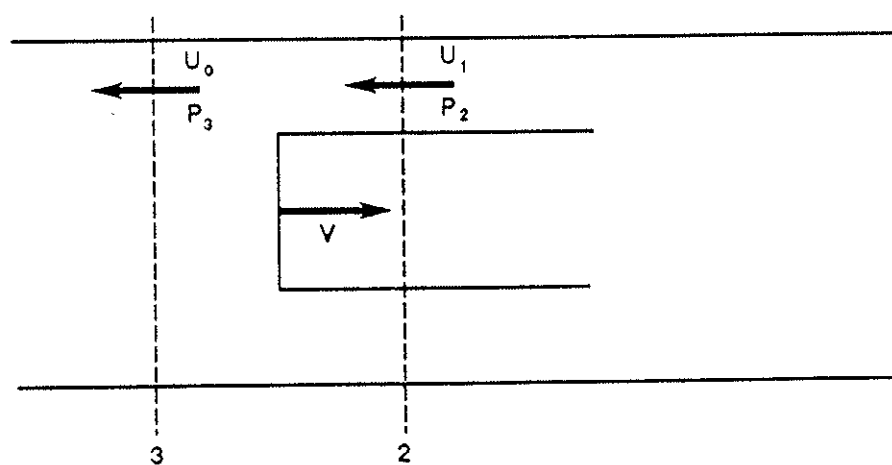
FIG. 6.4.2. FLOW OVER NOSE  
(RELATIVE TO TRAIN)FIG. 6.4.3. FLOW OVER TAIL  
(RELATIVE TO TRAIN)

FIG. 6.4.4.

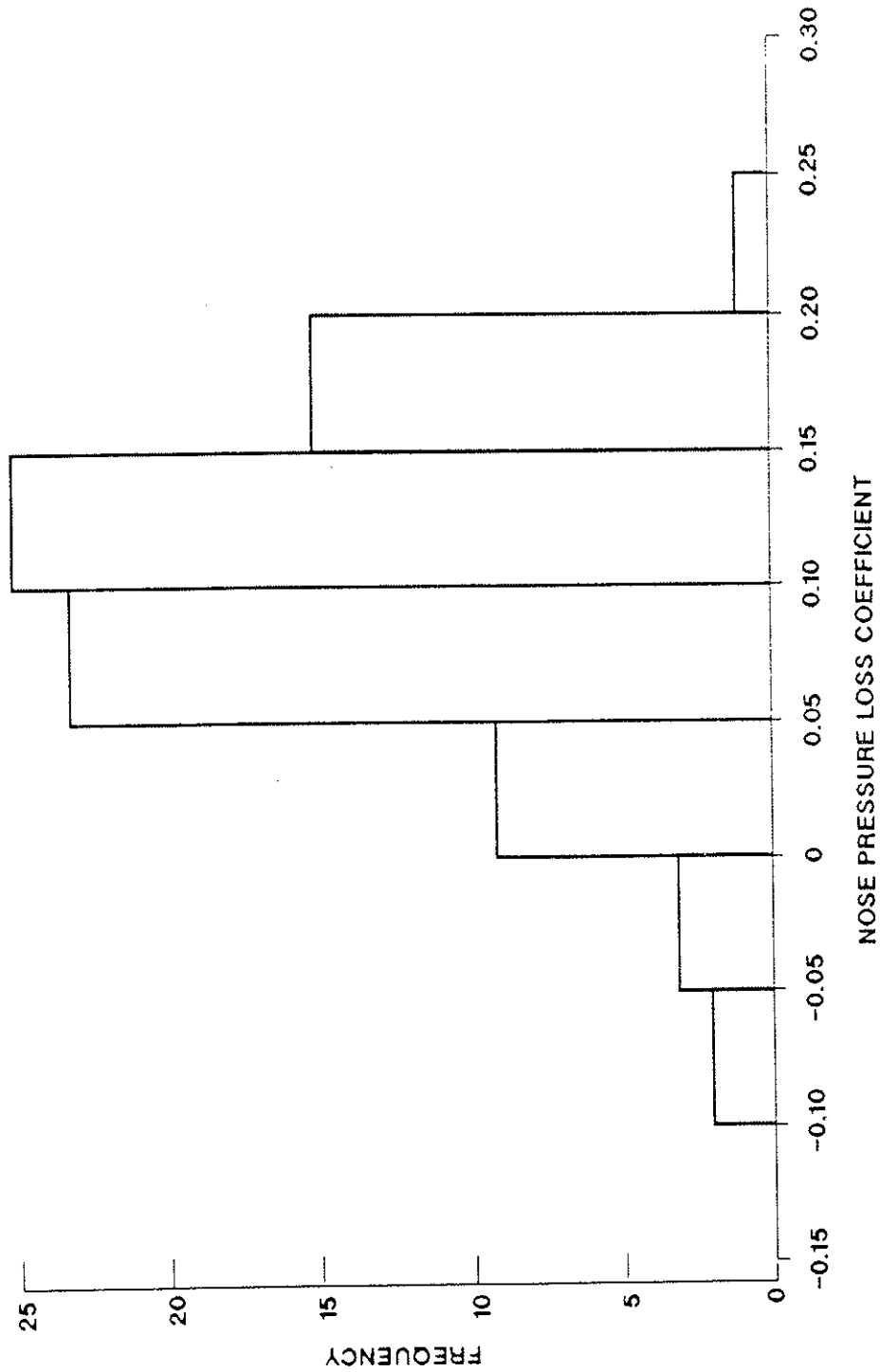


FIG. 6.4.4. DISTRIBUTION OF TRAIN NOSE PRESSURE LOSS COEFFICIENT MEASUREMENTS

FIG. 6.4.5.

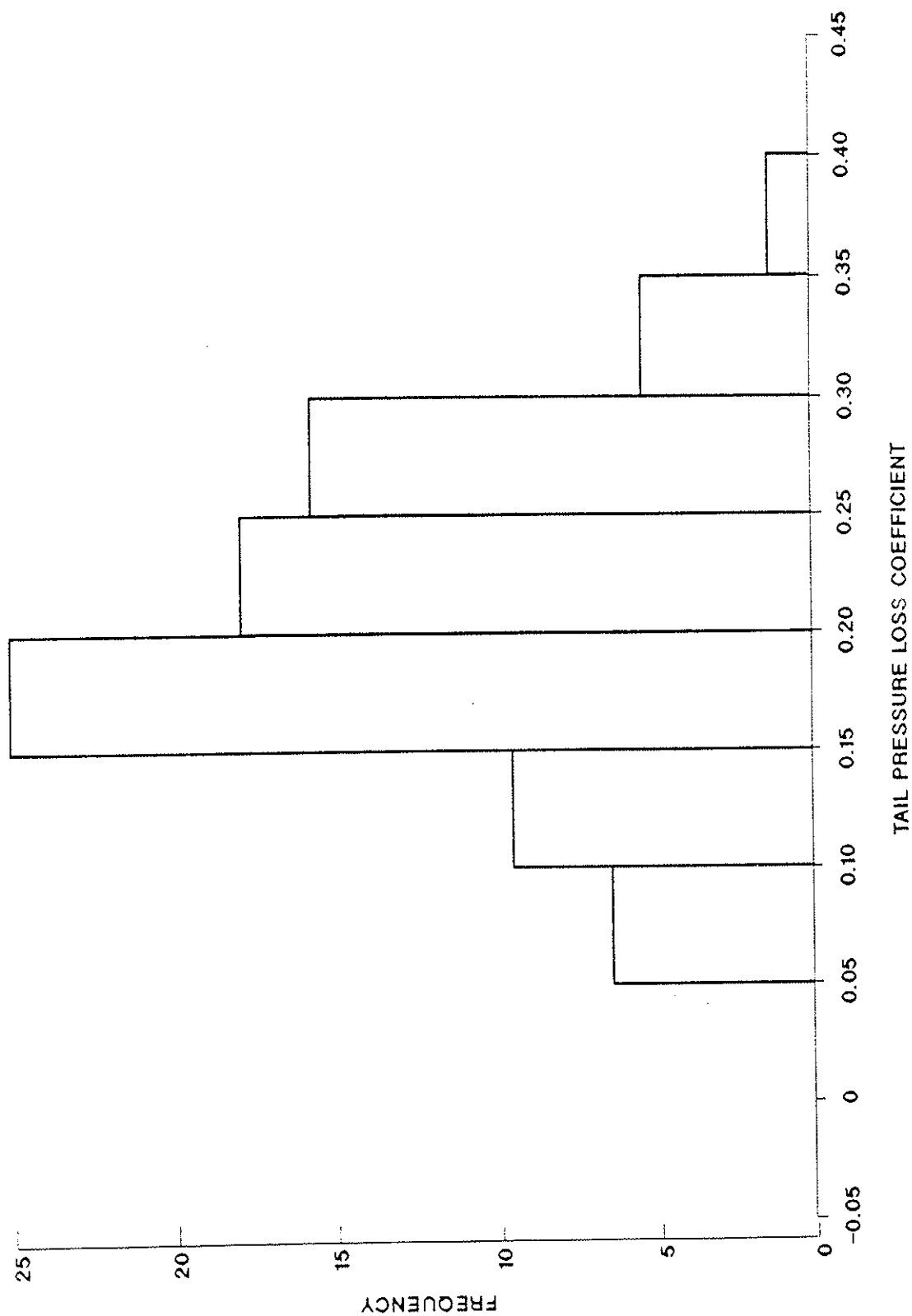


FIG. 6.4.5. DISTRIBUTION OF TRAIN TAIL PRESSURE LOSS COEFFICIENT

## 6.5 LEAKAGE BETWEEN TUNNELS WITH DOORS CLOSED

### 6.5.1 Flow measurements

An assessment was made of the leakage through the cross passages with the isolating doors closed. This was carried out using the vane anemometers mounted in the running tunnels close to cross passage 30 (Channels 7 and 9) and in the cross passage itself. (Channel 8) see Fig 5.1.1.1. Consideration was given to the leakage effect caused by train movements both in Tunnel 1 and in Tunnel 2.

The leakage effects produced by train transits in Tunnel 1 from Brig to Iselle and in Tunnel 2 from Iselle to Brig are well illustrated by Run 34011, 3.12.87 and Run 34028, 8.12.87 respectively. Figs 6.5.1 and 6.5.2 show the following excursions measured during the respective runs.

- (a) The flow velocity in Tunnel 2 (Ch 7).
- (b) The flow velocity in the cross passage (Ch 8).
- (c) The flow velocity in Tunnel 1 (Ch 9).
- (d) The static pressure in Tunnel 2 (Ch 13).
- (e) The static pressure in the cross passage (Ch 14).
- (f) The static pressure in Tunnel 1 (Ch 15).

We will begin by considering the movement of the test train through Tunnel 1, Run 34011, 3.12.87, Fig 6.5.1.

Fig 6.5.1, Graph (c) shows that when the train enters, a progressive acceleration of the flow occurs in Tunnel 1 in the direction of train motion. At the measurement point, the velocity reaches a peak of about 13.5 m/s before the train passes cross passage 30 and then falls progressively. Quite a rapid deceleration of the flow subsequently occurs after the train passes the cross-over close to the mid point of the tunnel, Fig 6.5.1.

In parallel with the generation of flow in Tunnel 1, a flow is produced in Tunnel 2 by the effect of leakage through the cross passages, Fig 6.5.1, Graph (a). Qualitatively, the flow behaviour with time is very similar to that in Tunnel 1 but in the opposite direction. At the measurement point, the peak velocity of the flow is about 11 m/s and occurs just after the train passes cross passage 30.



As the train approaches cross passage 30 a leakage flow of approximately 2 m/s is generated through the cross passage, Fig 6.5.1 Graph (b). When the train passes the cross passage, however, the leakage falls and changes direction<sup>+</sup>. During the interval which elapses between the tail passing the cross passage and the train reaching the cross-over, the leakage flow fluctuates between about 0.1 m/s and 1 m/s. Thereafter the leakage flow progressively falls to zero.

Just before the train nose passes cross passage 30, the ratio of the volume flow through the cross passage to the local volume flow through Tunnel 1\* is approximately 1.5%. At this juncture, local to the cross passage, the ratio of the volume flow in Tunnel 2 to the volume flow in Tunnel 1 is 79%. Clearly the cumulative effect of leakage through the cross passages together with the flow at the cross-over is very significant.

Consideration will now be given to the movement of the test train through Tunnel 2, Run 34028, 8.12.87, Fig 6.5.2. Graphs (a) and (c) show that the passage of a train through Tunnel 2 generates a situation which is qualitatively similar to that produced by the transit of a train through Tunnel 1. The displacement effect of the train in Tunnel 2 produces a flow in the direction of train motion. At the same time a flow which is in the opposite direction to the motion of the train in Tunnel 2, is generated in Tunnel 1 by the effect of leakage through the cross passages.

Prior to the train passing cross passage 30, a flow velocity of 14 m/s is produced in Tunnel 2 in the section of tunnel flanking the cross passage. At the same time, the flow velocity in the section of Tunnel 1 alongside cross passage 30 is 9.2 m/s. The resulting ratio of the volume flow in Tunnel 1 to the volume flow in Tunnel 2 is about 66%. This demonstrates that the cumulative effect of leakage from Tunnel 2 to Tunnel 1 is considerable but not as great as from Tunnel 1 to Tunnel 2.

Graph (b) shows that as the train approaches cross passage 30 a leakage flow of about 4 m/s is generated through it from Tunnel 2 to Tunnel 1. When the train passes the cross passage, the flow reverses and a leakage flow of around 2 m/s is established in the opposite direction. This persists until the train leaves the tunnel whence the flow decays to zero.

<sup>+</sup> Direction determined by pressure differentials between tunnels.

\* Note : ratio of cross passage c/s area to tunnel c/s area.

Just before the train nose passes cross passage 30, the ratio of volume flow through the cross passage to the volume flow in Tunnel 2 adjacent to the cross passage is about 2%. This is larger than for the equivalent condition involving a train in Tunnel 1. Nevertheless it indicates that the flow through the cross passage is still a small proportion of the flow in the adjacent running tunnel.

The magnitudes of the leakage flows through cross passage 30 appear to be somewhat variable. The doors are not fitted with a locking arrangement which holds them in a precise position when they are closed. They are simply pushed up against a joint and the degree of sealing depends on how tightly they are closed after use.

For both runs, Figs 6.5.1 and 6.5.2 show that the pressure changes generated by train movements in the running tunnels are transmitted into the cross passage. There are, however, quite significant reductions in the magnitudes. Only very minor changes in pressure are transmitted to the adjacent running tunnel.

#### 6.5.2 Comments

- (a) The cumulative effect of leakage through the cross passages when closed results in the generation of a substantial flow in the second running tunnel. It appears that in the section of tunnel adjacent to the tunnel containing the train, the volume flow generated by leakage can be as high as 80% of the volume flow produced by the displacement effect of the train in the first tunnel.
- (b) On the basis of measurements taken in cross passage 30, the flows through individual cross passages appear to be relatively small. In cross passage 30 the largest volume flow rates were of the order of  $7 \text{ m}^3/\text{s}$ . This contrasts with peak volume flow rates of about  $340 \text{ m}^3/\text{s}$  generated in the running tunnels by train movements.

FIG. 6.5.1.

TRANSMARK

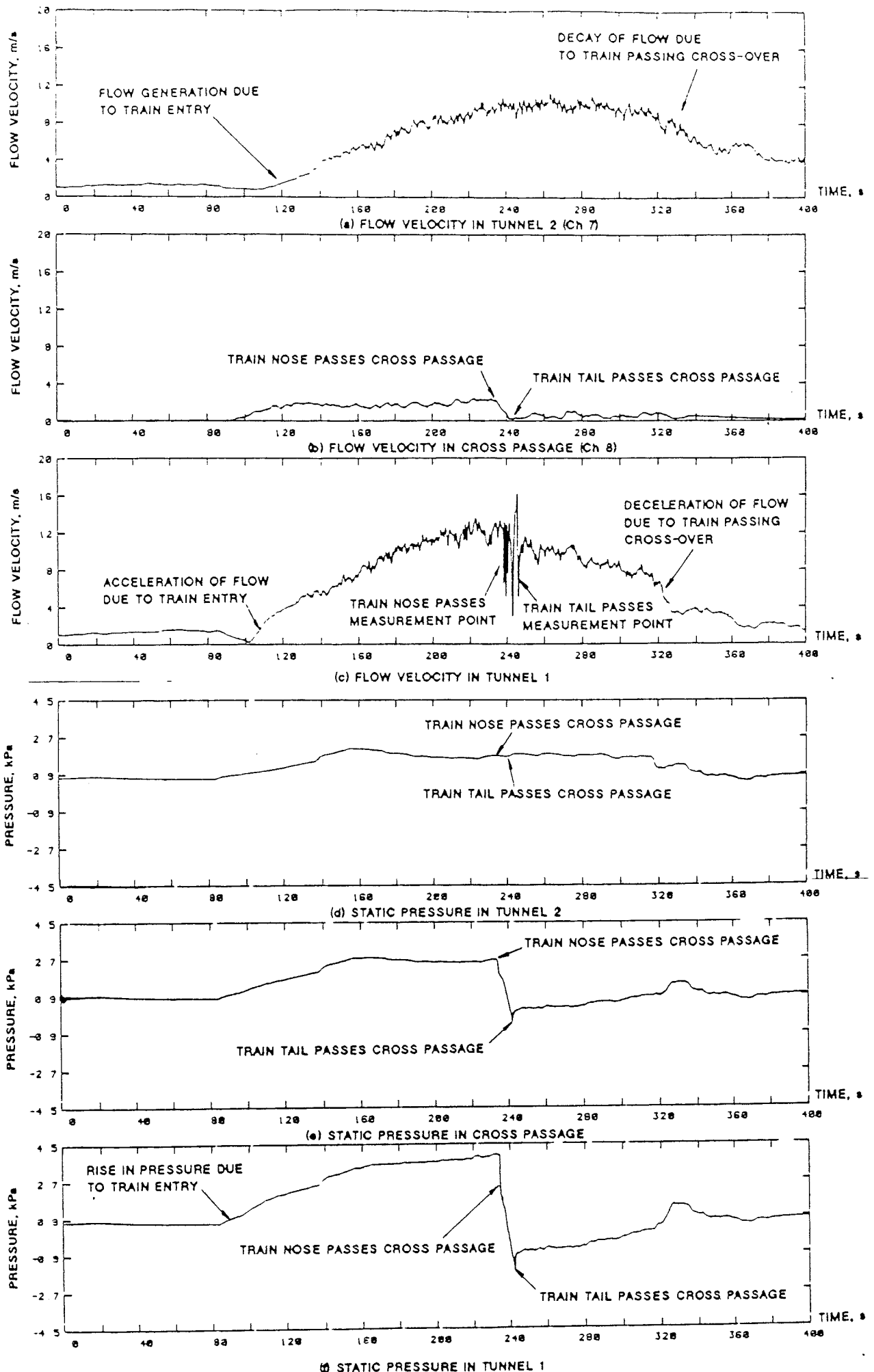


FIG. 6.5.1. TRAIN IN TUNNEL 1 RUN 34011 3/12/87  
FLOW VELOCITIES AND PRESSURES IN AND ADJACENT TO

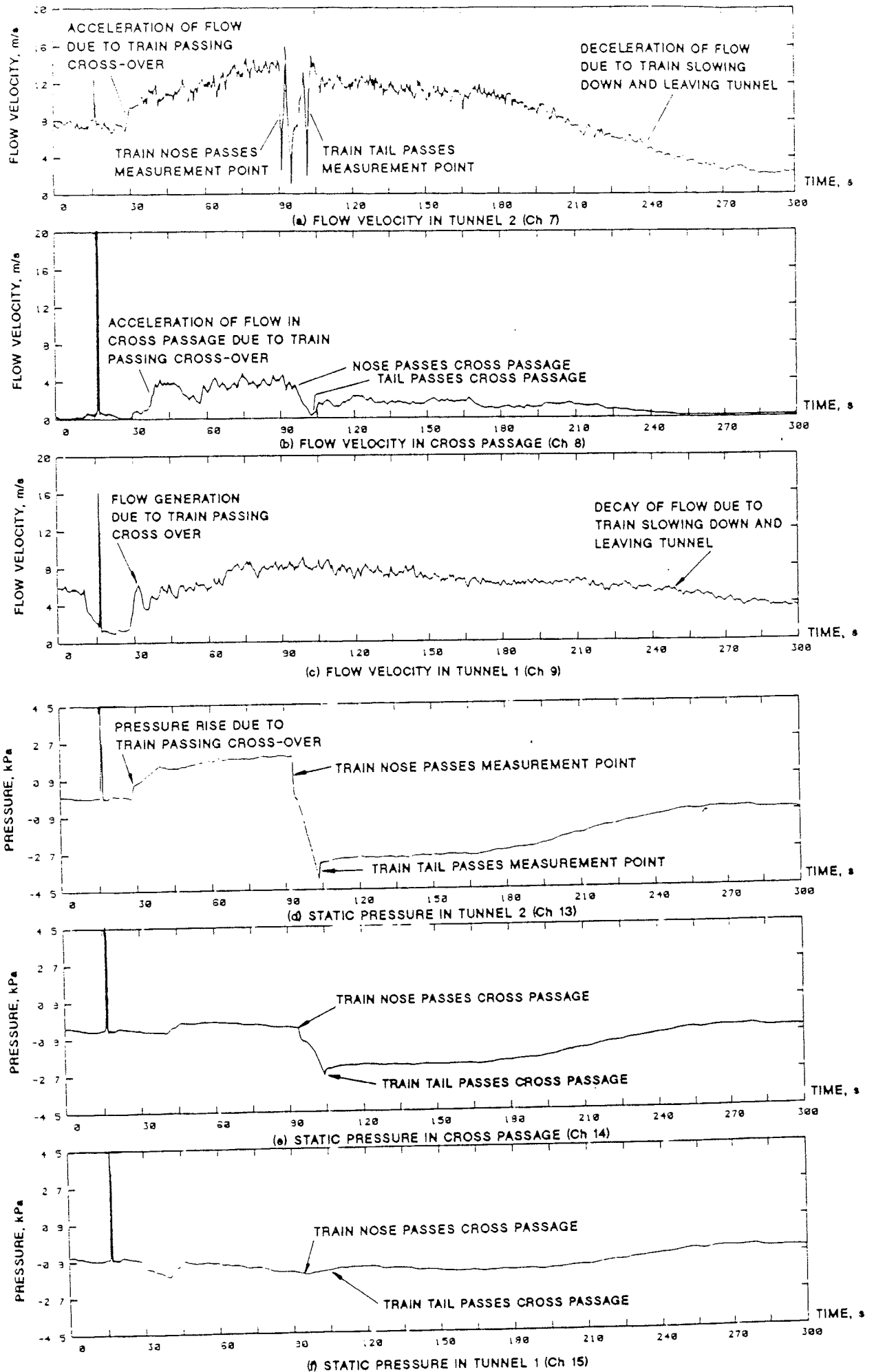


FIG. 6.5.2. TRAIN IN TUNNEL 2 RUN 34028 8/12/87  
FLOW VELOCITIES AND PRESSURES IN AND ADJACENT TO

## 6.8 Piston Duct Lateral Effects

### 6.8.1 Relationship between train position and air velocity

Fig 6.8.1.1 shows the airflow behaviour generated in cross passage 30 by the test train passing through Tunnel 1 in the direction Brig to Iselle. The flow measurements were obtained during run 34065 on 9th December. Fig 6.8.1.1 features the recordings obtained from the two gust anemometers mounted in the cross passage, Channels 3 and 4. The positions of the gust anemometers are shown in Fig 5.1.1.1. Fig 6.8.1.2 shows the recordings obtained from the gust anemometers during the passage of the train past the cross passage on an expanded time scale. Superimposed on the flow velocity excursions shown on Fig 6.8.1.2 are two vertical lines which indicate the times of the nose and tail passing the cross passage. The times were deduced from the infra red sensors placed 10 m to the left and right of the cross passage in Tunnel 1, Channels 20 and 21 respectively (see Section 5.1.3). The signals obtained from the sensors are shown in Fig 6.8.1.3.

As the train approaches cross passage 30, the number of cross passages between cross passage 30 and the train nose decreases. Consequently there is a reduction in the leakage flow between Tunnel 1 and Tunnel 2 and an increase in the flow displaced by the train along the section of tunnel adjacent to cross passage 30. In turn this results in an increased flow of air through cross passage 30 from Tunnel 1 to Tunnel 2, Fig 6.8.1.1. The flow of air through the cross passage from Tunnel 1 to Tunnel 2 reaches a maximum just before the nose passes, Figs 6.8.1.1 and 6.8.1.2.

When the nose passes the cross passage a sudden fall in the flow velocity in the cross passage occurs. This is then followed by a more gradual fall as the sides of the train draw past.

After just over 60% of the train has passed, the flow in the cross passage reverses. The flow in the cross passage then steadily increases from Tunnel 2 to Tunnel 1. The flow reversal is due to the generation of a suction effect towards the rear of the train.

The flow through the cross passage from Tunnel 2 to Tunnel 1 reaches a maximum just before the tail passes, Fig 6.8.1.2. After the tail passes, the flow in the cross passage progressively falls. This is due to the appearance of an increasing number of open cross passages between the back of the train and cross passage 30. These promote flow from Tunnel 2 to Tunnel 1 and progressively reduce the effect of

suction induced by the movement of the train in the section adjacent to cross passage 30. As a result the flow through the cross passage falls.

The flow behaviour in the cross passage is qualitatively similar for all other train runs in Tunnel 1 in the direction Brig to Iselle.

Fig 6.8.1.4 shows the flow behaviour sensed by the two gust anemometers (Ch 3 and Ch 4) in cross passage 30 during a test train run through Tunnel 2 from Iselle to Brig. The measurements were obtained during Run 34028 on 9th December and are quite typical of other transits in Tunnel 2. Qualitatively the flow behaviour is similar to that produced by train movements from Brig to Iselle through Tunnel 1. It is, however, important to note that there is quite a rapid increase in the cross passage flow velocity when trains travelling in Tunnel 2 pass the cross-over close to the mid point of the tunnel. Fluid dynamically, the cross-over has the effect of dividing the tunnel into two sections. As a result, when trains pass into the section of Tunnel 2 on the Brig side of the cross-over a rapid acceleration of the airflow occurs. In turn this causes a correspondingly rapid acceleration of the flow through the cross passage, Fig 6.8.1.4.

For transits through Tunnel 1 in the direction Brig to Iselle, the acceleration of the flow in the tunnel at entry is much more gradual. The reason for this is that, at entry, the trains were in the process of accelerating from Brig and travelling at relatively low speed. In Tunnel 2 test trains were travelling at speeds of 130 km/h as they passed the cross-over section.

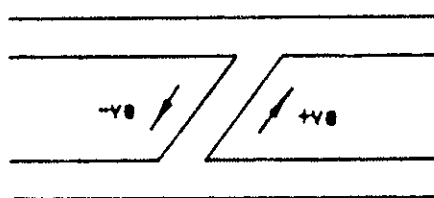
Run 34012 on 9th December was conducted in Tunnel 1 in the opposite direction to normal, ie Iselle to Brig. For this run, the flow characteristics in the cross passage were similar to those produced by transits in Tunnel 2, Fig 6.8.1.5.

Tables 6.8.1.1 and 6.8.1.2 show the peak velocities generated in the cross passage for test train runs conducted on 9th and 10th December respectively. The largest flow velocity recorded in the cross passage was 44.6 m/s. This occurred during Run 34012 on 9th December with the test train running from Iselle to Brig in Tunnel 1. The sense of the peak flow velocity was from Tunnel 1 to Tunnel 2 and was generated just before the nose passed the cross passage.

TABLE 6.8.1.1

LARGEST INSTANTANEOUS FLOW VELOCITIES  
IN CROSS PASSAGE AS TEST TRAIN PASSES  
(9.12.87)

SBB RUN NO	BR RUN NO	TIME	TUNNEL	V m/s	V <sub>B3</sub> m/s	V <sub>B4</sub> m/s	V <sub>A3</sub> m/s	V <sub>A4</sub> m/s	COMMENTS
34011	901	06.24	1	44.7	-33.6	-27.2	36.8	40.0	
34012	902	06.56	1	44.7	-44.2	-44.6	26.8	32.0	Iselle-Brig.
34015	903	07.23	1	40.2	-36.0	-30.4	31.2	33.6	Passenger train in Tunnel 2 39.1 m/s 90 seconds later.
34016	904	07.58	2	42.0	39.2	40.8	-28.0	-25.6	Train in Tunnel 1 120 seconds after test train.
34019	905	08.45	1	44.7	-35.2	-28.8	24.8	24.0	Train in Tunnel 2 90 seconds before test train.
34020	906	09.13	2	44.7	36.0	39.2	-26.4	-20.8	
34024	908	10.12	2	44.7	40.6	39.4	-29.4	-23.8	Train in Tunnel 1 240 seconds after.
34027	909	10.56	1	44.7	-38.0	-31.3	26.7	34.0	
34028	910	11.27	2	44.7	36.4	36.4	-25.2	-22.4	
34057	911	14.26	1	42.5	-39.3	-31.7	31.2	31.5	
34058	912	15.25	2	44.7	38.4	40.0	-26.6	-21.0	Train in Tunnel 1.
34061	913	15.41	1	41.6	-38.6	-32.2	29.4	32.2	
34062	914	16.12	2	43.3	35.7	40.0	-29.4	-24.5	
34065	915	16.39	1	41.6	-30.8	-25.2	32.9	34.3	Shuttle train in Tunnel 2.
34066	916	17.07	2	42.5	36.4	40.9	-28.0	-21.0	Train in Tunnel 1 100 seconds before.
34069	917	17.51	1	42.5	-39.5	-29.4	32.2	32.2	
34070	918	18.24	2	42.5	39.2	40.0	-28.0	-22.4	



SIGN CONVENTION FOR FLOW  
VELOCITIES IN CROSS PASSAGE

TUNNEL 1

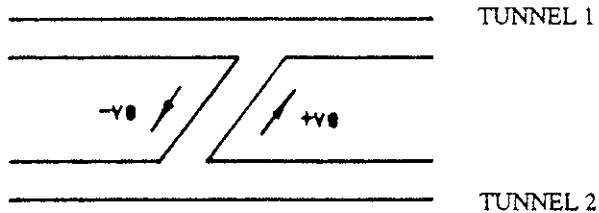
TUNNEL 2

- V Train velocity while passing cross passage.
- V<sub>B3</sub> Largest instantaneous flow velocity in cross passage prior to nose of test train passing (Channel 3).
- V<sub>B4</sub> As above but for Channel 4.
- V<sub>A3</sub> Largest instantaneous flow velocity in cross passage after passing of test train tail (Channel 3).
- V<sub>A4</sub> As above but for Channel 4.

TABLE 6.8.1.2

LARGEST INSTANTANEOUS FLOW VELOCITIES IN CROSS  
PASSAGE AS TEST TRAIN PASSES  
(10.12.87)

SBB	BR RUN	TIME	TUNNEL	V m/s	V <sub>B3</sub> m/s	V <sub>B4</sub> m/s	V <sub>A3</sub> m/s	V <sub>A4</sub> m/s	COMMENTS
34023	1006	09.43	1	44.7	38.0	40.0	-24.0	-20.0	
34024	1007	10.17	2	44.7	-33.0	-26.0	32.0	36.0	Train in Tunnel 1 130 seconds after.
34027	1008	10.48	1	44.7	40.0	42.0	-29.0	-25.0	
34028	1009	11.18	2	44.7	-36.0	-28.0	30.0	34.0	
34058	1012	15.05	2	44.7	42.0	44.0	-28.0	-22.0	Shuttle in Tunnel 1.
34061	1013	15.35	1	43.3	-35.0	-28.0	32.0	34.0	
34062	1014	16.15	2	44.7	38.0	40.0	-27.0	-22.0	
34065	1015	16.38	1	43.8	-36.0	-30.0	29.0	30.0	Shuttle in Tunnel 2 25 m/s.
34066	1016	17.21	2	44.7	32.0	32.0	-22.0	-18.0	
34069	1017	17.52	1	43.4	-34.0	-27.0	29.0	31.0	
34070	1018	18.24	2	43.8	43.0	41.0	-28.0	-24.0	



SIGN CONVENTION FOR FLOW  
VELOCITIES IN CROSS PASSAGE

- V Train velocity while passing cross passage.
- V<sub>B3</sub> Largest instantaneous flow velocity in cross passage prior to nose of test train passing (Channel 3).
- V<sub>B4</sub> As above but for Channel 4.
- V<sub>A3</sub> Largest instantaneous flow velocity in cross passage after passing of test train tail (Channel 3).
- V<sub>A4</sub> As above but for Channel 4.



FIG. 6.8.1.1.

01805DG

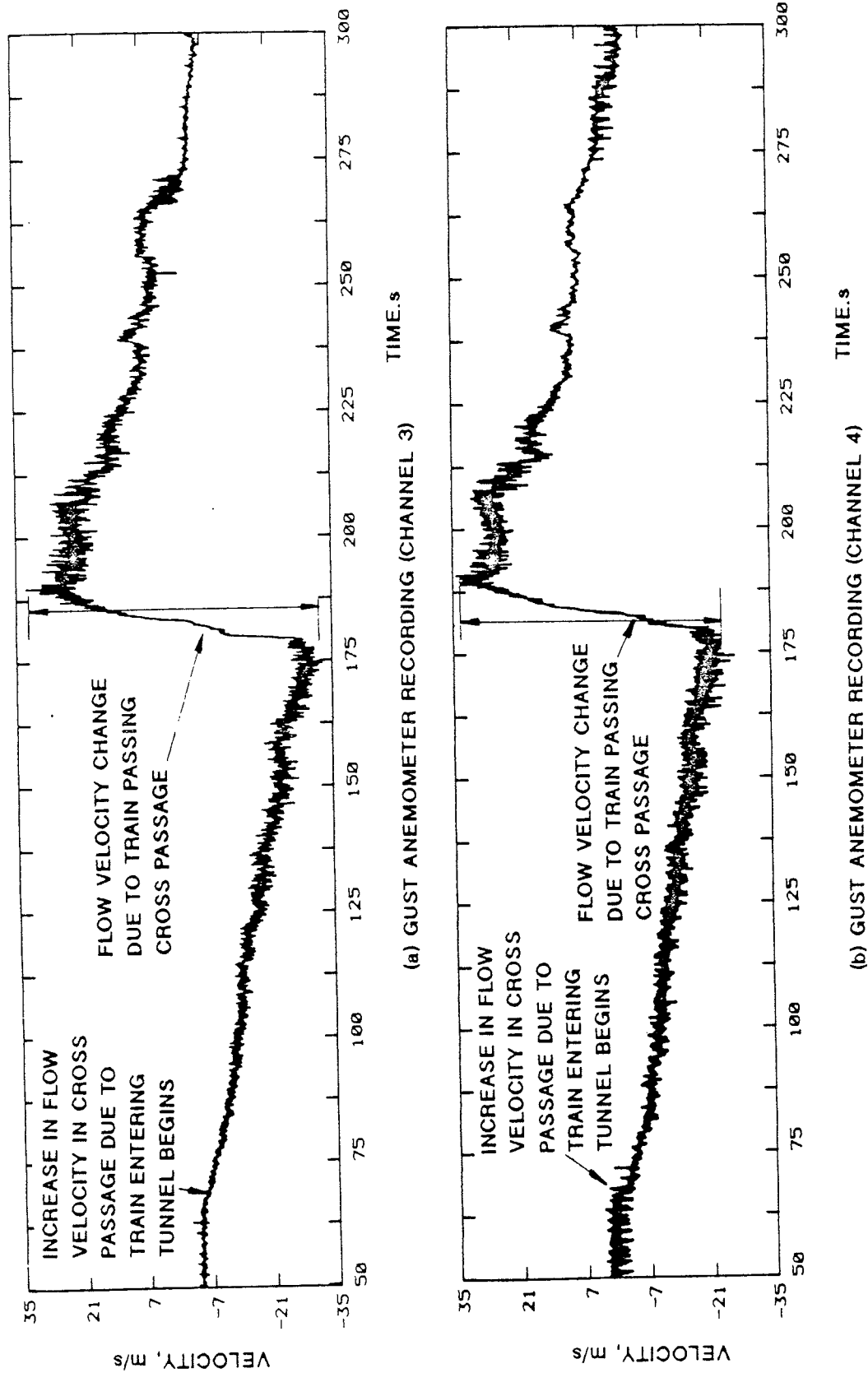
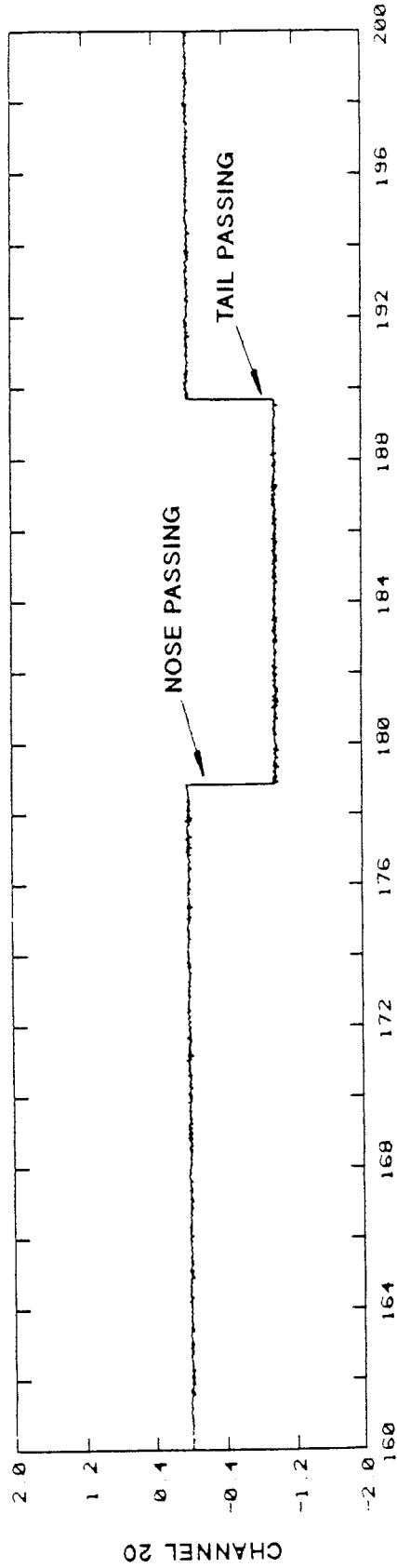
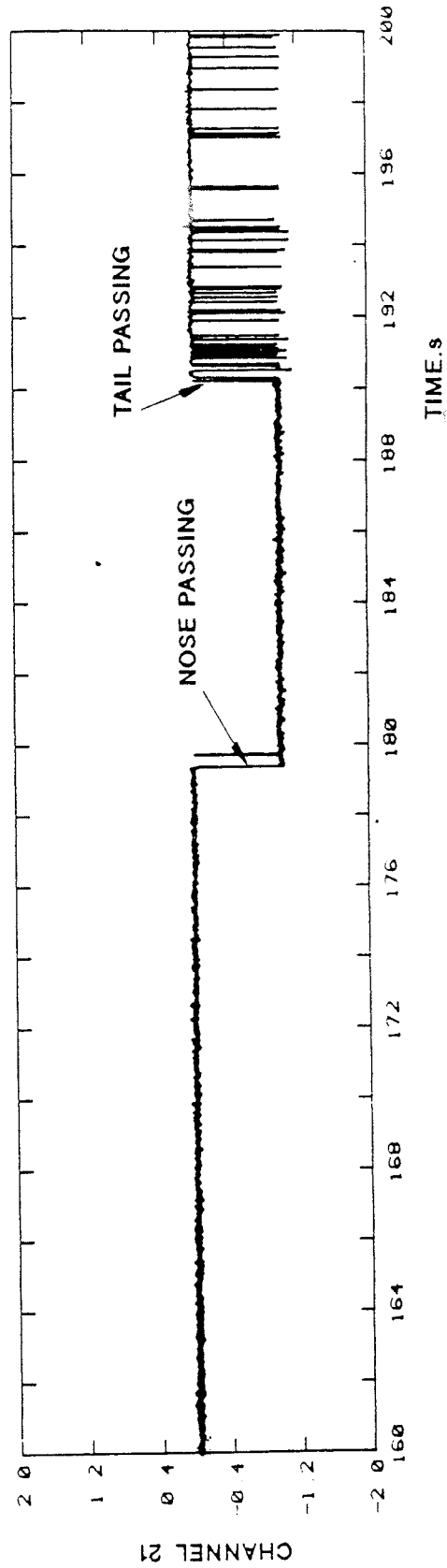


FIG. 6.8.1.1. FLOW BEHAVIOUR IN CROSS PASSAGE 30 RUN 34065 9/12/87 - TEST TRAIN IN TUNNEL 1 (DIRECTION BRIG-ISELLE)

FIG. 6.8.1.3.



(a) INFRA RED SENSOR IN TUNNEL 1-10m TO LEFT OF CROSS PASSAGE (BRIG SIDE)



(b) INFRA RED SENSOR IN TUNNEL 2-10m TO RIGHT OF CROSS PASSAGE (ISELLE SIDE)

FIG. 6.8.1.3. RUN 34065, 9/12/87 - TRAIN PASSING EVENTS OBTAINED FROM  
INFRA RED SENSORS

01808DG

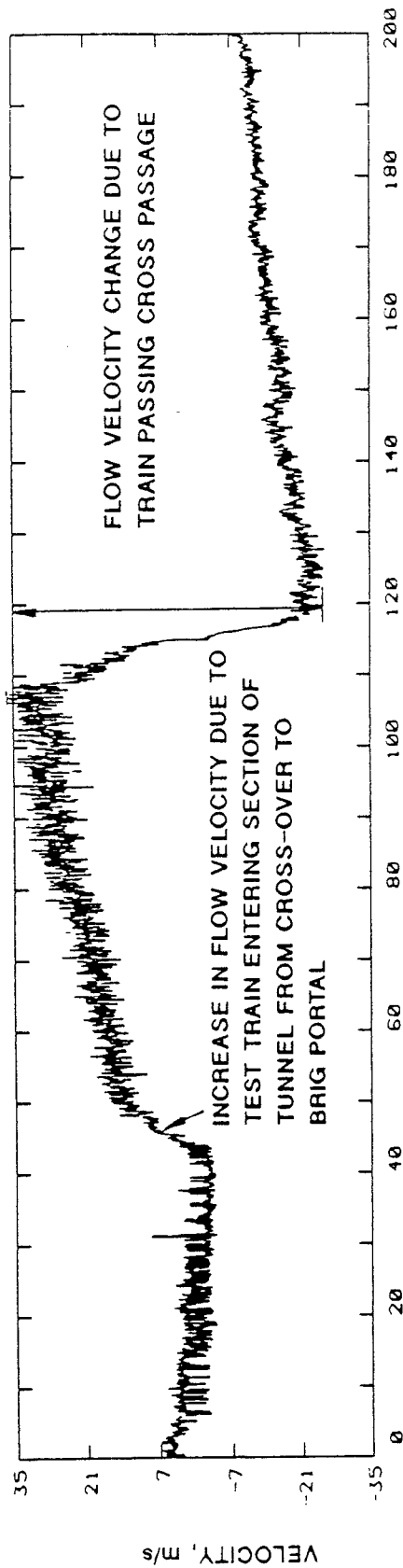


FIG. 6.8.1.4.

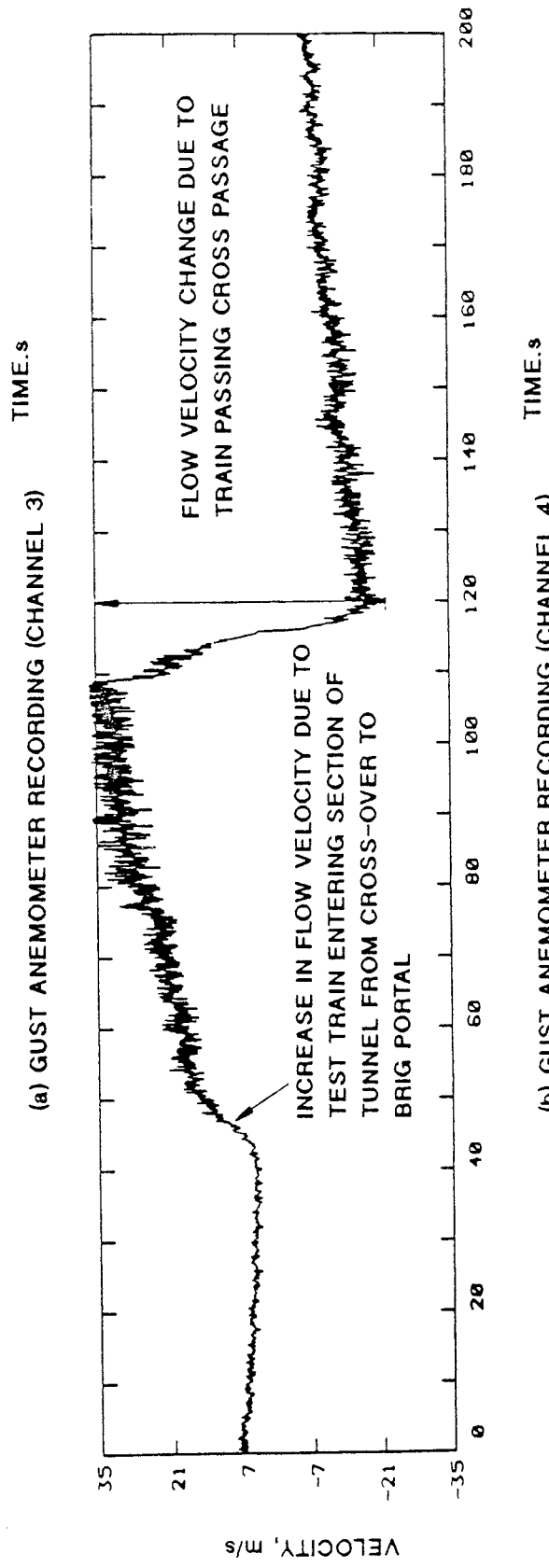


FIG. 6.8.1.4. FLOW BEHAVIOUR IN CROSS PASSAGE 30 RUN 34028 9/12/87  
TEST TRAIN IN TUNNEL 2 (DIRECTION ISELLE - BRIG)

FIG. 6.8.1.5.

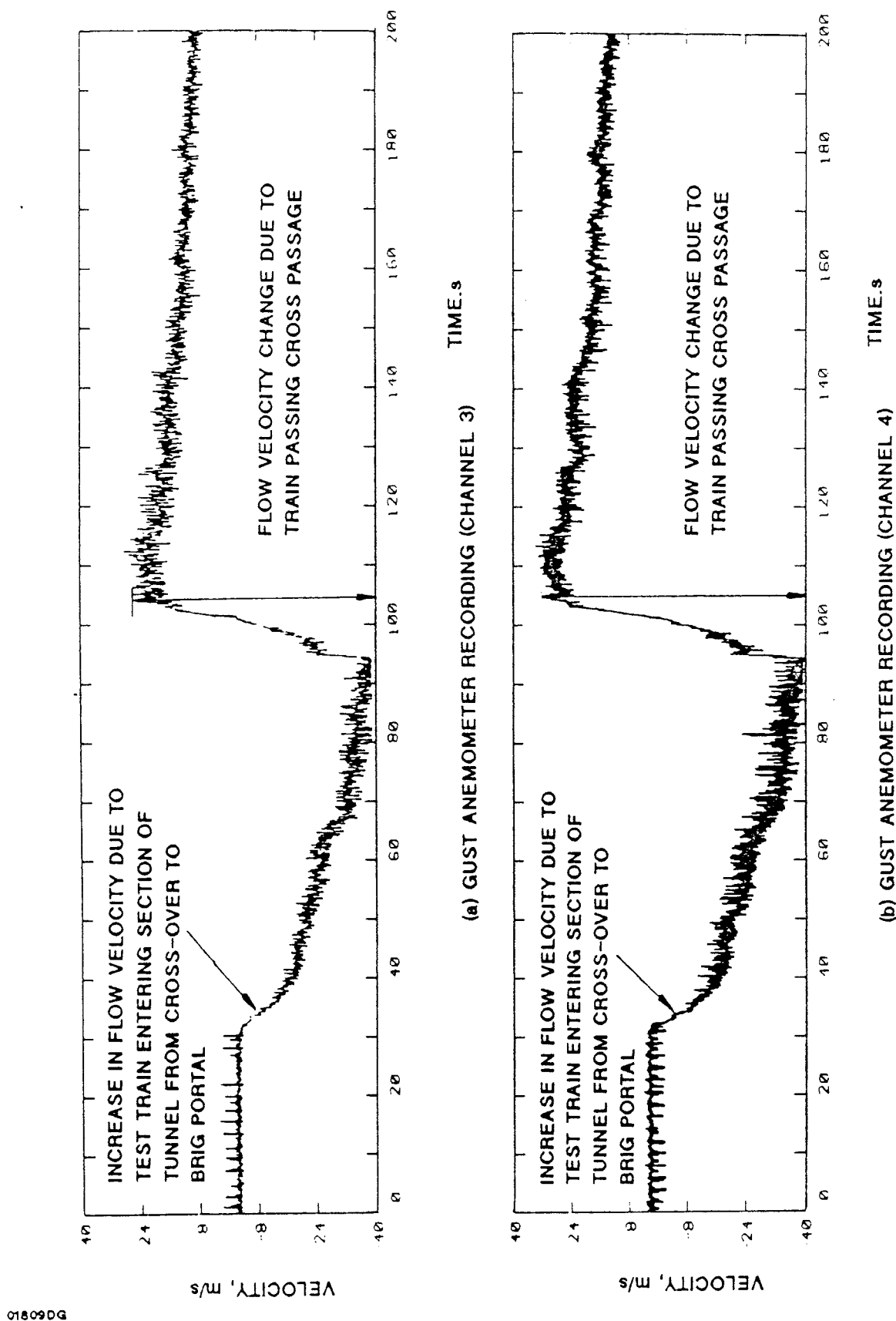


FIG. 6.8.1.5. FLOW BEHAVIOUR IN CROSS PASSAGE 30 RUN 34012 9/12/87  
TEST TRAIN IN TUNNEL 1 (DIRECTION BRIG - ISELLE)

### 6.10 Mean flow velocity in tunnels

This section considers the relationships between the local and mean flow velocities in the running tunnels. The relationships are derived with the help of velocity traverses conducted at Station "Ó" in Tunnel 2 and are used in the evaluation of the loss coefficients and friction factors presented in this report.

At Station "O" in Tunnel 2 (Fig 5.1.1.1), horizontal and vertical traverses were performed using a vane anemometer mounted on an adjustable pole, Fig 6.10.1. The horizontal traverse was carried out at 2.6 m above rail level which corresponded to approximately the half height of the cross section, Fig 6.10.2. The vertical traverse, Fig 6.10.2, was performed along a vertical running through the mid point between the rails. This was approximately at the half width of the cross section. Traverses were limited to a height of 2.6 m due to the presence of the overhead.

To assist in the process of traversing the anemometer horizontally, a scale was mounted transversely across the rails. The foot of the pole was placed on each graduation in turn and a spirit level attached to the side of the pole was used to align it vertically.

The anemometer was traversed vertically using various lengths of supporting pole.

The traverses were conducted using the draughts produced by train movements. These were in the direction Iselle to Brig. Following the passage of a train past the measurement station, the scale was placed on the rails and the traversing pole moved into position. Traverses, lasting between one and two minutes per point were then carried out while the flow was sufficiently strong to give a powerful recording signal, (ie with the flow velocity in excess of 2 m/s). When the flow fell below 2 m/s, traversing was suspended until after the next train movement. Care was taken to remove the traversing pole and scale from the track well in advance of oncoming trains.

The vane anemometer at the fixed location adjacent to the tunnel wall, Ch 7, was treated as a reference anemometer during the traverses. At each traversing point, simultaneous recordings were made on magnetic tape of the measurements from the traversing anemometer and the reference anemometer. This allowed the ratio  $U_T/U_{Ref}$  to be determined. ( $U_T$  - velocity measured by traversing anemometer,  $U_{Ref}$  - velocity measured by reference anemometer). The measured values of  $\frac{U_T}{U_{Ref}}$  at the traverse points are shown on Fig 6.10.2.

Having obtained the vertical and horizontal velocity profiles non dimensionalised with respect to  $U_{Ref}$ , two assumptions were made. These were as follows :-

- (a) The radial velocity profiles in the upper section of tunnel were taken to be a mean of the horizontal profiles to the right and left of the bisector of the cross section.

*(This is a reasonable assumption since the roughness over the roof area is similar to that of the side walls).*

- (b) The vertical velocity profiles between the horizontal traverse line and the tunnel floor were all taken to be of an identical shape to the profile along the bisector of the cross section.

*(This is acceptable since the roughness of the tunnel at ground level is dominated by the ballast and sleepers both of which extend across a large part of the width of the tunnel).*

It should be noted in adopting this assumption that the maximum velocity of the profiles is taken to be where the line of the profile intersects with the horizontal traverse.

In BS 848, recommended metering points are given for determining the mean flow velocity in a duct which consists of an upper semi circular section and lower rectangular section. This is sufficiently like the cross section of the Simplon Tunnel to use the same general distribution of points. The Simplon Tunnel cross section departs from the section featured in BS 848 in that the upper part of the tunnel conforms to an elliptical profile and the lower part tapers inwards towards the base.

The taper of the walls in the lower section does not represent too much of a departure from a rectangle. As a result the distribution of metering points is still judged to be appropriate. For the upper section, the shape departs fairly significantly from a semi circle. In view of this, the position of the metering points is distorted to conform to an ellipse. The distribution of points is presented in Fig 6.10.3.

Using the assumptions (a) and (b), flow velocities non dimensionalised with respect to  $U_{Ref}$  were generated at the metering points. In accordance with BS 848, the ratio  $U_m/U_{Ref}$  was then established by taking the mean of non dimensionalised flow velocities at the metering points.

$$\text{ie } \frac{U_m}{U_{Ref}} = \frac{1}{n} \sum_{i=1}^n \frac{U_i}{U_{Ref}}$$

where  $i$  is the  $i$  th. metering point and  $n$  is the total number of points.

From this exercise it was established that :-

$$U_m = 1.01 U_{Ref}$$

Now the fixed vane anemometer flow measurement points at measurement station A (Ch 10) and H (Ch 9) are at a slightly different position relative to the axis of Tunnel 1 to the reference point at measurement station "O" relative to the axis of Tunnel 2. Consequently it is necessary to examine the relationship between the flow measurements obtained at these points and the mean flow velocity.

The velocity profiles measured at Station "O" conform fairly well to  $1/7$  power law profiles, Fig 6.10.4.

The roughness characteristics of Tunnel 1 are very similar to Tunnel 2. On this basis it is assumed that the velocity profiles at station A and H are adequately approximated by  $\frac{1}{7}$  th power velocity distributions.

The locations of the vane anemometers at station A and H are as follows (See Fig 5.1.1.2a) :-

(i) *Ch 10, Station A*

Height from floor :- 1.15 m

Distance from wall :- 0.35 m

(ii) *Ch 9, Station H*

Height from floor :- 1.23 m

Distance from wall :- 0.34 m

Assuming  $\frac{1}{7}$  th power law profiles at Stations A and H results in the following relationships between the mean and measured velocities (reference velocities) :

(i) *Ch 10, Station A*

$$U_m = U_{Ref}$$

(ii) *Ch 9, Station H*

$$U_m = 0.99 U_{Ref}$$

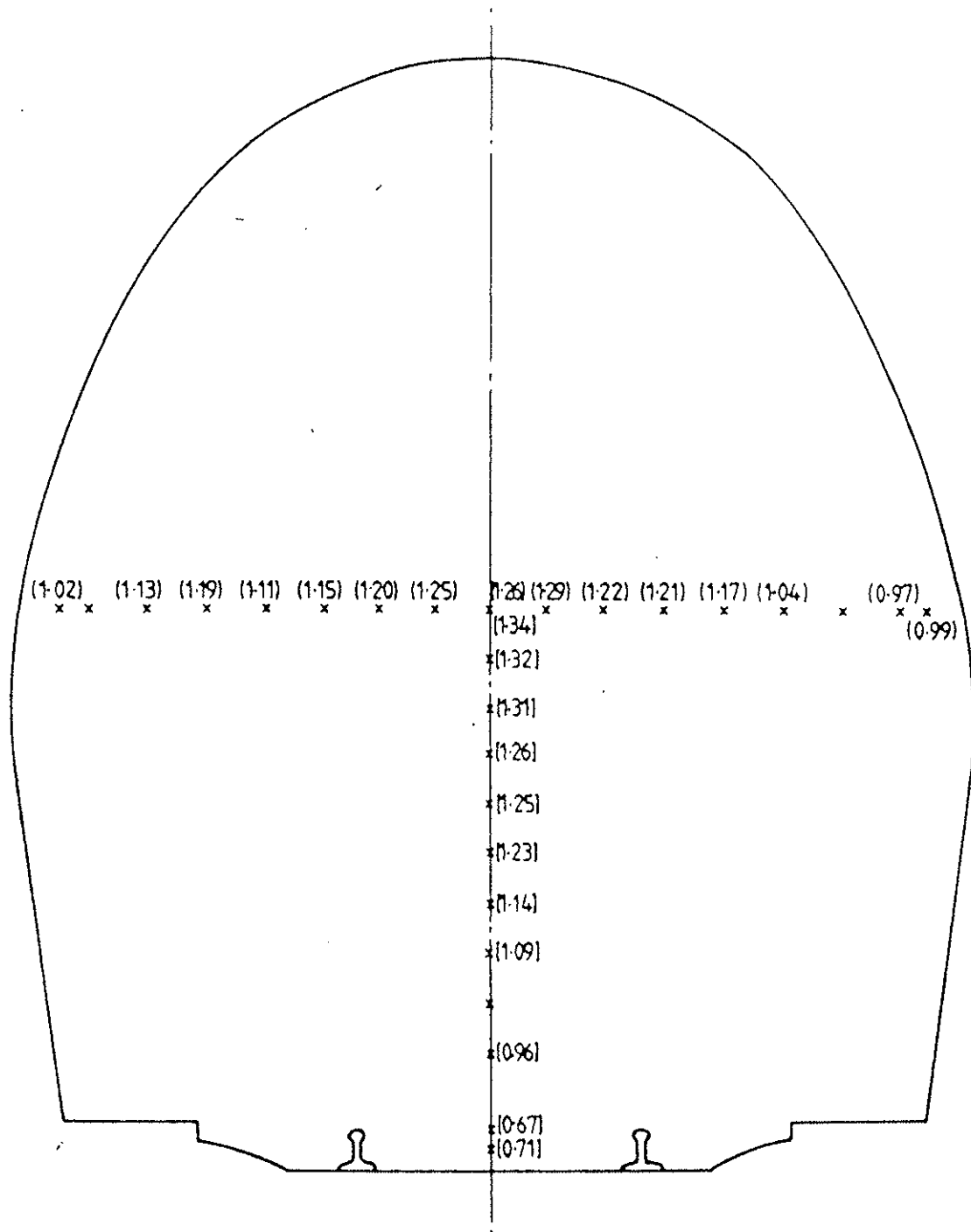
The reference vane anemometers at the fixed locations in the running tunnels therefore give a velocity which is very close to the mean. Consequently it is sufficient to take  $U_{mean} = U_{measured}$  for the vane anemometers positioned at stations A, H and O.



FIG. 6.10.1.



FIG. 6.10.1. TRAVERSING ANEMOMETER

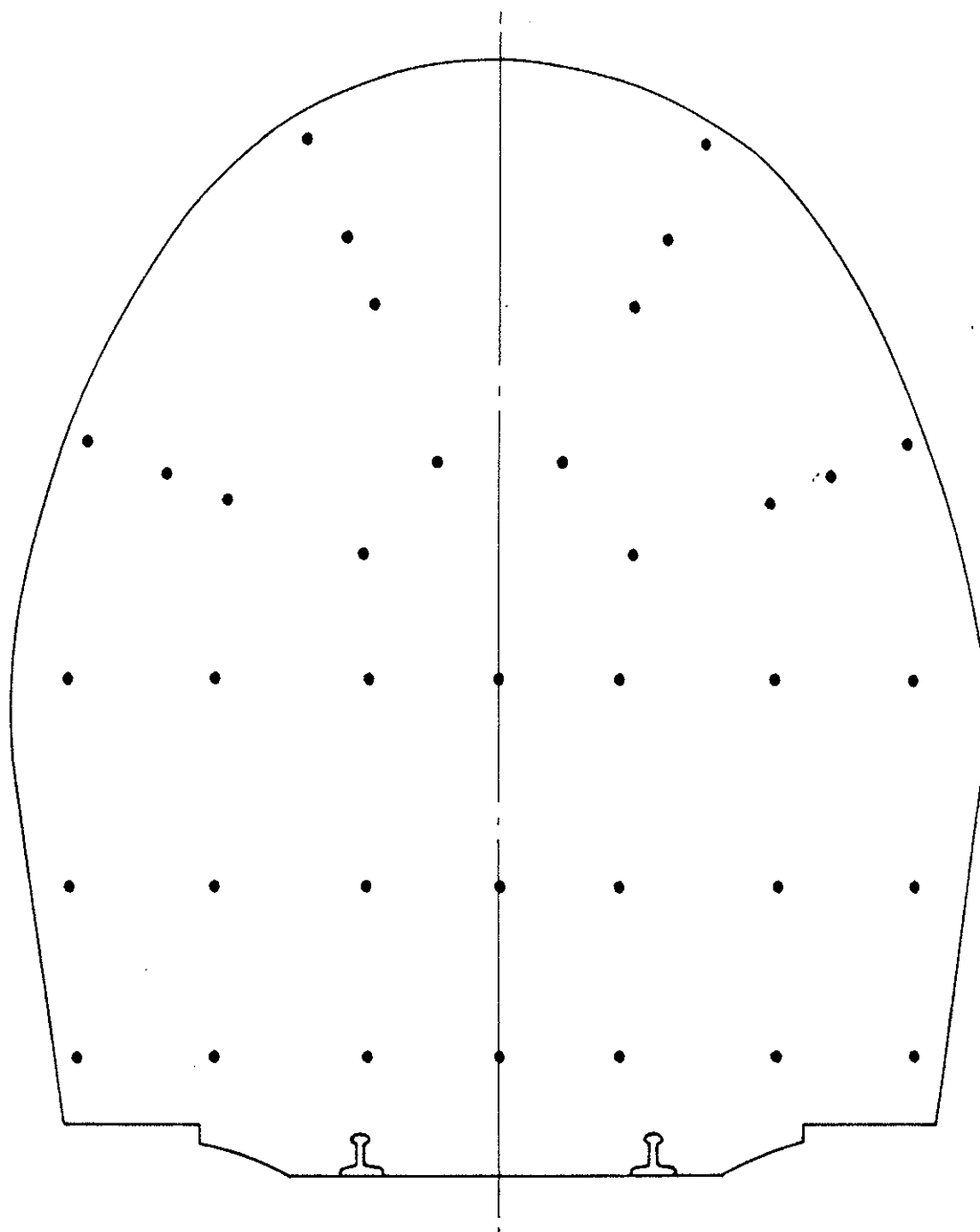


KEY:-

x TRAVERSE POINT

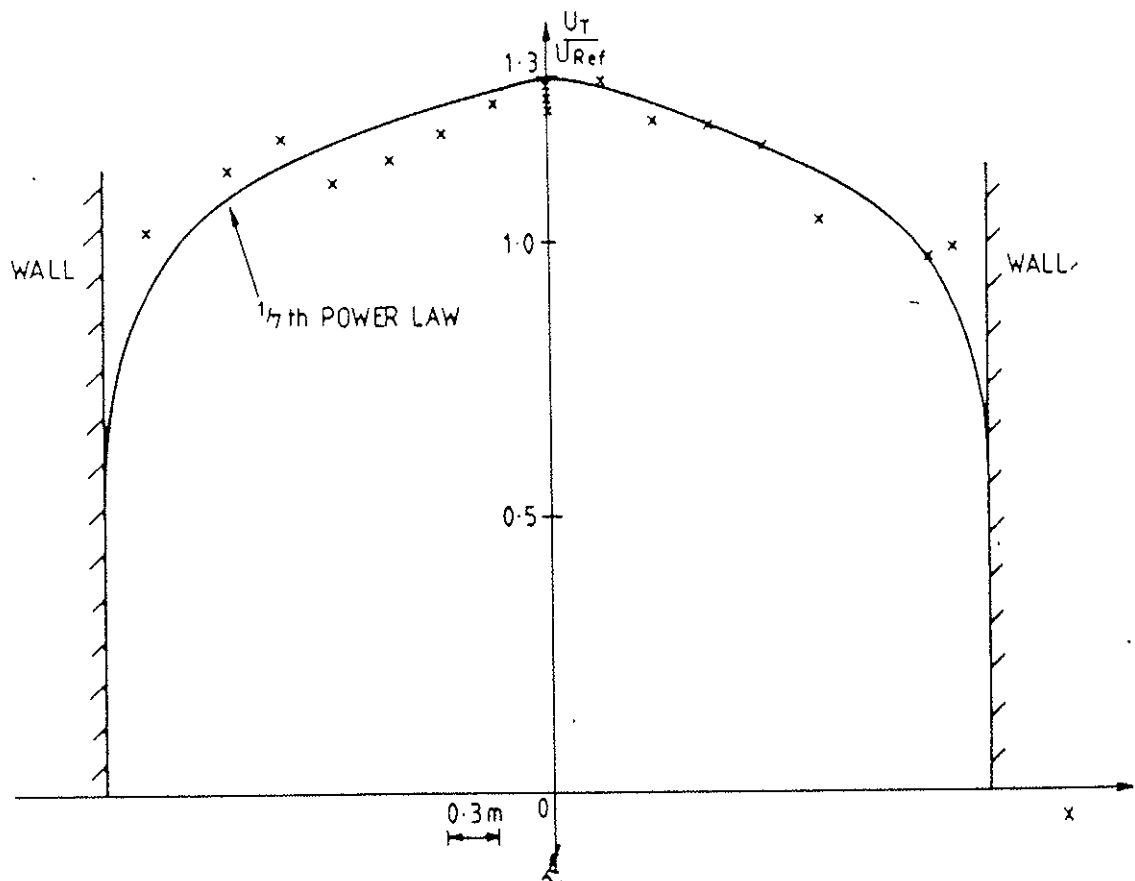
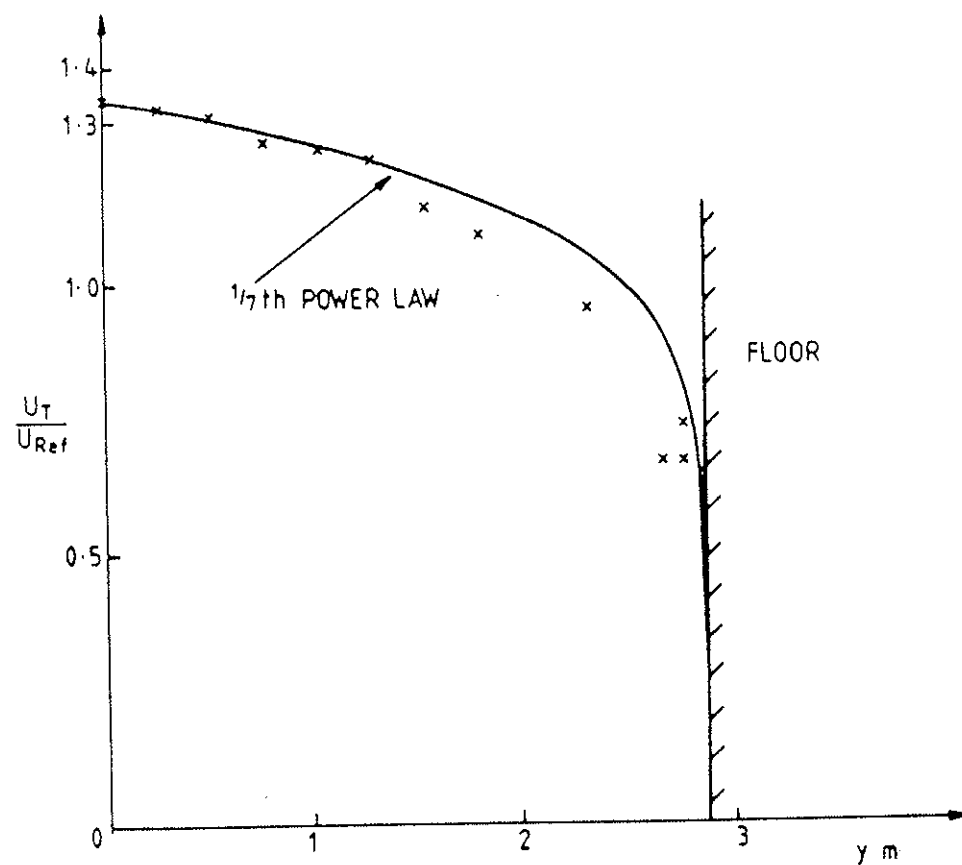
( )  $\frac{U_T}{U_{Ref}}$  (VERTICAL TRAVERSE)( )  $\frac{U_T}{U_{Ref}}$  (HORIZONTAL TRAVERSE)FIG. 6.10.2. HORIZONTAL AND VERTICAL TRAVERSE POINTS SHOWING MEASURED VALUES OF  $\frac{U_T}{U_{Ref}}$

FIG. 6.10.3.



SCALE 1 : 35.1

FIG. 6.10.3. DISTRIBUTION OF POINTS FOR DETERMINING MEAN FLOW VELOCITY (BASED ON RECOMMENDATION GIVEN IN BS. 848)

a) HORIZONTAL VELOCITY PROFILEb) VERTICAL VELOCITY PROFILEFIG. 6.10.4. REPRESENTATION OF HORIZONTAL AND VERTICAL VELOCITY DISTRIBUTIONS USING  $1/7$ TH POWER LAW PROFILES

## 7. CONCLUSION

The experimental investigations conducted in the SIMPLON tunnel provide valuable information on the steady and unsteady aerodynamic phenomena generated by the operation of a train in a long single track tunnel interconnected by cross-passages to another similar tunnel.

Most of the objectives defined in section two have been satisfactorily achieved. Nevertheless the procedure in certain cases has not been straight forward. For example it is realised that small but significant influences restricting the consistency of the results from one run to another must arise from the continuation of service train operation in the tunnel during the course of the tests. Consequently the degree of agreement can be regarded as very satisfactory.

These tests have assisted in the understanding of the three dimensional and turbulent nature of air flow generated by train operation in a complex tunnel. They have also confirmed the relatively important effect of the cross-passages on the aerodynamic resistance of the trains.

The tests were performed with a specially constituted test train up to 453 m long. This ran at speeds between 140 and 160 km/h in amongst normal train services. The operating speeds of the test train were higher than the other trains giving it an aerodynamically predominating influence over the flow conditions in the tunnel. As a result it was possible to obtain definitive data on the flow displacement and drag associated with the movement of the test train.

The most important results of the tests are as follows :-

1. The friction factor for the tunnel has been derived by a steady state method and a technique based on the method of characteristics. The former method gave an average value of 0.0072 and the latter a value of 0.0069. Averaging the results of both methods gives a friction factor for the tunnel of 0.0071.
2. The train friction factor has been obtained by two methods. The first uses the pressure excursion produced by the train as it passes a stationary point in the tunnel. This yields a friction factor of 0.0082. The second method utilises the pressure drop measured between two points on the train. This yields a friction factor of 0.0069. Averaging the results suggests a friction factor for the train of around 0.0076. The friction factor is based on a train cross-sectional area of  $10 \text{ m}^2$  and a perimeter of 11 m.

3. Pressure loss coefficients have been determined for the lined cross passage (cross passage 30).

Four conditions have been considered. These are listed below with the derived loss coefficients.

- a) train in tunnel 1 approaching the cross-passage (dividing flow) - 4.2
- b) train in tunnel 1 moving away from the cross-passage (joining flow) - 2.1
- c) train in tunnel 2 approaching the cross-passage (dividing flow) - 2.6
- d) train in tunnel 2 moving away from the cross-passage (joining flow) - 2.8

The cross passage geometries of the SIMPLON tunnel are unusual. Published data does not exist to allow comparisons to be made with the measured pressure loss coefficients for these cross passages.

4. The nose and tail pressure loss coefficients for the train have been derived from the pressure excursion provided at a point in the tunnel as the train passes. Using this method the nose and tail pressure loss coefficients have been found to be 0.1 and 0.2 respectively.
5. With the cross passage doors closed in the SWISS section the combined effect of the leakage through the doors and cross-overs is considerable. The volume flow in the second tunnel generated by these leakage paths can be as much as 80% of the volume flow generated by the movement of a train in the first tunnel. The flows through individual cross passages are relatively small and are of the order of 1.5% of the peak of the volume flow displaced by the train.
6. With the cross passage in the SWISS section of the tunnel closed the drag of the longest test train formation was 2.4 to 3.3 times the open air drag. Opening the cross passages produced a slight reduction in the drag of 2.2 to 2.8 times the open air value. In the ITALIAN section where the cross passages were permanently open and approximately 1 m<sup>2</sup> larger in cross-sectional area than the ones on the SWISS side the drag was 1.7 to 2.2 times the open air drag. This represents a reduction in drag of approximately 30% compared with that in the SWISS section with the doors closed. Cx improvements resulting from the opening of PRDs doors on the SWISS side are quite insignificant in comparison with the doors closed configuration. The small opening provides a flow constriction that caused an increase in flow losses. The drag of the train was found to vary approximately linearly with train length.

7. With respect to the variation in pressure on vehicle sides, the difference in pressure between the interior and exterior of the test coach did not exceed 170 Pa. The most important values are associated with the sudden changes in pressure caused by wave motion outside the train.

When the front and rear vehicles pass a junction, pressure variations of an unsteady kind appear on the exposed parts of the vehicles. The duration of these variations does not exceed 0.2 second, the amplitude possibly reaching 1375 Pa. Under such conditions, the variation in pressure between opposing sides of the same vehicle can reach a slightly higher value (maximum noted 1625 Pa). This pressure variation is sustained on only a small part of the vehicle side. The orientation of the junction in relation to the tunnel axis has an important influence on the values likely to be observed.

8. The lower parts of the train draw along a considerable mass of air at body level and especially at the front, where there is a rearward movement of air into the train tunnel annulus. The difference in behaviour relative to a tunnel without junctions is very marked. The maximum air speed in relation to the train is 0.4 times the train speed at window level and in the opposite direction to the train motion.
9. The peak flow velocities generated in the lined cross passage by train movements were just under 45 m/s. As the train approaches the cross passage a progressive increase in the flow through the cross passage occurs. This peaks just before the nose passes and then falls. It subsequently reverses as the sides of the train draw past and then peaks in the opposite direction as the tail passes. The velocity of the flow then falls progressively as the train tail moves away from the cross passage.
10. Airflows within the train and differences in pressure on either side of a transverse partition can be quite significant. When the intercommunicating doors are open, the train head/tail pressure difference induces a longitudinal movement of air down the inside of the train. Although a transverse partition considerably reduces this flow, it can instead be subjected to substantial pressure forces which then can cause difficulties with the operation of corridor doors.